RICE UNIVERSITY

Characterization of serum amyloid P and Fc gamma receptor: A critical engagement implicated in fibrosing diseases

by

Jeffrey Ray Crawford

A THESIS SUBMITTED
IN PARTIAL FULFILLMENT OF THE
REQUIREMENTS FOR THE DEGREE

Doctor of Philosophy

APPROVED. THESIS COMMITTEE

Richard Gomer, Professor, Advisor,
Biology, Texas A&M

John Olson, Chair,Ralph & Dorothy Looney
Professor, Biochemistry and Cell Biology

James McNew, Associate Professor,
Biochemistry and Cell Biology

Michael Stern, Professor
Biochemistry and Cell Biology

K. Jane Grande-Allen, Associate Professor,
Bioengineering

HOUSTON, TEXAS

NOVEMBER, 2011

Abstract

Characterization of serum amyloid P and Fc gamma receptor: a critical engagement implicated in fibrosing diseases

by

Jeffrey Crawford

Fibrotic diseases have a poor prognosis with no FDA approved therapies. Monocyte-derived, fibroblast-like cells called fibrocytes participate in the formation of fibrotic lesions. The conserved pentraxin protein serum amyloid P (SAP) inhibits fibrocyte differentiation in cell culture, and injections of SAP significantly reduce fibrosis in several animal models. SAP binds to the receptors for the Fc portion of immunoglobulin G (FcγR), and has been crystallized bound to FcγRIIa. The *in vivo* activity of SAP appears to be dependent on the common γ chain (FcRγ) of activating Fc receptors. The goal of my project is to elucidate the functional domains of SAP and the receptor responsible for SAP bioactivity, which could lead to refinements for SAP as a therapeutic agent and additional drug targets.

I found that mutagenesis of the residues critical for SAP binding to FcγRIIa only moderately decreases SAP's ability to inhibit fibrocyte differentiation. In murine cells, deletion of FcRγ or FcγRI significantly reduced sensitivity to SAP. Deletion of the combination of FcγRIIb/FcγRIIIa/FcγRIV did not significantly affect sensitivity to SAP, while deletion of just the inhibitory receptor FcγRIIb increased sensitivity to SAP. In human cells, siRNA-mediated reduction of FcRγ or FcγRI levels significantly decreased sensitivity to SAP, while reduction of FcγRIIb levels increased sensitivity to SAP. These

observations suggest that SAP, at least in part, uses FcγRI and FcRγ to inhibit fibrocyte differentiation.

I am also interested in how SAP functions in various disease states. SAP is known to be elevated in Alzheimer's disease (AD) and binds to amyloid plaques in the brain, a key hallmark of AD. There is a significant population of individuals that have key hallmarks of AD but show no signs of cognitive impairment, termed non-demented with AD neuropathology (NDAN). I evaluated SAP levels in post mortem samples of hippocampus and frontal cortex in age-matched controls, AD, and NDAN individuals. AD individuals had significantly increased SAP levels, while NDAN samples had no significant difference in SAP levels compared to controls. These results suggest that low levels of SAP in plaques marks the brains of individuals that escape dementia despite the presence of beta amyloid plaques.

Acknowledgements

First and foremost I would like to thank my thesis advisor Dr. Richard Gomer for his support over the years for my thesis project. He encouraged independent thinking while at the same time providing insightful guidance.

I would also like to thank my thesis committee, including Dr. John Olson, Dr. Michael Stern, Dr. James McNew, and Dr. Jane Grande-Allen, for their helpful direction and insights during the progression of my thesis project.

I want to thank all past and current members of the Gomer lab. I would especially like to thank Dr. Darrell Pilling for all his advice in the design of my experiments, for mentoring me in my murine work, and for the critical reading of my manuscripts. I would like to thank Dr. Deenadayalan Bakthavatsalam for all the helpful discussions regarding the direction of my project, and I would like to thank Anu Maharjan for all her assistance and for being my fellow partner in crime in the fibrocyte portion of the lab at both Rice and Texas A&M.

I would like to thank Dr. Sjef Verbeek and Jill Claassens at LUMBC for the immense assistance with the donation of receptor knockout spleens. Similarly, I would like to thank Dr. Bryce Binstadt and Jennifer Auger at the University of Minnesota for additional spleens. I want to thank Dr. Susan Cates for all her assistance in the physical characterizations of my recombinant protein, and the good people at Promedior for providing key materials, including a vector that really helped the progression of my thesis. I would also like to thank Dr. Giulio Taglialatela and Dr. Nicole Bjurkland at UTMB Galveston for the brain samples and guidance regarding Alzheimer's disease.

Finally, I would like to thank my parents Richard and Jan Crawford for their continued support, without which I would have never gotten this far.

Table of Contents

List of Figures

List of Tables

List of Abbreviations

A	alanine
Aβ	beta amyloid
Ab	antibody
ACK	potassium bicarbonate
AD	Alzheimer's disease
ApoE	apolipoprotein E
Asn	asparagine
BSA	bovine serum albumin
$CaCl_2$	calcium chloride
CD	circular dichroism
CD32/64/etc	cluster of differentiation
cDNA	complementary deoxyribonucleic acid
CHO	Chinese hamster ovary
CO_2	carbon dioxide
CPHPC	R-1-[6-[R-2-carboxy-pyrrolidin-1-yl]-6-oxo-hexanoyl] pyrrolidine-2-carboxylic acid
CRP	C-reactive protein
D	aspartic acid
DTT	dithiothreitol
E.coli	*Escherichia coli*
EDTA	ethylenediamine tetraacetic acid

ELISA	enzyme-linked immunosorbent assay
Fab	fragment antigen-binding
FcγR	Fc gamma receptor
FcRγ	common gamma chain
FPLC	fast protein liquid chromatography
G	glycine
HCl	hydrochloric acid
hSAP	human serum amyloid P
I	isoleucine
IgG	immunoglobulin G
IL	interleukin
kDa	kilodalton
L	leucine
LTA	lipoteichoic acid
mAb	monoclonal antibody
MCI	mild cognitive impairment
M-CSF	macrophage colony-stimulating factor
mg	milligram
ml	milliliter
mM	millimolar
MMSE	mini-mental state exam
mSAP	murine serum amyloid P
MWCO	molecular weight cut off

N	asparagine
NaCl	sodium chloride
$NaPO_4$	sodium phosphate
NDAN	non-demented with Alzheimer's disease neuropathology
NINCDS-ADRDA	National Institute of Neurological and Communicative Disorders and Stroke and the Alzheimer's Disease and Related Disorders Association
nM	nanomolar
P	proline
pAb	polyclonal antibody
PBMC	peripheral blood mononuclear cells
PBS	phosphate buffered saline
PCR	polymerase chain reaction
PMI	postmortem interval in hours
Q	glutamine
S	serine
SAP	serum amyloid P
SDS-PAGE	SDS-polyacrylamide gel electrophoresis
S.E.M.	standard error of the mean
SPR	surface plasmon resonance
T	threonine
Tris	tris(hydroxymethyl)aminomethane
µg	microgram

µl	microliter
µM	micromolar
µm	micrometer
V	valine
Y	tyrosine
WT	wild-type

Chapter 1: Fibrocytes in fibrosing diseases and potential regulation by serum amyloid P.

1.1 Fibrosing diseases.

Fibrosis is an aberrant condition involving repeated tissue injury and inflammation, resulting in scar-like lesions composed primarily of extracellular matrix (ECM) proteins such as collagen and fibronectin (Kumar et al., 2005). This excess buildup of scar tissue leads to tissue dysfunction and eventual organ failure.

Fibrosing diseases are characterized by a chronic and severely debilitating condition with a high mortality rate. Idiopathic pulmonary fibrosis is one such disorder with a 70% mortality rate within 5 years of diagnosis due to the excessive remodeling of the lung and collagen deposition (Perez et al., 2003). Other fibrosing diseases include scleroderma, hypertrophic scarring, chronic kidney disease, liver fibrosis, and a major killer in the US, congestive heart failure (Lupher et al., 2006). There are currently no FDA approved therapies so there is a serious unmet medical need (Bouros et al., 2005). Increasing evidence suggests that fibroblast-like cells termed fibrocytes are implicated in the formation of fibrotic lesions and can potentially differentiate into or activate existing fibroblasts into a more active cell type involved in collagen production, the myofibroblasts (Lupher, et al., 2006; Herzog et al., 2010). My project deals with determining how a potential therapeutic for fibrosing diseases, serum amyloid P, functions in its ability to regulate fibrocyte differentiation, which could lead to new and even more effective therapeutics.

1.2 Fibrocytes are involved in wound healing and implicated in fibrosing diseases.

To heal wounds, several cell types help form new tissue. Local fibroblasts migrate to the source of the wound and proliferate (Clark, 2001). In addition, circulating monocytes can leave the blood, enter the wound, and differentiate into spindle-shaped, fibroblast-like cells called fibrocytes (Bucala *et al.*, 1994; Abe *et al.*, 2001). At the site of a wound, fibrocytes secrete extracellular matrix proteins such as collagen to rebuild tissue, secrete inflammatory cytokines, stimulate angiogenesis, and promote wound closure (Chesney *et al.*, 1998; Hartlapp *et al.*, 2001). In addition to their beneficial effects, fibrocytes have been implicated in the formation of the scar tissue-like lesions in a variety of fibrosing diseases such as pulmonary fibrosis, congestive heart failure, cirrhosis of the liver, renal fibrosis, and nephrogenic systemic fibrosis (Cowper *et al.*, 2003; Phillips *et al.*, 2004; Haudek *et al.*, 2006; Kisseleva *et al.*, 2006; Mehrad *et al.*, 2007; Sakai *et al.*, 2010). Fibrocytes have also been detected in bronchial asthma and hypertrophic scarring (Schmidt *et al.*, 2003; Yang *et al.*, 2005).

Fibrocytes derive from a subset of CD14+ monocytes in human peripheral blood, and mature fibrocytes express markers of both hematopoietic cells (CD34, CD45, LSP-1, MHC Class II) and stromal cells (collagen I and III, fibronectin) (Bucala *et al.* 1994; Abe *et al.*, 2001; Gomperts *et al.*, 2007; Pilling *et al.*, 2009b). Fibrocyte differentiation is inhibited by the serum protein serum amyloid P (SAP) as well as cross-linked IgG (Pilling *et al.*, 2003, 2006).

1.3 Serum Amyloid P as a regulator of fibrocyte differentiation.

The regulation of fibrocytes is essential for proper wound repair; thus, a factor is present in the serum to regulate fibrocyte differentiation. The Gomer lab has identified serum amyloid P (SAP), a member of the pentraxin family of proteins, as the factor that prevents the rapid appearance of fibrocytes in a human peripheral blood mononuclear cell culture (Pilling et al., 2003). SAP is a glycoprotein that is secreted by the liver into the blood and has 51% amino acid homology to C-reactive protein (CRP), another member of the pentraxin family (Pepys *et al.*, 1983). The pentraxin family is characterized by a planar disc arrangement of five, non-covalently associated monomers (Figure 1.1; Woo *et al.*, 1985; Thompson *et al.,* 2002). SAP monomers have a mass of 25.46 kDa and are folded as a two-layered β-sheet with a jelly roll topology (Thompson *et al.*, 2002; Aquilina *et al.*, 2003). On one side of the roll is an alpha helix, and on the opposite side are two calcium binding sites. As a pentamer, the SAP disc-like structure consists of an "A face" with five alpha helixes and a "B face" that binds calcium (Figure 1.1; Thompson *et al.*, 2002).

SAP is a pattern recognition protein that binds a variety of ligands in a calcium dependent manner, including pathogen components like bacterial lipopolysaccharide (LPS), and autoimmune / apoptotic components like chromatin, histones, and phosphoethanolamine (Emsley et al., 1994; Pepys et al., 1997). CRP binds to similar ligand types, but the exact role of SAP and CRP within the body remains unclear (Pepys et al., 1997). Both proteins likely play a role in the initiation and clearance of an immune response because SAP and CRP can opsonize cells for phagocytosis to eliminate

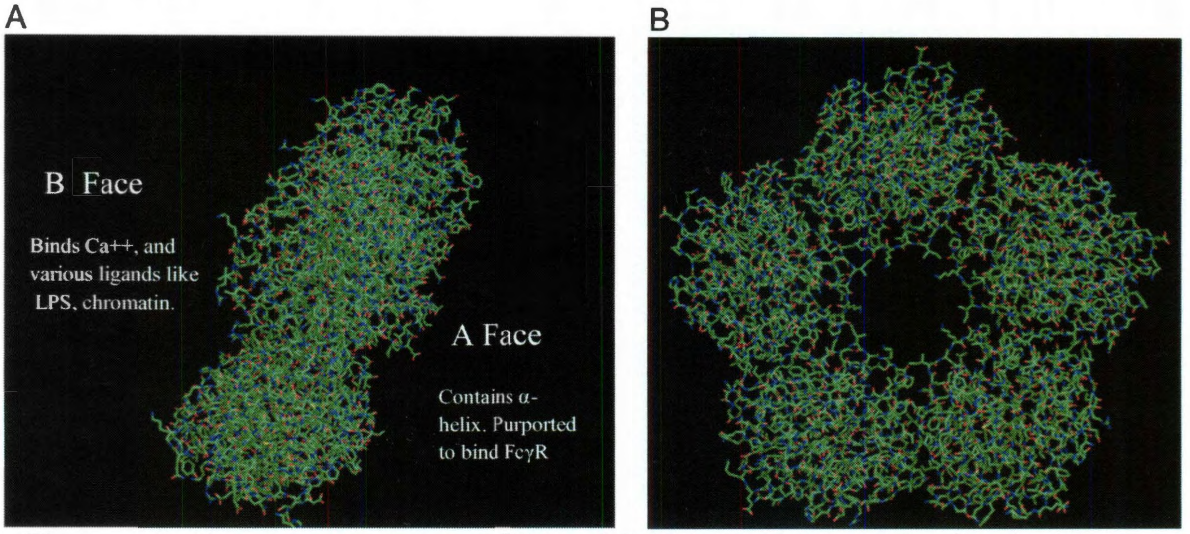

Figure 1.1: Crystal structure of SAP. MMDB ID: 2151. Visualized with Pymol (Delano, 2002). **(A)** Side view of SAP "disc". The "A" face is purported to bind the Fcγ receptor, the "B" face binds ligands such as bacterial lipopolysaccharide, chromatin, and phosphoethanolamine. **(B)** Overhead view of SAP "A" face.

pathogens and cellular debris (Bharadwaj et al., 2001). It has been proposed that SAP and CRP opsonize cells by binding to a ligand (such as bacteria or an apoptotic cell) on the B face, and then binding through its A face to a Fcγ receptor (FcγR) on a phagocytic cell (Figure 1; Bharadwaj et al., 2001; Bodman-Smith et al., 2002; Mold *et al.*, 2002). However, SAP and CRP likely have distinct roles in vivo because of differences in their biology and structure. For instance, SAP levels remain relatively constant within the blood, while CRP levels increase up to 1000 fold during an immune response and CRP can activate innate immunity through the complement cascade (Pepys et al., 1978 & 1983; Mold et al., 1999). Another difference is that SAP is glycosylated with a N-linked biantennary oligosaccharide at Asn32, while CRP is not glycosylated in serum except in some pathological conditions (Emsley et al., 1994).

One of the proposed roles of SAP in vivo is the regulation of fibrocyte differentiation within the circulation and peripheral tissues (Pilling et al., 2003). During resolution of an immune response, serum proteins are often cleared from the site of infection (Haslett et al., 1988). Within a wound, SAP may no longer be present due to such clearance or SAP's binding to other ligands to clear cellular debris. Without the presence of SAP to inhibit fibrocyte differentiation, monocytes can differentiate into fibrocytes and initiate wound repair. However, the monocyte will likely not immediately differentiate into a fibrocyte and close the wound, since closing an infected wound could result in gangrene and further cell death (Ferreira *et al.*, 2006). Instead, aggregated immunoglobulin, which binds pathogens and also inhibits fibrocyte differentiation, will

prevent premature appearance of fibrocytes until the wound is clear of pathogens (Pilling *et al.*, 2006).

Because fibrocytes participate and help regulate wound healing, manipulating SAP levels could also be beneficial to promote wound healing (Mori *et al.*, 2005). Fibrocytes are present in hypertrophic scars, and the ability to manipulate SAP levels could potentially reduce scarring (Yang *et al.*, 2005). Altering SAP levels could also potentially help diabetics who have slow wound healing. SAP-depleting bandages have been used to accelerate wound healing in pigs, and local and systemic injections of SAP slow woun healing in mice (Naik-Mathuria *et al.*, 2008; Gomer *et al.*, 2009).

In addition, since fibrocyte dysregulation has been associated with fibrotic diseases and SAP can inhibit fibrocyte differentiation *in vitro* (Pilling *et al.*, 2003), SAP has been tested as a therapeutic in a number of fibrosing disease model systems. We found that injections of SAP significantly reduced the levels of fibrosis in bleomycin-induced pulmonary fibrosis in a mouse and rat model system (Pilling *et. al*, 2007). We hypothesize that SAP prevents fibrosis by inhibiting fibrocyte differentiation. SAP has also successfully been used to treat model systems of ischemic cardiomyopathy, Aspergillus fumigatus-induced allergic airway disease, radiation-induced oral mucositis, renal fibrosis, and kidney fibrosis (Haudek *et al.*, 2006; Castano *et al.* 2009; Moreira *et al.,* 2010; Murray *et al.*, 2010). Additionally, SAP is undergoing Phase II clinical trials tests to inhibit scar formation in ocular surgery by Promedior (Malvern, PA). In these disease model systems, SAP appears to have acted through the reduction of fibrocytes

(Haudek *et al.*, 2006; Pilling *et al.*, 2007) or inhibition of pro-fibrotic inflammatory M2 macrophages (Castano *et al.*, 2009; Moreira *et al.*, 2010). Understanding how SAP functions could be beneficial not only for developing therapies for fibrosing diseases but also for promoting wound healing. My project could potentially impact both fields by allowing for fine tuned manipulation of SAP and its receptor.

1.4 SAP binds to Fcγ receptors (FcγR), key receptors in mediating the immune response.

To determine the functional domain of SAPs we will examine how SAP interacts with its receptor, FcγR. However, FcγR are known for mediating the immune response through the binding of immunoglobulin (IgG) antibodies. FcγRs are found on a variety of hematopoietic cells and bind the Fc portion of IgG antibodies (Ravetch *et al.*, 2001). Once aggregated IgG cross-links multiple receptors, a signaling cascade is activated through tyrosine kinases to initiate an immune response (Daeron, 1997). There are four activating Fcγ receptors: FcγRI (CD64), IIa (CD32a), IIIa (CD16a), and IIIb (CD16b). In contrast, FcγRIIb (CD32b) triggers an inhibitory signaling pathway to help modulate the immune response (Nimmerjahn *et al.*, 2008). The signaling cascades initiated by the receptors can be initiated directly by FcγRIIa and FcγRIIb, while FcγRI and IIIa/b require an accompanying gamma chain (FγcR) to initiate the signal (see figure 1.2). The signaling pathways initiated by the different receptors are quite similar. After the receptors are crosslinked, the tyrosine in the ITAM domain is phorphorylated by kinases of the SRC cellular activation. It is interesting to note that the binding of SAP to FcγRs initiates a family (Ravetch 2003). This leads to recruitment of the SYK family of

A

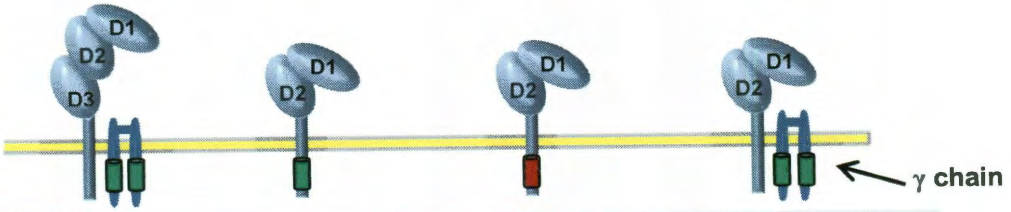

Human	FcγRI	FcγRIIa	FcγRIIb	FcγRIIIa	FcγRIIIb
Affinity for IgG	High	Low to medium	Low to medium	Low to medium	Low to medium
Affinity to hSAP	Medium	High	Very Low	Not tested	High
Signaling	Activating	Activating	Inhibiting	Activating	Activating
Needs γ chain?	Yes	No	No	Yes	Yes

B

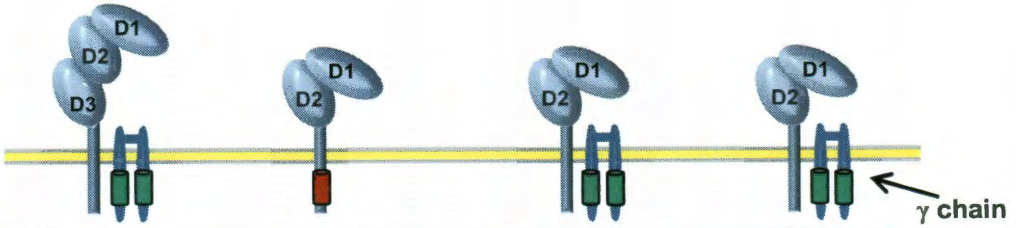

Mouse	FcγRI	FcγRIIb	FcγRIII	FcγRIV
Affinity for IgG	High	Medium/ low	Medium/ low	Medium/ low
Affinity to hSAP	Medium	Low	Medium	High
Signaling	Activating	Inhibiting	Activating	Activating
Needs γ chain?	Yes	No	Yes	Yes
Binds IgG Subtype	IgG2a (IgG3)	IgG1 IgG2a IgG2b	IgG1 (IgG2a) (IgG2b)	IgG2a IgG2b IgE^b

Figure 1.2: The family of Fcγ receptors in (A) humans and (B) mice. Green represents ITAM activating domains, red the ITIM inhibitory domain. Parenthesis around IgG subtypes indicates that the subtypes can bind *in vitro* to the FcγR but does not require the receptor *in vivo* to function. Adapted from Nimmerjahn *et al.* (2008).

kinases, followed by the activation of downstream pathways such as RAS-RAF-MAPK, important for similar but not identical pathway. SAP utilizes the SRC family of kinases but does not appear to rely on SYK since a SYK-agonist failed to block the bioactivity of SAP (Pilling *et al.*, 2006).

FcγRs are also defined by their affinity for binding monomeric or aggregated IgG. FcγRI is the high affinity receptor for both monomeric and aggregated IgG, while the remaining receptors bind only aggregated IgG with low to medium affinity. The extracellular region of the Fc receptors is composed of two domains containing immunoglobulin-like folds, termed D1 and D2, with IgG binding to D2. Additionally, FcγRI has a third extracellular domain D3, which accounts for its ability to bind IgG with high affinity (Hullet *et al.*, 1998; figure 1.2). IgG will intercalate into the groove formed by the two different extracellular domains, forming an asymmetrical contact between the single FcγR and the Fc binding portion of IgG, which prevents a second receptor from binding to the same Fc portion of IgG (Nimmerjahn *et al.*, 2008). Therefore, a single IgG molecule cannot cross-link multiple receptors and elicit an immune response. It requires multiple IgGs to form an immune complex by binding to an antigen like a pathogen or by heating IgGs to cause them to self aggregate.

The activating and inhibitory Fcγ receptors work together to modulate an immune response. This is further complicated by the fact that there are four specific IgG subtypes that also bind with varying affinity and specificity to the FcγRs to elicit specific responses (Dijstelbloem *et al.*, 2001; see Figure 1.2). As another complication, the

biology of the FcγRs is not consistent across species. A significant portion of my studies are in the murine system with distinct FcγR biology. Similar to humans, there are both activating and inhibitory FcγRs. In mice, the activating FcγRs are FcγRI, III, and IV, and all three require the accompanying gamma chain for signaling (Nimmerjahn *et al.*, 2008). The inhibitory receptor is FcγRIIb, similar to humans, while mice lack FcγRIIIb, an activating receptor unique to human neutrophils (Ravetch *et al.*, 1991). Based on sequence similarity of the extracellular domain, mouse FcγRIII is most closely related to human FcγRIIa, while FcγRIV is most closely related to human FcγRIIIa (Hughes *et al.*, 1996). Additionally, the affinity for specific IgG subtypes by murine FcγRs is much higher than those found in humans. These differences should be taken into account when trying to extrapolate any results from mice to humans.

Chapter 2: Determining the functional domains of SAP through mutagenesis.

2.1 Introduction

There are no FDA approved therapies for the treatment of fibrosing disorders. Because SAP is a potential therapeutic for such diseases and is currently undergoing Phase II trials, there is great interest in understanding how SAP functions. To determine the functional domains of SAP, residues were altered by site-directed mutagenesis. For the initial mutagenesis, residues were selected that could potentially bind to the SAP receptor, FcγR. There are multiple reasons why we are focusing on SAP's ability to bind FcγR in trying to determine the functional domain of SAP. The bioactivity in question is SAP's ability to inhibit monocytes from becoming fibrocytes. SAP was previously found to bind to monocytes, monocytes express all three main classical subtypes of FcγR, SAP has been found to initiate a signaling cascade consistent with FcγR ligation, and SAP has been crystallized bound to FcγRIIa (Bharadwaj *et al.*, 2001; Grage-Griebenow *et al.*, 2001; Chi *et al.*, 2002; Macdonald *et al.,* 2006; Lu *et al.*, 2008). Additionally, SAP's ability to inhibit fibrosis in mouse models of pulmonary and kidney fibrosis was dependent on activating FcγRs (Haudek *et al.*, 2008; Castano *et al.*, 2009).

To select residues for mutagenesis, I initially compared SAP to two conserved regions of IgG, ^{234}L(F)LGGPS^{239} and ^{327}ALPAPI^{333}, that contact the FcγR when IgG binds to the receptor (Radaev *et al.* 2001). Assuming that there is functional homology in having a similar amino acid motif, I selected residues 178-183 of SAP, which closely resembles the ^{327}ALPAPI^{333} sequence from IgG (See table 2.1). C-reactive protein

(CRP), a pentraxin and serum protein that also binds FcγRs, is known to have a sequence that resembles the IgG ^{234}L(F)LGGPS^{239} region (Bang *et al.*, 2005). CRP has distinct bioactivity from SAP and does not inhibit fibrocyte differentiation, and this difference in IgG-like binding domains could account for this.

A second region was also selected for mutagenesis based on a published SAP-FcγRIIa crystal structure, which suggests a completely separate region to focus upon. Lu *et al.*(2008) crystallized SAP binding to the extracellular domain of the human FcγRIIa receptor to 2.8 Å resolution. For crystallization, SAP was purportedly dissociated into monomers and mixed with a 1:1 molar ratio of *E.coli* expressed ecto-domain of FcγRIIa. The resulting complex suggests that one FcγRIIa molecule would bind across the face of one SAP pentamer with the D1 and D2 domains of the receptor contacting 2 subunits of the pentraxin (see Figure 2.1, contacts between 2 SAP monomers). SAP binds to the receptor along the ridge helix region (Pro 166 to Gln 174) with key residues being Tyr 173 and Gln 174 (Figure 2.1, highlighted red spheres). Additionally, the C-terminus residues near the SAP pentamerization domain (Srinivassan *et al.*, 1994) come in contact with the D1 and D2 domains of the receptor.

In this chapter, I show that recombinant SAP produced both in bacteria and human cells is bioactive. The bacterially expressed SAP displays some interesting biology such as promoting fibrocyte differentiation when altering reside 182, while reducing differentiation when residue 180 was mutagenized. However, only the SAP expressed by human tissue cultured cells retains native structure as a pentamer, which

Table 2.1: Sequence homology between SAP, CRP, and IgG binding regions.

SAP sequence	173	174	175	176	177	178	179	180	181	182	183
Human SAP	Y	Q	G	T	P	L	P	A	N	I	L
Human CRP	Y	L	G	G	P	F	S	P	N	V	L
Human IgG1	L	L	G	G	P	L	P	A	P	I	E
Human IgG2	V	A	-	G	P	L	P		P	I	E
Human IgG3	L	L	G	G	P	L	P	A	P	I	E
Human IgG4	F	L	G	G	P	L	P	S	S	I	E
IgG sequence (EU sys)	234	235	236	237	238	328	329	330	331	332	333

Comparison of SAP to two different IgG binding regions ^{234}L(F)LGGPS^{239} and ^{327}ALPAPI^{333} (Bang *et al.*, 2005). SAP closely resembles the 327-333 IgG sequence.

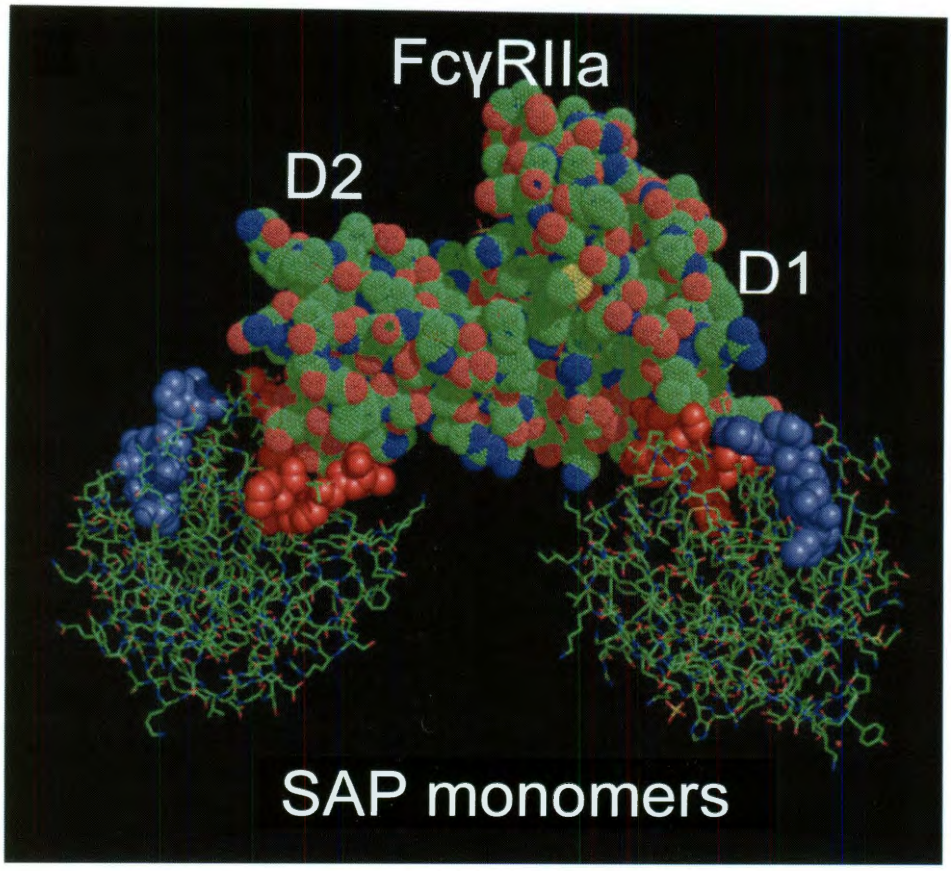

Figure 2.1: Crystal structure of SAP-FcγRIIa complex. MMDB ID: 67886 (Lu *et al.* 2008). Only the SAP monomers that come in contact with FcγR are shown. The FcγR is highlighted as multi-colored dotted spheres, the interface residues on SAP are highlighted as red spheres, and the purported IgG-like ^{234}L(F)LGGPS^{239} region is highlighted as blue spheres (initial site selected for mutagenesis).

ensures that any change in bioactivity when mutagenized is due to the alteration of a specific amino acid residue rather than a change in gross structure. Mutagenesis of the IgG like domain does not significantly alter SAP bioactivity, while mutagenesis of key residues from the SAP-FcγRIIa crystal structure only had a modest effect on SAP bioactivity. This suggests that these regions do not play a major role in the effect that SAP has on fibrocyte differentiation.

2.2 Methods

2.2.1 Construction of pTriEx vector & expression in E. coli.

The serum amyloid P (SAP) mature peptide coding region (Genbank Accenssion number 18375514) was amplified via PCR using a commercial human liver cDNA library as the template source (Agilent). The PCR primers contained restriction sites for Nco I (forward) and Xho I (reverse) for insertion into plasmids - Forward: 5'CAT GCC ATG GGC CAC ACA GAC CTC AGT GGG 3'; Reverse: 5'CCG CTC GAG GAC CCA CAC CAA GGG TTT G 3' (Invitrogen, Carlsbad, CA). A Geneamp PCR kit (Applied Biosystems) was used to amplify the cDNA, and the sequence was cloned into the pTriEx-3 Neo Vector (EMD Chemicals, Gibbstown, NJ).

The TriEx vector containing SAP cDNA was transformed into Tuner (DE3) pLacI competent cells (EMD Chemicals) and expressed following the manufacturer's protocol with a 4 hour induction time at 37° C with 0.5 mM IPTG.

2.2.2 Protein purification for pTriEx vector

Cell pellets were resuspended in 20 mM Tris, 200 mM NaCl buffer pH 8.0 with protease inhibitors (Roche), run twice through an Avestin Emulsiflex-C5 homogenizer, and the inclusion body was collected by centrifugation for 30 minutes at 20,200 x g (r. avg., Sorvall SS-34 rotor). Inclusion bodies were dissolved in 8M urea, 20 mM Tris, 200 mM NaCl, pH 8.0 and clarified by centrifugation at 125,000 x g (r. avg., Beckman 45Ti rotor) for 30 min at 4° C. The supernatant was loaded onto an AKTA FPLC and applied to a His-binding HiTrap column (Amersham). Protein was refolded slowly on the column and eluted with a linear 0 to 500 mM imidazole gradient at a rate of 1 ml/min. The eluted protein was exchanged to 20 mM sodium phosphate, pH 7.4, using a spin concentrator (Amicon). When samples needed additional purification to remove contaminants, the procedure in *2.2.6* was followed with bead purification.

2.2.3 Construction of pBad vector & expression in E. coli

The cDNA was originally cloned into a pTriEx expression vector (EMD Chemicals), but was subsequently transferred to the pBad gIIIA vector (Invitrogen). The pBad/gIIIA vector containing SAP cDNA was transformed into Top10 competent cells (Invitrogen) and expressed following the manufacturer's protocol with a 4 hour induction time at 37° C with 0.1% arabinose.

2.2.4 Protein purification for pBad vector

Cell pellets were resuspended in 20 mM sodium phosphate, 150 mM NaCl buffer pH 8.0 with protease inhibitors (Roche), run twice through an Avestin Emulsiflex-C5 homogenizer, and the homogenized pellet was mixed with a final concentration of 5% n-

lauroylsarcosine (sarcosyl) for 2 hours at room temperature. The homogenized cell mix was clarified by centrifugation at 125,000 x g (r. avg., Beckman 45Ti rotor) for 30 min at 4° C. The supernatant was loaded onto a Bio-Rad Biologic FPLC and applied to a His-binding HiTrap column (GE Lifesciences, Piscataway, NJ) at a rate of 0.2 ml/min. Protein was slowly washed overnight in a 25 mM imidazole Tris wash buffer, and eluted with a 500 mM imidazole, 50 mM Tris, pH 8, 150 mM NaCl, 5% glycerol buffer. The sample was dialyzed overnight in a Slide-a-Lyzer dialysis cassette with 10k MWCO (Pierce).

2.2.5 Construction of pcDNA3.1- vector & expression in HEK293 cells

The serum amyloid P (SAP) coding region (Genbank Accession number 18375514), including the secretion signal, was amplified via PCR using a commercial human liver cDNA library (Agilent). The cDNA was cloned into the pcDNA3.1(-) plasmid (Invitrogen) using Not I and Age I restriction sites, with an RNA export enhancer element cloned in 3' to SAP (Pacl to Eco RI). The vector with SAP was generously donated by Promedior.

The SAP-pcDNA3.1(-) vector was transfected into Freestyle 293F cells (Invitrogen) using Lipofectamine 2000 (Invitrogen) following the manufacturer's protocol. Cells were grown at 37° C with 5% CO_2 in Freestyle 293 media (Invitrogen), supplemented with 2 mM glutamine and 0.75 mg/ml Geneticin to select for the vector. After 5 days, conditioned media were collected for protein purification.

2.2.6 Protein purification from HEK293 cells

20 ml of conditioned medium from the SAP-expressing 293F cells were clarified by centrifugation at 900 x g for 10 minutes at room temperature (RT). 1 M $CaCl_2$ was added to a final concentration of 2 mM, and the conditioned medium was then mixed with 1 ml of 50% slurry of Sepharose Fast Flow (GE Healthcare BioSciences, Piscataway, NJ) for 1 hour at RT using an end-over-end mixer (in the presence of Ca^{++}, SAP binds strongly to Sepharose; Pepys *et al.*, 1977). The Sepharose beads were collected by centrifugation at 900 x g for 1 minute at RT. The beads were washed five times with 15 ml of 20 mM Tris pH 7.4/ 140 mM NaCl/ 2 mM $CaCl_2$ buffer. Bound protein was eluted overnight at 4° C with 400 µl of 20 mM Tris pH 7.4/ 140 mM NaCl/ 50 mM EDTA. The eluted protein was dialyzed in a 500 µl, 10kDa MWCO dialysis cassette (Thermo Scientific Pierce, Rockford, IL) using 1.5 L of 20 mM $NaPO_4$ pH 7.4/10% glycerol overnight at 4° C. The protein was further dialyzed in 20 mM $NaPO_4$ pH 7.4 buffer six times with a minimum 3 hour period between buffer exchanges. Protein was filter sterilized with a 0.2 µm acrodisc syringe filter (Millipore, Billerica, MA) and concentration was checked via Western blot as previously described (Pilling *et al.*, 2003; Pilling *et al.*, 2007) with the exception that samples were run on 4-15% Tris-Glycine gels (Bio-Rad, Hercules, CA) and the detection antibody was a 1:20,000 dilution of rabbit anti-SAP polyclonal antibody (Epitomics, Burlingame, CA). The purity of the SAP was also checked by Coomassie or silver stain.

2.2.7 Construction of pMT/BiP/V5-His vector, expression, and purification of SAP

The SAP cDNA was originally cloned into a pTriEx expression vector (Novagen), but was subsequently transferred to the pMT/BIP/V5-His vector (Invitrogen). The pMT/BIP/V5-His vector containing SAP cDNA was cotransfected with pCoHygro vector (Invitrogen) into S2 cells with calcium phosphate and selected for with hygromycin in Schneider's Drosophila medium (Invitrogen) with 10% FBS. Cells were grown at 23° C in air. Before induction, the medium was changed to serum free medium, and SAP expression was induced with 500 μM copper sulfate. SAP was purified from the media as per *2.2.6*.

2.2.8 Generation of SAP mutants

Using the SAP-pTriEx, SAP-pBad, and SAP-pcDNA3.1(-) vectors as templates, the primers in Table 2.2 were used to generate point mutations in the SAP sequence. The PCR reaction and transformation was carried out using a QuikChange II Site-Directed Mutagenesis Kit (Stratagene, La Jolla, CA), following the manufacturer's protocol. The resulting plasmids were sequenced to confirm the point mutations and absence of other mutations. Transfection and expression were then carried out as described above.

2.2.9 Circular dichroism

Samples were prepared by placing the protein in 20 mM sodium phosphate, 150 mM NaCl buffer at a volume of 400 μl and a concentration of at least 2 μM (250 μg/ml). 400 μl of the 20 mM Na phosphate, 150 mM NaCl buffer was used as the "blank"

Table 2.2: List of primers for mutagenesis.

Mutant	Forward/Reverse Primer
R38A	5' ACCTTGTGTTTTGCAGCCTATAGTGATCTC 3' 5' GAGATCACTATAGGCTGCAAAACACAAGTT 3'
S171A	5'GAA AAT ATCCTG GCT GCCTATCAGGGTACC 3' 5' GGTACCCTGATAGGCAGCCAGGATATTTTC 3'
Y173A	5' ATCCTGTCTGCCGCTCAGGGTACCCCTCTC 3' 5' GAGAGGGGTACCCTGAGCGGCAGACAGGAT 3'
Q174A	5' CTGTCTGCCTATGCGGGTACCCCTCTC 3' 5' GAGAGGGGTACCCGCATAGGCAGACAG 3'
S171A/Y173A/Q174A[a]	5'ATCCTGGCTGCCGCTGCGGGTACCCCTCTC 3' 5' GAGAGGGGTACCCGCAGCGGCAGCCAGGAT 3'
Y173A/Q174A/T176V[b]	5' TCTGCCGCTGCGGGTGTCCCTCTCCCTGCC 3' 5' GGCAGGGAGAGGGACACCCGCAGCGGCAGA 3'
L178A	5'CAGGGTACCCCTGCCCCTGCCAATATC 3' 5' GATATTGCCAGGGGCAGGGGTACCCTG 3'
P179A	5' GGTACCCCTCTCGCTGCCAATATCCTG 3' 5' CAGGATATTGCCAGCGAGAGGGGTACC 3'
A180G	5' GGTACCCCTCTCCCTGGCAATATCCTGGAC 3' 5' GTCCAGGATATTGCCAGGGAGAGGGGTACC 3'
A180S	5' GGTACCCCTCTCCCTTCCAATATCCTGGAC 3' 5' GTCCAGGATATTGGAAGGGGAGAGGGGTACC 3'
N181A	5' CCTCTCCCTGCCGCTATCCTGGACTGG 3' 5' CCAGTCCAGGATAGCGGCAGGGAGAGG 3'
I182A	5' CTCCCTGCCAATGCCCTGGACTGGCAG 3' 5' CTGCCAGTCCAGGGCATTGGCAGGGAG 3'
I182N	5' CTCCCTGCCAATGTCCTGGACTGGCAG 3' 5' CTGCCAGTCCAGGACATTGGCAGGGAG 3'
I182V	5' CTCCCTGCCAATGTCCTGGACTGGCAG 3' 5' CTGCCAGTCCAGGACATTGGCAGGGAG 3'
I182L	5' CTCCCTGCCAATCTCCTGGACTGGCAG 3' 5' CTGCCAGTCCAGGAGATTGGCAGGGAG 3'
L183A	5' CCTGCCAATATCGCGGACTGGCAGGCTCTG 3' 5'CAGAGCCTGCCAGTCCGCGATATTGGCAGG 3'
D184A	5' GCCAATATCCTGGCCTGGCAGGCTCTG 3' 5' CAGAGCCTGCCAGGCCAGGATATTGGC 3'

[a] S171A cDNA was used as the template.
[b] Y173A cDNA was used as the template.

control. The spectra of protein samples were obtained from a CD Spectrometer model 62ADS (Aviv, Lakewood NJ), measuring a wavescan from 200 to 250 nm, every 1 nm. Each sample was measured three times.

For thermal denaturation studies, samples in sodium phosphate buffer were heated from 25 to 100° C in 1 degree increments at 220 nm with a 3 second averaging time and 1.5 minute equilibration time.

2.2.10 HEK Blue LPS detection, temperature denaturation, and proteinase-K digestion

To ensure that recombinant SAP bioactivity was not due to bacteria contamination, bacterially-expressed SAP was tested for LPS contamination using the HEK-Blue LPS detection kit (Invivogen), as per the manufacturer's protocol.

Additionally, bacterially-expressed SAP was heated at 98° C for 20 minutes. Bacterially-expressed SAP was also digested with a 1:20 ratio of Proteinase-K (Sigma-Aldrich) (5 μg/ml proteinase K per 100 μg/ml SAP) for 16 hours at 37° C. Proteinase K was deactivated by mixing the proteinase K digest with equimolar concentration of Pefabloc SC (AEBSF, Sigma Aldrich). The digest was checked by silver staining on a 4-15% SDS-PAGE gel. The heat denatured and digested SAP were tested for bioactivity using the fibrocyte differentiation assay in *2.2.13.*

2.2.11 Gel filtration

Conditioned media from SAP-expressing 293F cells was filtered with a 0.2 μ acrodisc syringe filter (Millipore) and diluted in running buffer (20 mM Tris, 140 mM NaCl, 10 mM EDTA, pH 7.4). 300 μl of sample was loaded onto a Superose 12 100/300 GL column (GE Healthcare) using an AKTA Purifier UPC-10 with a flow rate of 0.3 ml/min at 4° C. 300 μl fractions were collected and analyzed by Western blots for the presence of SAP. The apparent molecular weight of SAP was estimated by comparing the fractions to the elution profile of gel filtration standards (Bio-Rad), run in the same buffer.

2.2.12 Detection of SAP mutants by ELISA

Maxisorb 96-well plates (Thermo Scientific Nunc, Rochester, NY) were coated overnight at 4° C with anti-SAP monoclonal antibody CBL304 (Millipore) or SAP-5 (Sigma) at a 1:1000 dilution in PBS. Plates were washed 3 times with PBS/0.05% Tween-20. Plates were blocked in PBS-4% BSA for 1 hour at 37° C. Recombinant SAP and mutants were diluted to 5 μg/ml in PBS-4% BSA and incubated in the plates for 1 hour at 37° C. The presence of SAP was detected as described previously (Pilling *et al.*, 2003), using a rabbit polyclonal anti-SAP antibody (EMD Calbiochem, San Diego, CA). For bacterially-expressed SAP, the SAP and mutants were bound directly to the plate and then detected as described above.

2.2.13 Fibrocyte Differentiation Assay

Human peripheral blood was collected into heparin vacutainer tubes (#367874; BD Bioscience, Franklin Lakes, NJ) with written consent from healthy adult volunteers and with specific approval of Rice University's or Texas A&M's Institutional Review Board. Peripheral blood mononuclear cells (PBMC) were isolated by Ficoll-Paque Plus (GE Healthcare Biosciences, Piscataway, NJ), as previously described (Pilling *et al.*, 2009). PBMCs were cultured in serum-free medium (SFM) as described previously using Fibrolife basal media (LifeLine Cell Tech, Walkersville, MD) (Pilling *et al.,* 2009). 5x RPMI medium was prepared by mixing 2.5 ml of 10x RPMI (Sigma Aldrich) with 250 µl of each supplement described previously (Pilling *et al.,* 2009), 833 µl of 6% $NaHCO_3$, and 170 µl of H_2O. Recombinant SAP was added to flat-bottomed, 96-well, tissue-culture plates and diluted as follows. 0.8 µg recombinant SAP in 20 mM $NaPO_4$ pH 7.4 or an equal volume of buffer, was added to the first column of wells along with a $1/4^{th}$ volume of 5x RPMI medium. The wells were brought to 200 µl with SFM. 100 µl was removed from the first column and serially diluted with an equal volume of SFM across the plate to achieve the indicated SAP concentrations. 100 µl of PBMCs at $5x10^5$ cells/ml in SFM was then added to each well. After a 5 day incubation period, the plate was air dried, fixed with methanol, and stained with Hema 3 stain (Fisher Scientific, Hampton, NH). For each well, fibrocytes were counted in five different 900 µm diameter fields, with fibrocytes defined as adherent, elongated spindle-shaped cells with oval nuclei (Pilling *et al.,* 2003 and 2006; Shao *et al.*, 2008).

2.3 Results

2.3.1 Bacterially-expressed SAP is bioactive.

To perform mutagenesis to determine SAP's functional domains, I first needed to express recombinant SAP that was bioactive and retained its native structure. I initially expressed SAP in the pTriEx vector in *E.coli* and human CHO cells, experiencing low yields, especially in the mammalian system. For the *E.coli* expressed SAP, all of the protein was in the inclusion body, which required urea denaturation to extract the protein, followed by dialysis and refolding (Figure 2.2A). I was able to obtain approximately 50 μg protein from a 500 ml culture of LB broth. However, to avoid refolding from the inclusion body, I also tried expressing SAP in the baculovirus system, which failed. Finally, I expressed SAP in the pBAD vector in *E.coli* and was able to extract the protein using Sarkosyl detergent in 2-3 times larger yields than the TriEx vector without having to refold the protein from the inclusion bodies (Figure 2.2B).

TriEx and pBad expressed SAP significantly reduced the number of fibrocytes, signifying bioactivity (Figure 2.3), and had IC50s that were statistically indistinguishable from native SAP (Table 2.4). Additionally, mock expression of both vectors were carried out, purified, and tested for bioactivity. Neither mock expression showed bioactivity (Figure 2.3 and data not shown).

2.3.2 The observed bioactivity of bacterially-expressed SAP is due to expressed protein rather than bacteria components or detergent.

Bacterial components such as lipoteichoic acid (LTA) inhibit fibrocyte differentiation, so one worry is that any observed effect of the bacterially-expressed SAP

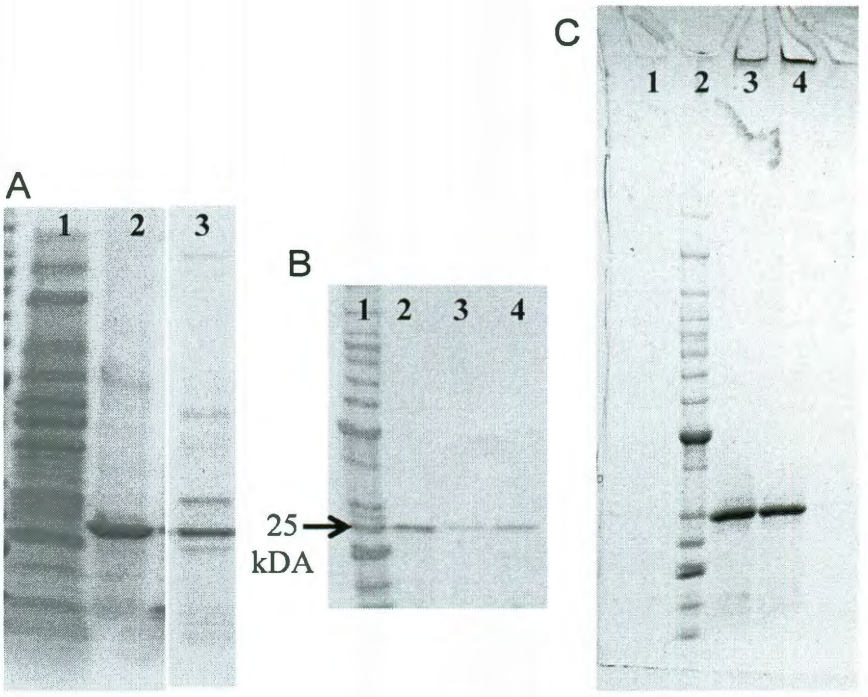

Figure 2.2: Purification of SAP from pTriEx and pBAD vectors. **(A)** Purification of recombinant SAP expressed from pTriEx. Lane 1 – cell pellet, Lane 2 – urea extract from inclusion body, Lane 3 – elution off His beads. **(B)** Purification of pTriEx expressed SAP with agarose beads. Lane 1 – M, Lane 2 – SAP after dialysis, Lane 3 – flow through off agarose beads, Lane 4 – elution off agarose beads. **(C)** Purification of recombinant SAP expressed from pBAD. Lane 1 – blank, Lane 2 – M, Lane 3 – final elution off nickel column (his tag), Lane 4 – final SAP after dialysis in phosphate buffer + 150 mM NaCl.

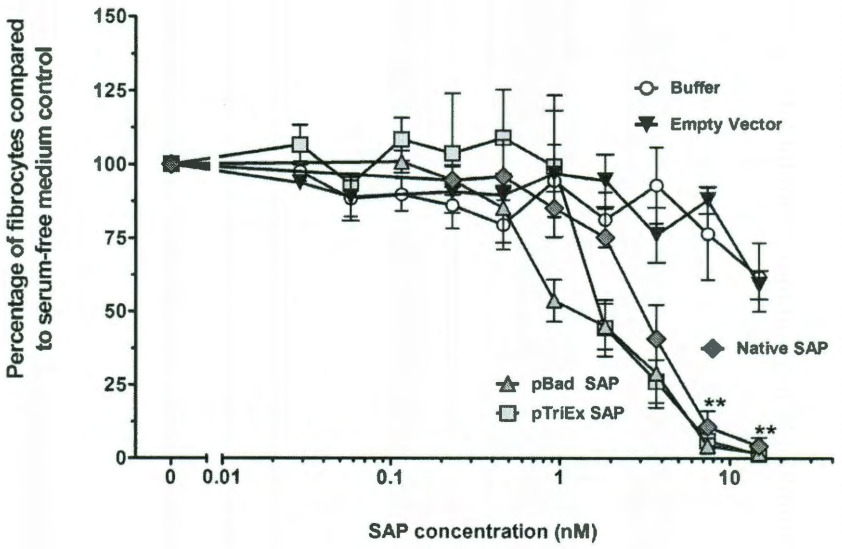

Figure 2.3: Recombinant SAP from pTriEx and pBAD vectors have bioactivity similar to native SAP. PBMCs at $2x10^5$ cells/ml were cultured for 5 days in the presence of SAP or an equal volume of serum-free medium/buffer. Results are normalized to the number of fibrocytes per 2.5×10^5 cells/ml in serum-free medium only wells, and the results are expressed as the mean percentage ± SEM. Recombinant SAP expressed from pTriEx (n=3) and pBAD (n=5) vectors were compared to native SAP (n=4), buffer only, and eluent from a mock purification of empty TriEx vector (n=3). Recombinant SAP significantly reduced the number of fibrocytes compared to buffer controls as, determined by Student's t-test. **, $p < 0.01$

was due to contamination (Maharjan *et. al,* 2010). I initially checked for lipopolysaccharide (LPS) contamination with the HEK-Blue LPS detection kit (Invivogen), and there was no contamination in recombinant SAP or the mutants. Although LPS does not inhibit fibrocyte differentiation, LPS contamination would be a general indicator of other bacterial component contamination (Maharjan *et al.*, 2010).

A common method to inactivate proteins and test contamination is through heat denaturation. Recombinant SAP was heated at 98° C for 20 minutes, but the sample still retained full bioactivity (Figure 2.4A). To determine if the result was due to contamination or due to the thermastability of SAP, I performed thermal denaturation studies using circular dichroism. The secondary structure of SAP was not significantly altered when heated from 25 to 100° C, indicating that SAP is a very stable protein (Figure 2.4B), while the closely related pentraxin CRP was fully denatured by 80° C Figure 2.4C). Because SAP is not readily denatured at 98° C like most proteins, the bioactivity observed in 2.4A could still be from recombinant SAP instead of a non-protein contaminant.

As an alternative approach to check for bacterial contamination, recombinant protein can be digested by proteolysis and measured for bioactivity. However, SAP is known to be highly resistant to proteolysis (Kinoshita *et al.*, 1992), so I selected a potent serine protease, proteinase K, that has broad selectivity (Elbeling et al., 1974) and tested

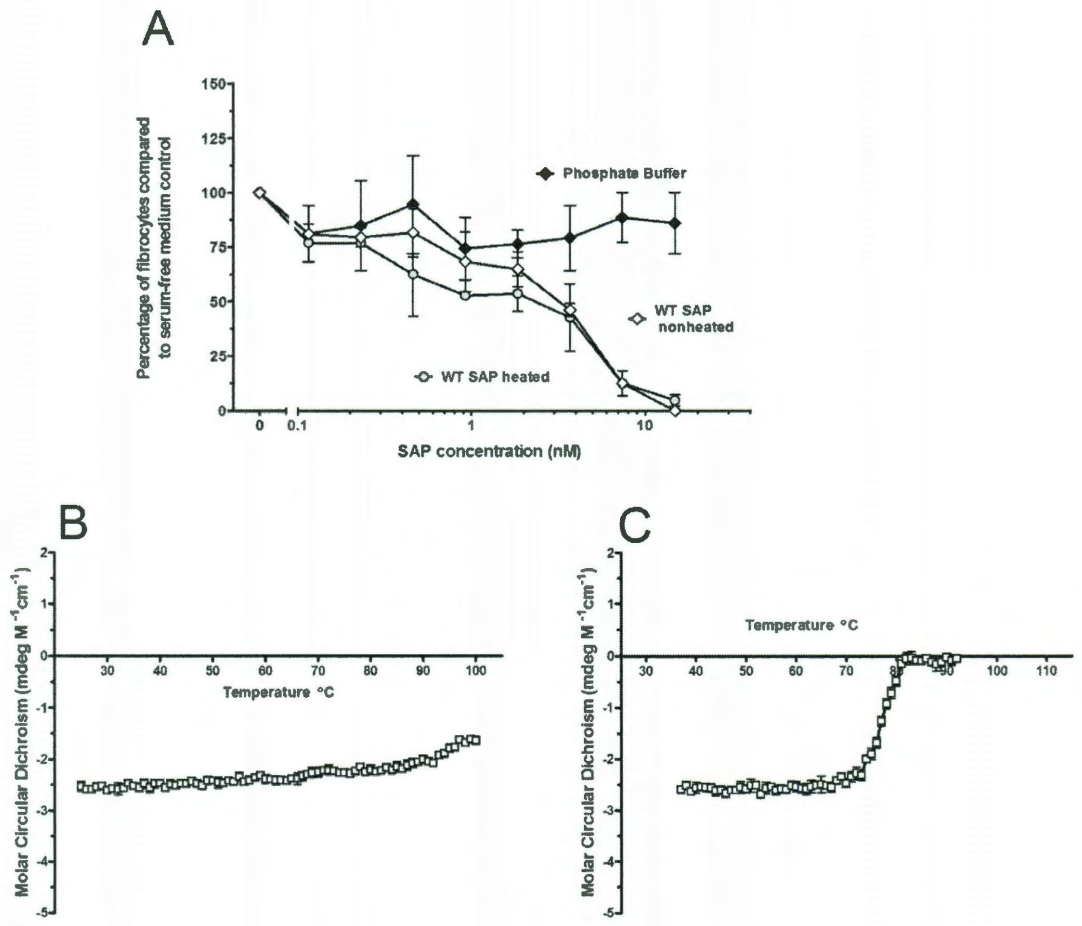

Figure 2.4: Bacterially-expressed SAP retains bioactivity after being heated to 98° C and is thermally stable as determined by circular dichroism. **(A)** Bacterially-expressed SAP was heated at 98° C for 20 minutes. PBMCs at $2x10^5$ cells/ml were cultured for 5 days in the presence of SAP, heat denatured SAP, or an equal volume of serum-free medium/buffer. Results are normalized to the number of fibrocytes per 2.5 x 10^5 cells/ml in serum-free medium only wells, and the results are expressed as the mean percentage ± SEM (n=2). Heat denatured SAP did not lose bioactivity. **(B and C)** The thermal stability of SAP and the closely related pentraxin CRP were measured by circular dichroism at 220 nm while heating the sample from 25 to 100° C in 1 degree increments. SAP does not readily denature even when reaching 98° C, while CRP readily denatures by 75 ° C.

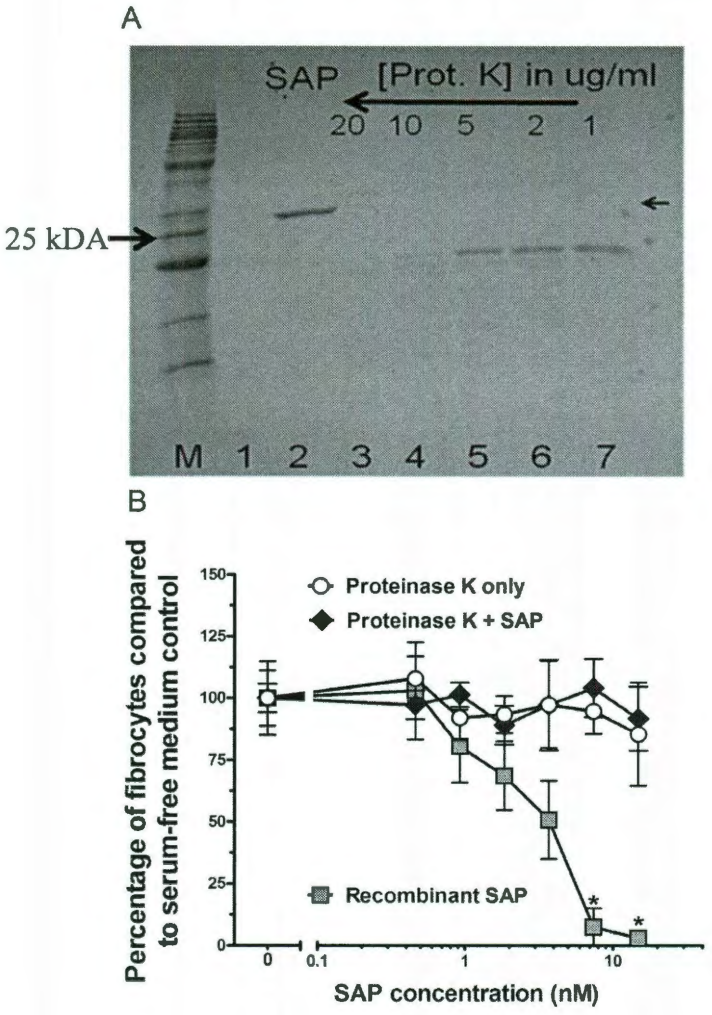

Figure 2.5: Proteinase K fully digests SAP in a 1:20 ratio, and digested recombinant SAP has no bioactivity. **(A)** Proteinase K was added to 100 μg/ml native SAP and incubated overnight at 37° C. Digestion of SAP was checked via Coomassie. M - MW marker, lane 1 – empty, lane 2 – SAP control 100 μg/ml, lane 3 – SAP + 20 μg/ml proteinase K, lane 4 – SAP + 10 μg/ml proteinase K, lane 5 – SAP + 5 μg/ml proteinase K, lane 6 - SAP + 2 μg/ml proteinase K, lane 1 - SAP + 1 μg/ml proteinase K. Arrow indicates very light band in lanes 6 and 7 at this location, indicating low levels of native SAP still present that is undigested. **(B)** 100 μg/ml of recombinant WT SAP was mixed with 5 μg/ml of proteinase K and incubated overnight. AEBSF proteinase K inhibitor was added in equimolar amounts to the SAP digest and buffer control containing proteinase K. PBMCs at $2x10^5$ cells/ml were cultured for 5 days in the presence of

recombinant SAP, proteinase K-digested SAP, or inactivated proteinase K in buffer control. Results are normalized to the number of fibrocytes per 2.5 x 10^5 cells/ml in serum-free medium only wells, and the results are expressed as the mean percentage ± SEM (n=2). The proteinase K digested SAP had significantly less bioactivity compared to recombinant WT SAP, as determined by Student's t test. *, $p < 0.05$.

for digestion at various protease:SAP ratios (Figure 2.5A). I found that to fully digest SAP, it requires a 1:20 ratio. Recombinant SAP was digested with proteinase K, checked for complete digestion with a silver stain (data not shown), and then the proteinase K was inactivated with AEBSF. As a control, buffer with proteinase K was also inactivated with AEBSF. The digest was cultured along with the deactivated proteinase K control with PBMCs to measure fibrocyte inhibition. The proteinase K-digested recombinant SAP had no bioactivity, while recombinant SAP significantly inhibited fibrocyte differentiation, as determined by Student's t test (Figure 2.5B). The lack of activity by the proteinase K digest indicates that the observed bioactivity was due to the presence of a protein. Because the recombinant SAP sample did not show additional protein contaminants when stained via Coomassie and the fact that a mock purification of empty vector did not inhibit fibrocyte differentiation (Figure 2.3), this suggests that the observed bioactivity is due to recombinant SAP.

One additional source of contamination was the use of lauroylsarcosine sodium salt (sarcosyl) to purify recombinant SAP from the bacteria cell pellet. This method resulted in higher yield and did not require isolating and refolding protein from the inclusion body using 8M urea. However, if sarcosyl is not fully removed by dialysis, low levels of detergent could remain in the samples and alter the bioactivity. Therefore, the bioactivity of SAP purified using 8M urea was compared to that of SAP purified using sarcosyl (Figure 2.6). Both recombinant SAPs were bioactive, as they significantly reduced the number of fibrocytes found in culture compared to buffer-only controls. As there was little difference in the bioactivity between recombinant SAP purified with urea

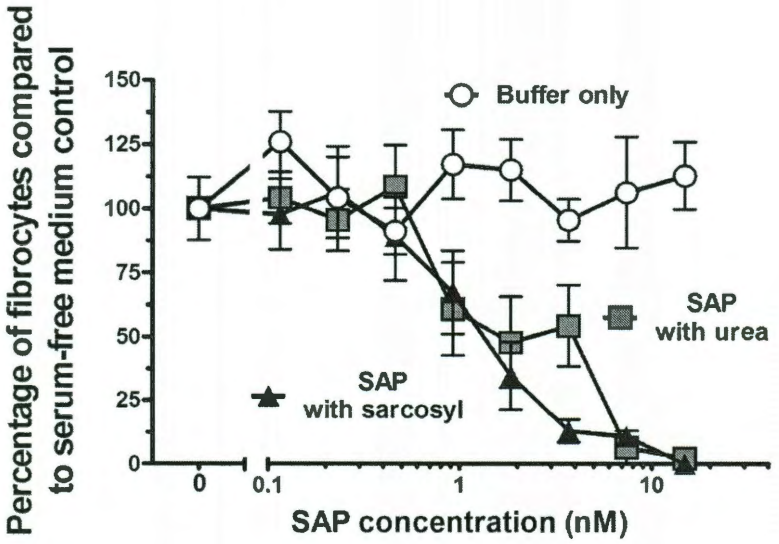

Figure 2.6: Purifying recombinant SAP with sarcosyl does not affect bioactivity. PBMCs at $2x10^5$ cells/ml were cultured for 5 days in the presence of SAP or an equal volume of buffer. Results are expressed as number of fibrocytes per $2x10^5$ cells/ml. Recombinant WT SAP using the pBad expression system was purified from inclusion bodies with urea, followed by protein refolding during dialysis. Recombinant SAP was also purified by solubilizing the cell pellet with sarcosyl. Purifying the protein with sarcosyl had no significant difference in its bioactivity compare to SAP purified with urea, as determined by Student's t-test.

and sarcosyl, the sarcosyl either had no affect on fibrocyte differentiation or was fully removed by dialysis. Therefore, the purification method could continue to be utilized.

2.3.3 Bacterially-expressed SAP and mutants have secondary structure similar to native SAP, but appear to mostly be aggregates in solution.

To elucidate the functional domains of SAP, I mutagenized a region of SAP that bears resemblance to the region of IgG which comes in contact with the FcγR, the purported SAP receptor. IgG residues ^{327}ALPAPI^{333} have similarity to SAP region 178-182 (Table 2.1). To ensure that any observed changes in bioactivity of SAP mutants are due to the change in the amino acid residue rather than a gross change in structure, I measured the physical characteristics of the recombinant SAP and mutants by circular dichroism, native antibody binding, and size exclusion chromatography. I initially tried analytical ultracentrifugation and size exclusion chromatography to determine protein size to see if the recombinant SAP was a pentamer at 135 kDa rather than 25 kDa monomers or some sort of aggregate. However, the initial runs failed to either show recombinant protein or give measurable data. I later rectified the problem with size exclusion chromatography through the use of a Tris-EDTA buffer on a fresh Superose-12 column. Before that breakthrough, I relied on CD to determine if the recombinant SAP had similar secondary structure as native SAP. Native and recombinant SAP had very similar circular dichroism spectra, while the mutants such as SAP I182A showed slightly more disorder while retaining similar alpha helix and beta sheet structure (Table 2.3). These results suggest that the recombinant SAP folded properly but it does not give

Table 2.3: Comparison of 2° structure between native and recombinant SAP.

Sample	H1: α Helix	H2: Distorted α Helix	S1: β strand	S2: Distorted β strand	Turns	Unordered
Native SAP	0.28	0.19	0.12	0.15	0.13	0.13
Recomb. WT	0.27	0.19	0.11	0.15	0.13	0.15
SAP I182A	0.28	0.16	0.13	0.10	0.13	0.19

Ellipticity of bacterially-expressed SAP was compared to native SAP. Standard wavelength scans were performed with an Aviv 62A DS Circular Dichroism Spectrometer from 200 to 250 nm using a 1 mm path length (Starna 21-Q-1 quartz cuvette) with a 3 second averaging time. All measurements were taken at 25° C in 20 mM sodium phosphate buffer, pH 7.4, 150 mM NaCl. Recombinant SAP percent structure was calculated using CDPro with the CDSSTR Fit algorithm and the SMP56 (43 soluble and 13 membrane protein reference set).

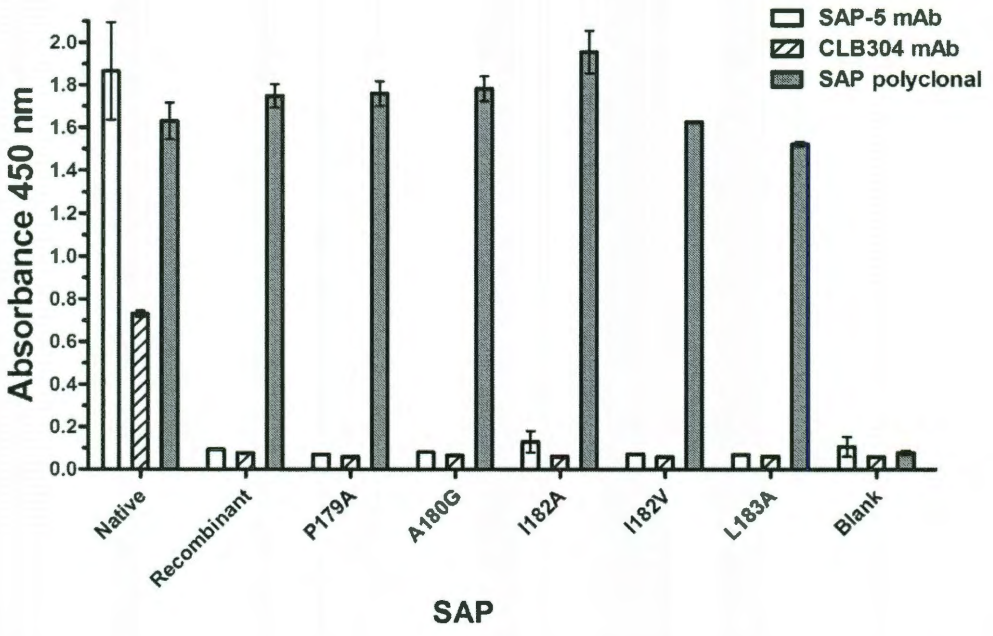

Figure 2.7: Recombinant SAP and mutants expressed in bacteria do not bind anti-SAP monoclonal antibodies that only recognize native SAP. Wells were coated with capture antibodies Sap-5 mAb (Sigma) or CBL304 mAb (Millipore). The presence of SAP bound to the capture antibodies was detected using a rabbit anti-SAP polyclonal Ab (Calbiochem). Both of the capture antibodies only bind native SAP. Alternatively, SAP was bound directly to the plate and then detected throught the use of rabbit anti-SAP polyclonal Ab (Calbiochem). Biotinylated goat anti-rabbit was used as the secondary antibody. Blank control had all the antibodies added, but no SAP was added. The plate was developed with Extravidin-conjugated peroxidase.

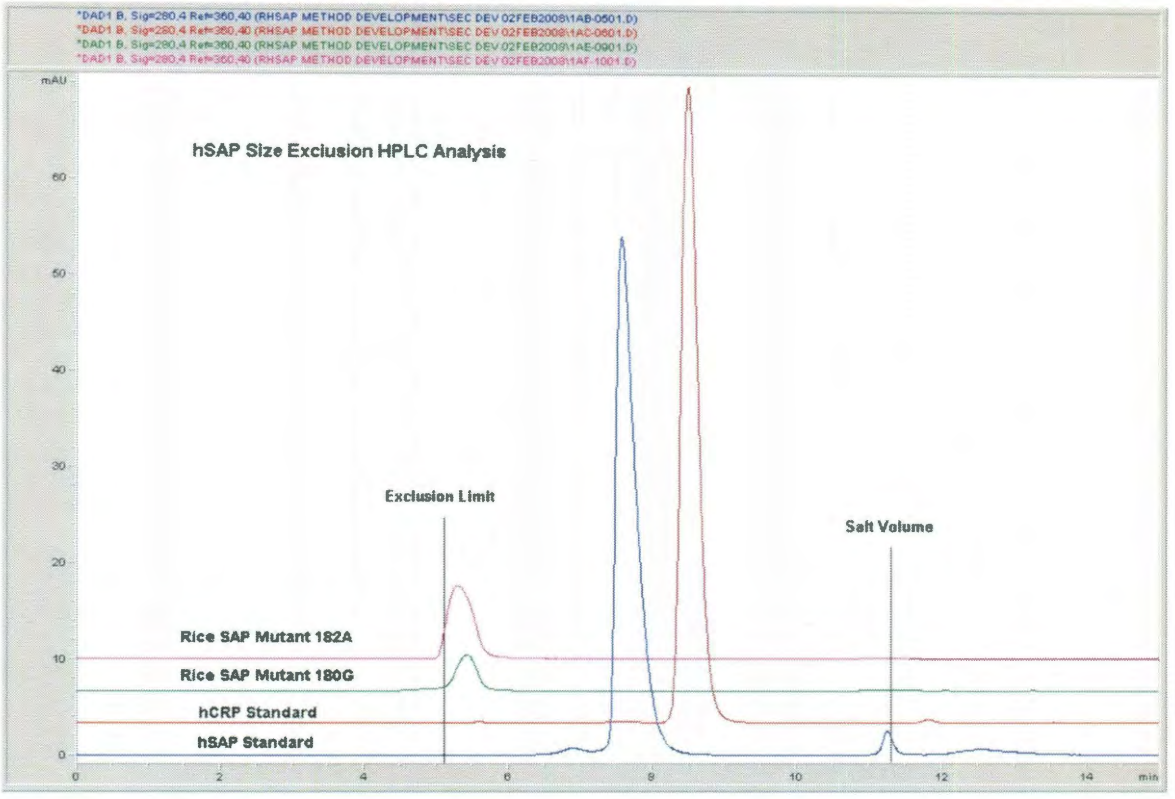

Figure 2.8: pBAD-expressed SAP mutants are predominantly aggregates in solution. Recombinant SAP was fractionated by size exclusion chromatography on a Superose 12 10/300 GL column and compared to native SAP and CRP. The two recombinant mutants ran near the void volume, suggesting a molecular weight greater than 670,000. Graph provided by Rick Caimi of Promedior.

information about whether the SAP was pentameric. Since the protein was not grossly misfolded, I bioassayed the mutant SAPs, further discussed in section *2.3.4.*

I further characterized the bacterially expressed SAP through the use of monoclonal antibodies that bind only native protein, as per the manufacturer's instructions, SAP-5 mAb (Sigma Aldrich) and CBL304 mAb (Millipore). Wells of an ELISA plate were coated with recombinant SAP and mutants, the plate was blocked, and the presence of SAP was detected with the monoclonal antibodies or a rabbit polyclonal (EMD Chemicals) that can also bind denatured SAP, as per the manufacturer's instructions. The recombinant SAP and mutants failed to bind to the monoclonal antibodies and were only detected with the rabbit polyclonal antibody (Figure 2.7). These results suggest the possibility that the recombinant protein is not in its native structure.

Finally, we successfully analyzed the bacterially-expressed mutants by size-exclusion chromatography with the assistance of Promedior (Malvern, PA). The bacterially expressed SAP mutants ran as aggregates near the void volume, suggesting a molecular weight greater than 670,000 (Figure 2.8). Therefore, any observed biological effects of the mutants could be due to SAP aggregation.

2.3.4 Bacterially-expressed SAP mutants A180G and L183A has reduced bioactivity while I182A has a proliferative effect.

After mutagenizing these residues, I found that altering residues 174, 178, and 179 had little effect on the ability of SAP to inhibit fibrocyte differentiation (Table 2.4). Residues A180G and L183A had reduced bioactivity, with A180G showing a statistically significant decrease compared to WT, as determined by ANOVA with Dunnett's test ($p < 0.05$) (Figure 2.9 and Table 2.4). Reduced bioactivity would suggest that these residues are part of SAP's functional domain. Additional mutations of these residues, including a double mutant, would need to be done to answer this question. However, the bacterially-expressed SAP mutants were found to predominantly be aggregates in solution (Figure 2.8), so this was not pursued further.

Although the recombinant mutants were mostly aggregates in solution, mutations in residue 182 gave interesting effects (Figure 2.9B and Table 2.4). Mutants I182N and I182V appeared to be more bioactive than WT SAP, although this was not a statistically significant change by one-way ANOVA. I182A actually resulted in a proliferative effect resulting in an increase in fibrocyte number above that of serum free controls. This effect was obtained when expressed from either pTriEx or pBad vector, although no such effect was observed for n=2 out of a total of n=7.

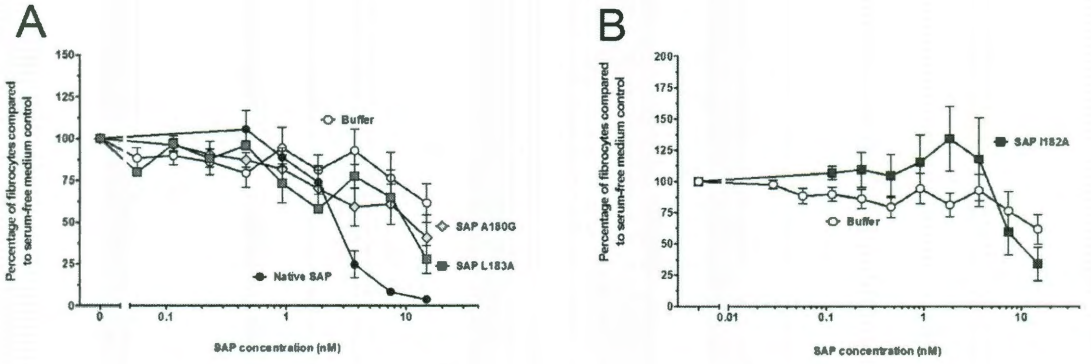

Figure 2.9: Bacterially-expressed SAP mutants have altered bioactivity in their ability to inhibit fibrocyte differentiation. PBMCs at $2x10^5$ cells/ml were cultured for 5 days in the presence of SAP or an equal volume of serum-free medium/buffer. Results are normalized to the number of fibrocytes per 2.5 x 10^5 cells/ml in serum-free medium only wells, and the results are expressed as the mean percentage ±SEM. **(A)** SAP mutants A180G (n=5, pBad and pTriEx expressed) and L183A (n=3, pBad only) were compared to buffer only control and commercial SAP. The A180G and L183A mutants did not significantly inhibit fibrocyte differentiation as determined by Student's t-test, although both mutants did retain some bioactivity. **(B)** SAP mutant I182A (n=7, pBad and pTriEx expressed) was compared to buffer control. At concentrations between 1 and 4 nM, SAP I182A increased the number of fibrocytes compared to buffer control, but this change was not statistically significant due to variance between assays.

Table 2.4: IC_{50} values for bacterially-expressed SAP mutants inhibiting fibrocyte differentiation.

Sample	IC50, nM
Native SAP	3.3 ± 0.2
Rec. SAP (pTriEX)	2.5 ± 0.6
Rec. SAP (pBad)	1.7 ± 0.5
Q174A	4.5 ± 0.5
L178A	3.0 ± 0.8
P179A	3.3 ± 0.8
A180G	14 ± 7.1*
I182A	6.5 ± 2.5
I182V	0.9 ± 0.2
I182N	1.1 ± 0.3
L183A	8.1 ± 3.1

IC_{50} was calculated as the concentration at which the inhibitor, SAP, reduces fibrocyte number by half. Bacterially-expressed (rec.) SAP and mutants had similar IC_{50} as native SAP. IC_{50} levels were obtained by fitting a sigmoidal dose response curve with normalized response and variable slope, using normalized fibrocyte levels compared to serum-free controls (n=3 except n=5 for native SAP and A180G, n=4 for pBad SAP and SAP P179A). For I182A, four sets of data failed to converge so they were excluded. IC_{50} values were compared to native SAP and recombinant SAP for significance using ANOVA with Dunnett's post-test. *, $p < 0.05$.

2.3.5 Human cell culture expressed SAP is pentameric and bioactive.

I initially utilized bacterially-expressed SAP because I was not able to express SAP in human cell culture using the pTriEx vector in CHO cells. However, the bacterially-expressed SAP was not an appropriate choice for mutagenesis because any observed changes in SAP bioactivity could be due to the fact that the recombinant SAP formed aggregates instead of a native pentamer structure. Therefore, I looked to alternative expression systems with a focus on human cell lines, as native SAP is glycosylated and has a native secretion signal that could be utilized by mammalian cells. I was able to express SAP using the pcDNA3.1(-) vector in HEK293 human cell culture. As the coding region contained SAP's native secretion signal, the SAP was secreted into the media and readily purified by binding to Sepharose beads. The resulting SAP was highly pure (Figure 2.10A) with yields between 5-40 μg from 10 ml of conditioned media. To try to increase the yield, I expressed SAP in different cell lines using the same procedure as the HEK293 system. I tried K562, HL-60, THP-1, U937, CHO K1, and NSO cells. SAP expression was only observed in HEK293 and CHO K1 cells, and the expression levels in the two cell lines were not significantly different (data not shown).

To determine if the HEK293-expressed SAP was pentameric, I performed size exclusion chromatography. The recombinant SAP was predominantly in fractions 38-41 as a wide peak of approximately 135 kDa (Figure 2.10B), as determined by the peaks of molecular weight standards. The recombinant WT SAP had no apparent aggregation

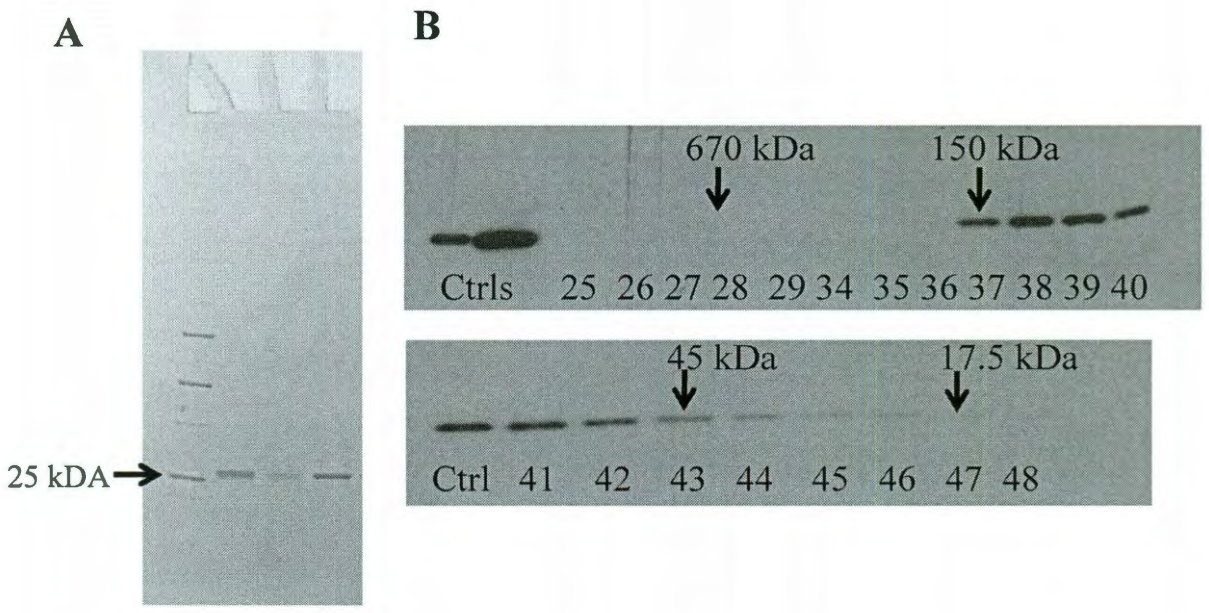

Figure 2.10: Recombinant SAP secreted from HEK293 cells can be readily purified and is predominantly a pentamer. **(A)** Purified recombinant SAP expressed from HEK293 cells. Fractions were analyzed by SDS-PAGE on a 4-15% reducing gel and stained with Coomassie. Lane 1 – marker, Lane 2 – recombinant SAP , Lane 3 – recombinant SAP mutant S171A/Y173A/Q174A, lane 4 – native SAP control. **(B)** Recombinant SAP was fractionated by size exclusion chromatography on a Superose 12 10/300 GL column. Fractions were analyzed by Western Blot using a rabbit anti-SAP primary antibody (Epitomics). The first two lanes contain native SAP controls. The remaining lanes represent 300 µl fractions collected off the column. Arrows indicate the molecular weight of known standards (Pierce) previously run on the column.

(fractions 25-29), and there was only a small amount of monomers (27 kDa, fractions 45-46). This suggests that the 293-expressed SAP was predominantly pentameric with no apparent aggregates. To further demonstrate that the recombinant SAP was folded properly, I determined by ELISA that a monoclonal antibody that can only bind native SAP was able to bind the HEK293-expressed SAP (Figure 2.11). The CBL304 (Millipore) antibody did not bind the bacterially-expressed SAP aggregates (Figure 2.7), while it was able to bind the 293-expressed SAP.

I tested for bioactivity using an *in vitro* fibrocyte differentiation assay. The HEK293-expressed SAP significantly reduced the number of fibrocytes, signifying bioactivity (Figure 2.12), and had an IC50 that was statistically indistinguishable from native SAP (Table 2.5).

2.3.6 SAP mutants expressed from human cells retain bioactivity similar to native SAP.

To elucidate the functional domains of SAP, I mutagenized two regions of SAP potentially involved in FcγR binding. For the first region, SAP region 178-182 was mutagenized similar to the bacterially-expressed SAP in section *2.3.3*, as the IgG-like region. Although the bacterially expressed SAP did not show these residues as critical, the results are suspect due to the bacterially-expressed SAP mainly being composed of aggregates. For the second region, residues were selected that were critical for SAP binding to the extracellular domain of FcγRIIa in a published crystal structure (Lu *et al.*, 2008). The crystal structure indicated that SAP residues 38, 171-176, and 200-205 are

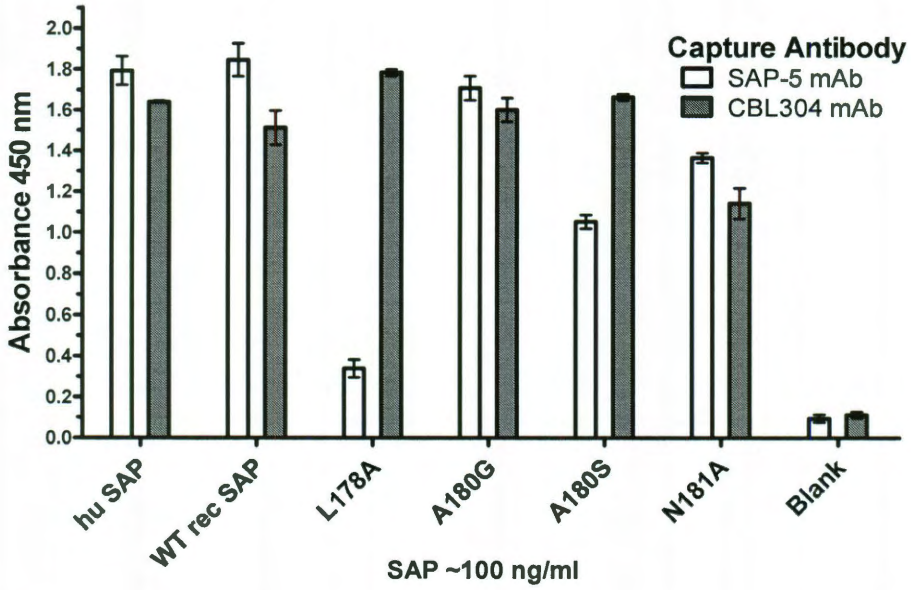

Figure 2.11: Recombinant SAP and mutants expressed by HEK293 cells can bind to anti-SAP monoclonal antibodies, that only bind native SAP. Wells were coated with a capture antibody as indicated. The presence of SAP bound to the capture antibodies, Sap-5 mAb (Sigma) or CBL304 mAb (Millipore), was detected using a rabbit anti-SAP polyclonal Ab (Calbiochem). Both of the capture antibodies only bind native SAP. Biotinylated goat anti-rabbit was used as the secondary antibody. Blank control had all the antibodies added, but no SAP was added. The plate was developed with Extravidin-conjugated peroxidase.

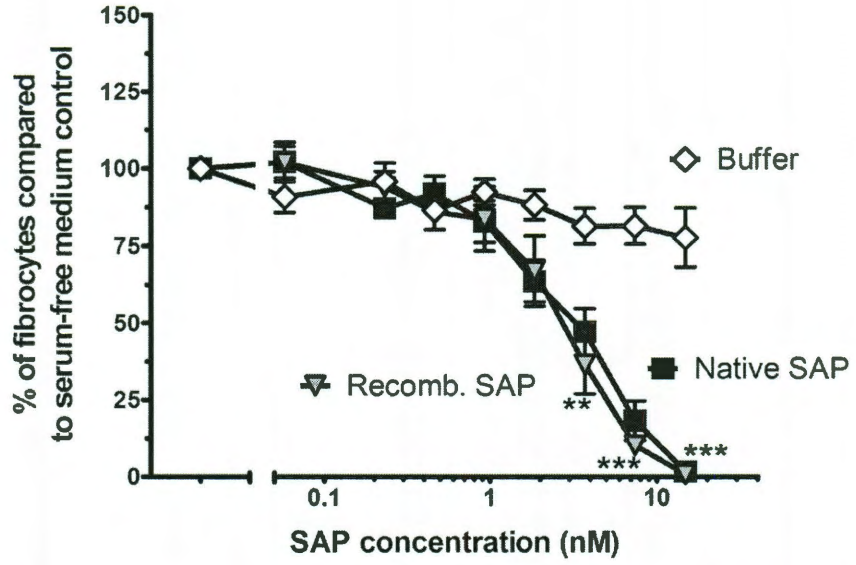

Figure 2.12: HEK293-expressed SAP inhibits fibrocyte differentiation of PBMCs. PBMCs at $2x10^5$ cells/ml were cultured for 5 days in the presence of SAP or an equal volume of buffer in serum-free medium (SFM). Results are normalized to the number of fibrocytes per 2.5×10^5 cells/ml in SFM only wells, and the results are expressed as the mean percentage ±SEM (n=3). Recombinant SAP at and above 4 nM significantly reduces fibrocyte differentiation compared to buffer only control, as determined by Student's t-test. **, $p < 0.01$; ***, $p < 0.001$.

the key contacts for SAP binding to FcγRIIa; however, residues 200-205 were not mutagenized as they are near the SAP pentamerization domain and could interfere with native structure formation. A series of single and multiple point mutations were made in these two regions of SAP and the mutagenized protein was subsequently expressed by HEK293 cells, except for SAP I182A which was not secreted into the media. Instead, SAP I182A was expressed in S2 cells, as well as WT SAP as a control. Size exclusion chromatography performed as described in Figure 2.10 indicated that all the resulting SAP variants were pentameric and could bind the native antibody CBL304. However, ~10% of SAP I182A was determined to be aggregates, while still predominantly pentameric.

Altering residues in the two selected regions of SAP had a modest effect at best on the ability of SAP to inhibit fibrocyte differentiation (Table 2.5). Mutagenizing residues in the IgG-like region did not significantly alter SAP bioactivity (Table 2.5 and data not shown), while a slight reduction in bioactivity was observed for the residues implicated in the SAP-FcγRIIa crystal structure (Figure 2.13). Altering residue 171 did not significantly reduce SAP bioactivity due to assay variability (Figure 2.13A). Altering residues 173 and 174 and removing the hydrogen bonding potential from residues 173, 174, and 176 reduced SAP bioactivity (Figure 2.13B-D). Focusing only on mutants derived from the SAP-FcγRIIa crystal structure, no significant differences were observed compared to native SAP (Figure 2.13E) unless the highly variable results of mutant S171A were excluded from the analysis. Excluding the S171A data, mutants Y173A and Q174A showed a significant increase in IC50 compared to native hSAP, suggesting that

Table 2.5: IC_{50} values for HEK293-expressed SAP mutants inhibiting fibrocyte differentiation.

Sample	IC_{50}, nM
Native SAP	2.9 ± 0.3
Rec. SAP	2.6 ± 0.7
S2 SAP	2.9 ± 0.6
R38A	2.7 ± 0.1
S171A	6.8 ± 4.3
Y173A	5.9 ± 1.4
Q174A	5.6 ± 0.6
S171A/Y173A/Q174A	3.5 ± 0.5
Y173F/Q174L/T176V	5.0 ± 0.4
L178A	4.1 ± 0.5
P179A	3.5 ± 0.5
A180G	4.3 ± 0.4
A180S	2.2 ± 0.3
N181A	2.7 ± 0.3
I182A	3.7 ± 0.5
D184A	3.5 ± 0.4

IC_{50} was calculated as the concentration at which the inhibitor, SAP, reduces fibrocyte number by half. No significant change in IC_{50} was observed for HEK293-expressed (rec.) SAP, S2-expressed SAP, or SAP mutants compared to native SAP (1-way ANOVA, Dunnett's test). IC_{50} values were obtained by fitting a sigmoidal dose response curve with normalized response and variable slope, using normalized fibrocyte levels compared to serum-free controls (n=3 except n=12 for native SAP, n=5 for S171A, A180S, and N181A; n=4 for Y173A and 173/174/176).

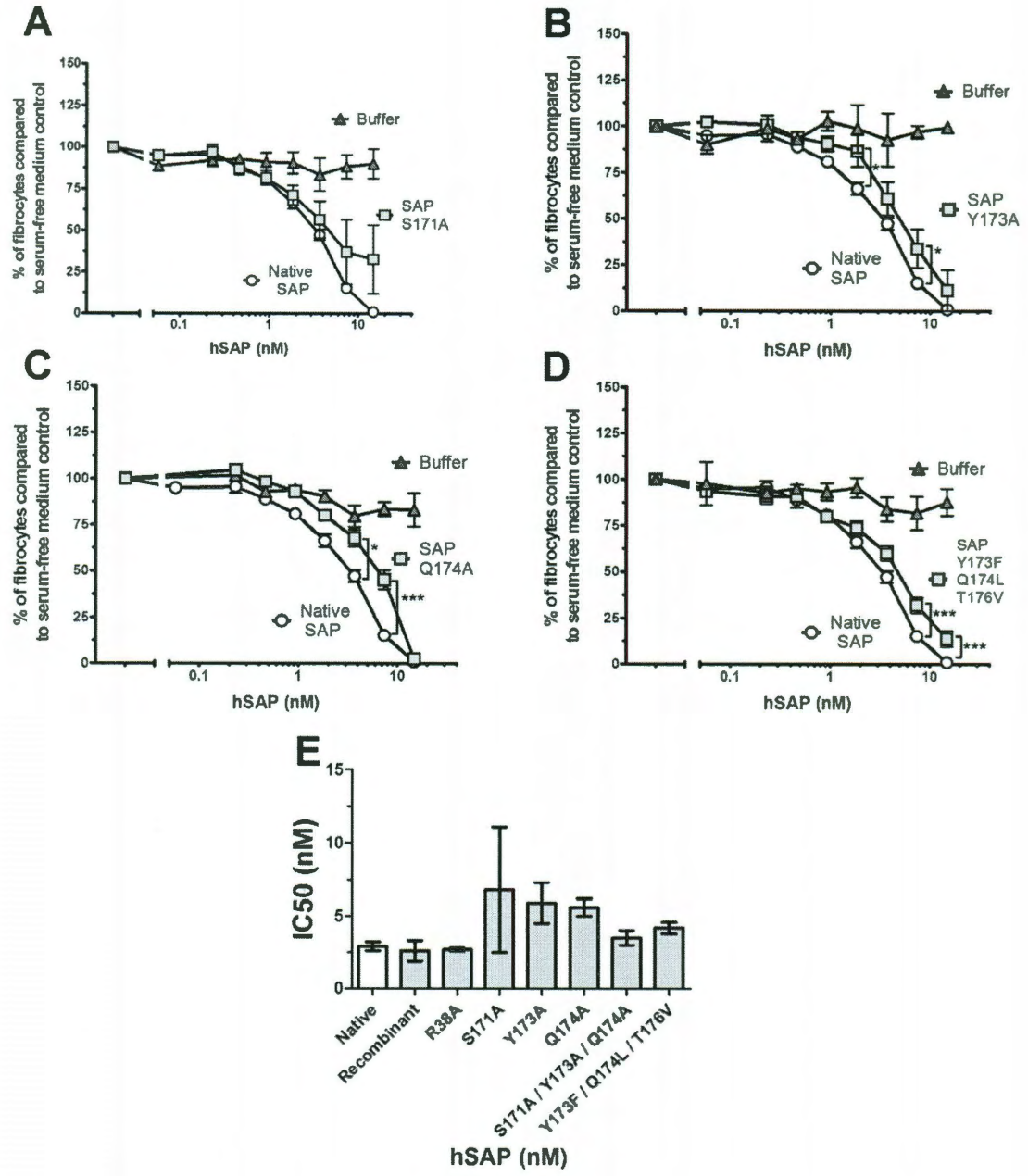

Figure 2.13: Human SAP mutants Y173A, Q174A, and Y173F/Q174L/T176V have reduced bioactivity compared to native SAP. PBMCs were cultured for 5 days in the presence of hSAP or an equal volume of serum-free medium/buffer. Results are normalized to the number of fibrocytes in serum-free medium, and the results are expressed as the mean percentage ± SEM. n=12 for native, n = 5 for S171A, n=4 for

Y173A and 173/174/176, and n=3 for Q174A. **(A)** hSAP S171A did not have significantly reduced bioactivity compared to native hSAP due to the significant variance between assays (2 assays showed reduced bioactivity, 3 assays showed a response similar to that of native SAP). **(B - D)** hSAP Y173A, Q174A, and Y173F/Q174L/T176V at 7.4 nM have significantly reduced bioactivity compared to native hSAP, as determined by t-test. *, $p < 0.05$; ***, $p < 0.001$. **(E)** IC_{50} values for SAP mutants focusing on the residues critical in the SAP-FcγRIIa crystal structure. No significant differences were observed in the IC50s between the mutants and native SAP (1-way ANOVA, Dunnett's test). If mutant S171A is excluded from the ANOVA analysis, mutants Y173A and Q174A have significantly increased IC50 values compared to native hSAP, suggesting reduced hSAP bioactivity ($p < 0.01$; 1-way ANOVA, Dunnett's test).

the mutants have reduced activity (Figure 2.13E). However, when these residues were changed to alanine in a triple 171/173/174 mutant, the bioactivity of the mutant was similar to that of native hSAP (Figure 2.13E). Additionally, the IC 50 of R38A was similar to that of hSAP (Figure 2.13E). The data suggest that hSAP residues 173 and 174 may mediate some but not all of SAP bioactivity.

2.4 Discussion

To elucidate the functional domains of SAP, residues were mutagenized that were believed to be critical for SAP signaling through its receptor, FcγR. Bioactive SAP was expressed both from bacteria and human cells. Initially, human SAP was expressed in bacteria because of the extremely low yields when the recombinant protein was expressed in human cells. The bacterially-expressed SAP appeared to have folded properly as determined by circular dichroism and digestion of the protein eliminated all bioactivity, suggesting any observed effect was not due to bacterial contamination. However, the bacterially-expressed proteins were eventually found to be predominately aggregates after refining the size exclusion chromatography assay to include EDTA in the buffer. Therefore, any observed biological effect could be purely due to SAP being aggregated rather than a specific change to its primary structure. Nonetheless, aggregated proteins in general do not inhibit fibrocyte differentiation. Specifically, heat aggregated IgG, which acts through the same receptor as SAP, inhibits fibrocyte differentiation, while other heat aggregated immunoglobulins have no effect on fibrocyte differentiation (Pilling *et al.*, 2006). Additionally, the observed biological effects are not just a generic aggregation effect because different mutations gave interesting results, including I182A

promoting fibrocyte number, while A180G and L183A had reduced bioactivity. However, these results did not carry over when the same mutations were expressed in human cells, although L183A was not expressable in HEK293 or S2 cells. Finally, the bacterially-expressed SAP results should not necessarily be discounted because protein aggregation was not measured immediately, so these recombinant proteins could be pentameric when immediately assayed after purification. Additionally, the bacterially-expressed protein could be predominantly pentameric when diluted down to nM concentrations utilized in the bioassays.

Although the key functional domain of SAP was not found, I was able to successfully express recombinant SAP and mutants that retain SAP's native pentameric structure. The pentameric SAP was expressed in human HEK293 cells, which has the benefit of glycosylating the protein, as SAP has a single glycosylation site at Asn32 (Emsley et al., 1994). We were able to discern additional aspects of SAP's biology, including the fact that SAP is highly thermostable, unlike CRP which has 51% sequence identity, and that SAP requires a very high 1:20 ratio for full proteinase K digestion. Additionally, two specific regions were eliminated for future studies in determining SAP's functional domain. Altering the sequence with similarity to IgG ^{327}ALPAPI^{333} had no significant effect on SAP bioactivity when the mutants were expressed by human HEK293 cells. Altering residues critical for SAP binding to FcγRIIa in the Lu *et al.* (2008)'s crystal structure only had a very modest effect on SAP bioactivity. Residues 173 and 174 may mediate some but not all of SAP bioactivity and do not appear to be a critical part of SAP's functional domain.

A possible explanation regarding the lack of success with mutagenizing the ridge helix region (Pro 166 to Gln 174) suggested by the Lu *et al.* (2008) crystal structure, is that the crystal structure may not be biologically relevant. The Lu paper states that SAP was dissociated into monomers and then crystallized, whereas biologically relevant SAP is pentameric. The crystal structure published at NCBI (MMDB ID: 67886) only shows 4 out of 5 SAP monomers on the same plane as a partial pentamer.

Even if the crystal structure is biologically relevant, SAP could act through a different receptor or predominantly through a different FcγR subtype. While FcγRIIa and III have similar structure, FcγRI contains an additional immunoglobulin D3 domain that accounts for its high affinity to IgG (Hullet *et al.*, 1998) and could potentially interact with SAP. For instance, the closely related pentraxin CRP was mutagenized at residues critical for FcγRIIa binding, which disrupted the binding of CRP to FcγRIIa and III but not to FcγRI, which contains the additional D3 domain (Lu *et al.*, 2008).

Finally, because SAP is part of the pentraxin family that is highly conserved across species and the closely related CRP does not inhibit fibrocyte differentiation, for any future mutagenesis we will be looking towards residues on the surface of SAP that are conserved in humans, mice, and rats (human, mouse, and rat SAP's inhibit fibrocyte differentiation) and are different than the residues found in CRP (Baltz *et al.*, 1982; Pilling *et al.*, 2003).

Chapter 3: Potential characterization of SAP's functional domain through SAP peptides and receptor binding

3.1 Introduction

In addition to mutagenesis of residues, we can also determine the active domain of SAP by producing peptides containing the critical regions of SAP. The peptide could not only tell us which residues are sufficient for SAP bioactivity but also have potential as a therapeutic since peptides are preferred over whole protein for their cheaper cost and are easier to manipulate. The two regions we selected for mutagenesis in Chapter 2 are also the regions we focused on for the peptides (Figure 3.1).

Although our initial mutagenesis study did not find any residues critical for SAP bioactivity, any future critical residues will need to be further characterized. We will need to determine if the recombinant and mutant SAP are still binding to the Fcγ receptors to fully understand any biological effects the mutants have on PBMC cultures. If the binding of SAP to FcγR is essential for bioactivity, any SAP mutants that fail to inhibit fibrocyte differentiation will likely fail to bind to the FcγRs or bind with different affinity so that the mutant no longer activates the FcγR. Also, mutants that are bioactive might be found that no longer bind to any FcγR, which would suggest that the other receptors and/or ligands are involved in regulating differentiation.

SAP has previously been found to bind to FcγRs through the use of cells expressing only specific receptors, as well as through surface plasmon resonance (SPR);

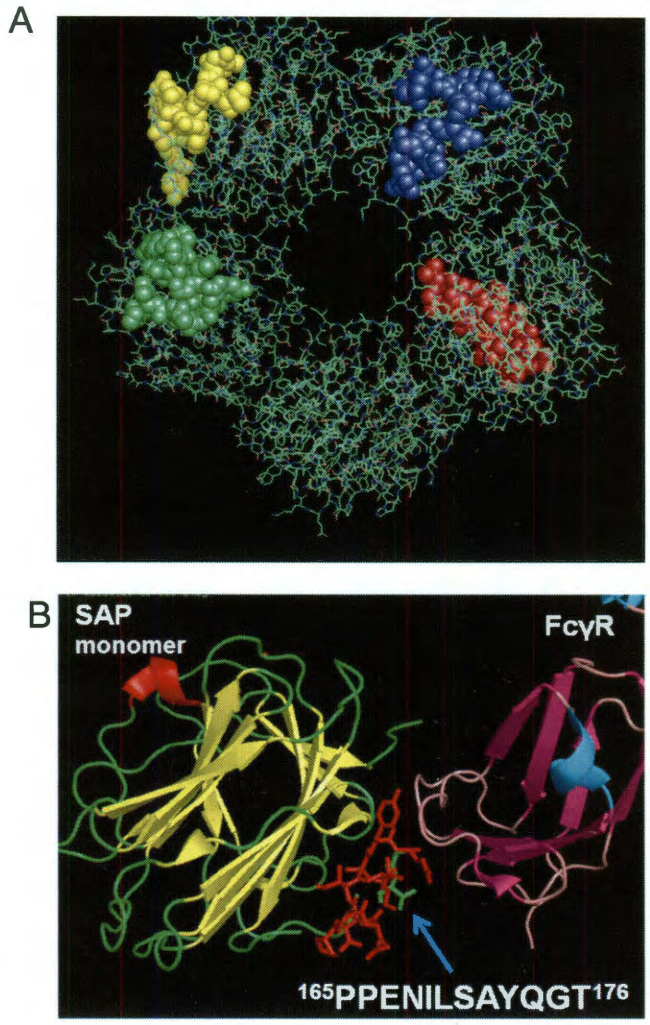

Figure 3.1: SAP peptide locations along the pentamer and Bethyl peptide position relative to the SAP-FcγRIIa complex crystal structure. **(A)** SAP was visualized with Pymol (Delano, 2002). Residues were highlighted by peptide with blue representing the peptide ^{171}SAYQGTPLPANILDWQ^{186}, yellow representing the ^{178}LPANILDWQALNYEIRGY^{195}, green representing ^{163}VLPPENILSAYQGTPLPA^{179}, and red representing ^{61}LLVYKERVGEYSLYIGRHK^{79}, which is found on the opposite face of the SAP planar disc. **(B)** The SAP monomer and FcγRIIa complex is represented as a cartoon and colored by their secondary structure (Lu *et al.*, 2008). The SAP peptide comprises residues ^{165}PPENILSAYQGT^{176} and its location within a SAP monomer is represented as stick figures. The peptide is at the interface of the SAP-FcγRIIa complex.

however, significantly different affinities were reported (Lu *et al.*, 2008; Castano *et al.*, 2009). To evaluate SAP mutants, we need a quick, efficient, and relatively inexpensive method to test the binding of our mutants to the receptor. The most successful method for SAP receptor binding was surface plasma resonance (SPR), but that process is expensive due to the Biacore machine and due to the fact that you need a significant amount of protein. Additionally, to get SPR to work, Castano *et al.* (2009) had to bind SAP in the presence of calcium to a dextran ligand present on a Biacore CM5 chip. In a typical SPR run, you bind the receptor to the chip and have the ligand flow over the chip. Having to bind SAP to the chip would make it very inconvenient and costly to analyze multiple mutants. Therefore, we focused on binding SAP through ELISAs using the recombinant extracellular domain of FcγR.

In this chapter, I show that peptides based off areas we mutagenized do not have bioactivity except at 500x molar excess, which makes it irrelevant as a potential therapeutic and suspect as biologically relevant. I also show that receptor binding ELISAs do not require having SAP bound to a ligand like dextran, suggesting that Ca^{++} dependent ligand binding is not necessary for FcγR engadgment. Additionally, IgG is found to be a poor competitor to use against SAP in a competitive ELISA assay, suggesting that IgG and SAP bind to different locations on the FcγRs. Finally, I show that the optimum binding conditions for SAP occurs when the receptor is not bound directly to an ELISA plate, suggesting that proper orientation is critical for efficient SAP binding in an ELISA receptor assay.

3.2 Methods

3.2.1 SAP f(ab')$_2$ antibody preparation.

A SAP polyclonal antibody was made by Bethyl Laboratories in a goat against the human SAP peptide ^{165}PPENILSAYQGT^{176}. The nonspecific Fc portion of the antibody was removed via papain digestion using a Fab preparation kit (Pierce), as per manufacturer's instructions. The digestion was checked via Western blot and compared to goat Fab (Abcam), the full length SAP antibody, and full length goat IgG (Jackson Immunoresearch) as controls. Fab fragments and full-length antibodies were detected using a biotinylated donkey anti-goat F(ab')$_2$ (Jackson ImmunoResearch), along with Extravidin-HRP (Sigma Aldrich).

3.2.2 SAP Fab antibody fibrocyte differentiation assay.

PBMCs were prepared and cultured as described in *2.2.13*. The SAP Fab antibody and goat Fab control antibody (Abcam) were mixed at 40 and 10 nM with 7.7 nM (1 μg/ml) SAP (EMD Chemicals) or buffer control in a final 200 μl volume with 2.5 x 10^5 cells/ml PBMCs. Additionally, serum-free only wells and SAP only wells at 7.7 nM were plated with the same concentration of PBMCs. After 5 days, cells were fixed and stained as previously described (Pilling *et al.*, 2003).

3.2.3 Biotinylation of peptide and SAP

The ^{165}PPENILSAYQGT^{176} peptide was biotinylated using NHS-PEG$_4$-Biotin (Thermo Scientific), following the manufacturer's protocol. The biotinylated peptide was purified via size exclusion gravity chromatography with Sephadex G15 (GE Healthcare) column bedding at room temperature. Fractions were collected via gravity

in 300 µl fractions, and peptide concentration was measured via Bradford protein assay. Biotinylation of fractions was confirmed by ELISA. The fractions were incubated overnight in a Maxisorb 96-well plates (Thermo Scientific Nunc), blocked with TBS-4% BSA for 1 hour, and washed 3 x in TBS-0.05% Tween 20. Biotinylated peptide was detected using Extravidin Peroxidase (Sigma-Aldrich). Undiluted peroxidase substrate 3,3,5,5-tetramethylbenizidine (Sigma-Aldrich) was incubated for 4 minutes at room temperature before stopping the reaction with 1 N HCl, and the plate was read at 450 nm (Biotek Instruments, Winooska, VT).

SAP was biotinylated using the Pierce EZ-Link Micro Biotinylation kit (Pierce), following the manufacturer's protocol, and the degree of biotinylation was checked via depletion using neutravidin beads (Pierce). Biotinylated SAP in the presence and absence of neutravidin beads were assayed via electrophoresis on 4-15% Tris-glycine gels (Bio-Rad laboratories) and stained with Coomassie blue dye.

3.2.4 Peptide fibrocyte differentiation assay

PBMCs were prepared and cultured as described in *2.2.13*. Biotinylated peptides were generated by Biomer Technology (Pleasanton CA), or from *3.2.3* using the Bethyl peptide. The peptides were resuspended in ddH_20 or 20 mM sodium phosphate buffer, pH 7.4. Biotinylated peptides were plated in serum-free media at 10 µM, as well as doubling dilutions ranging from 1 µM to 7.8 nM. Additionally, the biotinylated peptides were conjugated with neutravidin (Pierce) at 1/4th molar concentration by mixing for 1 hour at room temperature in an end-over-end mixer before plating in serum-free media.

As a control, neutravidin was plated by itself in serum free media. Originally, the neutravidin was added at much higher concentration based on the estimated binding capability via weight, but these high concentrations were toxic to the cells. For the Bethyl ^{165}PPENILSAYQGT^{176} peptide, biotin (Sigma-Aldrich) was also added to the neutravidin + peptide, neutravidin-only, and buffer control wells at 5x molar concentrations to the neutravidin.

3.2.3 Detection of SAP binding to FcγR by ELISA

Maxisorb 96-well plates (Thermo Scientific Nunc, Rochester, NY) were coated overnight at 4° C with 2 μg/ml of the extracellular domain of recombinant Fcγ receptor (R&D Systems). Plates were washed 3 times with PBS/0.05% Tween-20. Plates were blocked in PBS-4% BSA for 1 hour at 37° C. SAP (EMD Chemicals) was diluted to 0.5-50 μg/ml in PBS-1% BSA and incubated in the plates for 1 hour at 37° C. Alternatively, SAP was pre-incubated in a 20 mM Tris, 140 mM NaCl, 2 mM $CaCl_2$ binding buffer in the presence or absence of equimolar carboxymethyl dextran (GE Healthcare) for 30 minutes, followed by incubation in the receptor-coated plates for 1 hour, 2 washes with PBS-Tween-20, and fixation with ice-cold 4% PFA-PBS. The presence of SAP was detected as described previously (Pilling *et al.*, 2003), using a mouse monoclonal anti-SAP antibody (SAP-5, Sigma Aldrich or CBL304, Millipore) or a rabbit polyclonal (Calbiochem). Bound SAP was detected using biotinylated goat $F(ab')_2$ anti-mouse IgG or goat $F(ab')_2$ anti-rabbit IgG (Southern Biotech), followed by Extravidin peroxidase (Sigma-Aldrich). Undiluted peroxidase substrate 3,3,5,5-tetramethylbenizidine (Sigma-

Aldrich) was incubated for 4 minutes at room temperature before stopping the reaction with 1 N HCl, and the plate was read at 450 nm (Biotek Instruments, Winooska, VT).

Biotinylated SAP was also tested for binding to the Fcγ receptor. The same procedure as above was followed, except the SAP that was added was biotinylated. Additionally, biotinylated human IgG (Jackson ImmunoResearch) was heated 45 minutes at 60 °C to aggregate the IgG, and the aggregated IgG was added to the wells at 50 μg/ml as a positive control. Bound IgG or SAP was detected with Extravidin peroxidase (Sigma-Aldrich).

An indirect ELISA for SAP binding was performed through competitive binding with IgG. Wells were coated with 2 μg/ml of receptor overnight. The wells were blocked with PBS-4% BSA. Human IgG (Jackson ImmunoResearch) was heated 45 minutes at 60 °C to aggregate the IgG, and the aggregated IgG was added to the wells at 50 μg/ml along with SAP at concentrations between 0.3 – 30 μg/ml in PBS-1% BSA. Bound IgG was detected with a biotinylated mouse $F(ab')_2$ anti-human IgG (Jackson Immunoresearch), followed by Extravidin peroxidase (Sigma-Aldrich).

Alternatively, rabbit anti-his (1:1000) was coated overnight on the 96 well plates, the plates were washed twice the next day and blocked with PBS-4% BSA, and the recombinant Fcγ receptors were incubated at 2 μg/ml for 1 hour. The remaining procedure was as above, except SAP was incubated in a PBS-1% BSA solution with 2

mM $CaCl_2$. Bound SAP was detected with a mouse monoclonal anti-SAP antibody (CBL304, Millipore), followed by Extravidin peroxidase (Sigma-Aldrich).

3.2.4 Detection of SAP binding to FcγR bound to Tosyl beads

Alexa-594 conjugated SAP and albumin were kindly donated by Promedior (Malvern, PA) and was prepared using an Alexa Fluor 488 kit (Invitrogen) on human SAP (EMD Chemicals) and albumin (Sigma-Aldrich), as per the manufacturer's protocol.

Dynabeads M-280 Tosylactivated (Invitrogen) were prepared as per the manufacturer's instructions binding 5 μg/ml of recombinant extracellular domain of the Fcγ receptors (R&D Systems) in a 0.1 M Na-phosphate buffer, pH 7.4. The beads were mixed overnight at 37° C, blocked the next day in phosphate buffer-0.1% BSA two times for 5 minutes, and finally blocked with 0.2 M Tris, pH 8.5 with 0.1% BSA for 4 hours at 37° C. Due to nonspecific binding by SAP, the blocking step was later changed to include washes with sodium phosphate-3% BSA and 0.5 M Tris, pH 8.5 with 1% BSA. Alexa-594 conjugated SAP or BSA were incubated with 8 μl of bead slurry per protein concentration in a 20 mM Tris, 140 mM NaCl, 2 mM $CaCl_2$, 0.1% BSA binding buffer in the presence or absence of equimolar carboxymethyl dextran (GE Healthcare) for 1 hour at 37° C. The beads were placed on a Dynal magnet (Invitrogen) and washed twice with PBS-0.5% Tween-20. The beads were resuspended in 60 μl PBS-1% BSA and 30 μl were placed in a black 96 well plate (Nunc), and the fluorophore was excited at 594 nm and read at 620 nm using a Tecan plate reader (Durham, NC) and Magellan data analysis software.

3.3 Results

3.3.1 Anti-SAP Fab that recognizes an epitope near the purported FcγR binding region blocks SAP bioactivity.

We had a goat polyclonal antibody made against SAP and the sequence selected just happens to be in the same region that SAP binds FcγRIIa in the Lu *et al.* (2008) crystal structure (Figure 3.1B). Therefore, I decided to try to block SAP bioactivity through the binding of the antibody. Since the SAP pentamer acts like a planar disc with one side binding ligands like bacteria, while the opposite side binds the FcγR (Figure 1.1A), we would expect this antibody to block SAP bioactivity if our hypothesis for SAP receptor binding holds true. First, I digested the goat polyclonal with papain to remove the Fc constant region that could nonspecifically bind to monocytes in culture and interfere with fibrocyte differentiation (Figure 3.2A). SAP bioactivity was significantly reduced in the presence of the Fab anti-SAP fragment as expected (Figure 3.2B & 3.2C). This helps confirm that SAP's active domain is on the "A" face of the planar disc (Figure 1.1A).

3.3.2 SAP peptides based around the two purported FcγR binding regions do not have significant bioactivity or block the action of SAP.

To help determine the functional domain of SAP, I tested peptides based around the purported FcγR binding regions from Chapter 2, the IgG-like domain and the FcγRIIa-SAP crystal structure (Figures 2.1 & 3.1). I initially selected 3 biotinylated peptides near the IgG-like domain and a 4^{th} peptide on the opposite face of the SAP pentamer as a negative control (Table 3.1, Figure 3.1A). The peptides weren't bioactive,

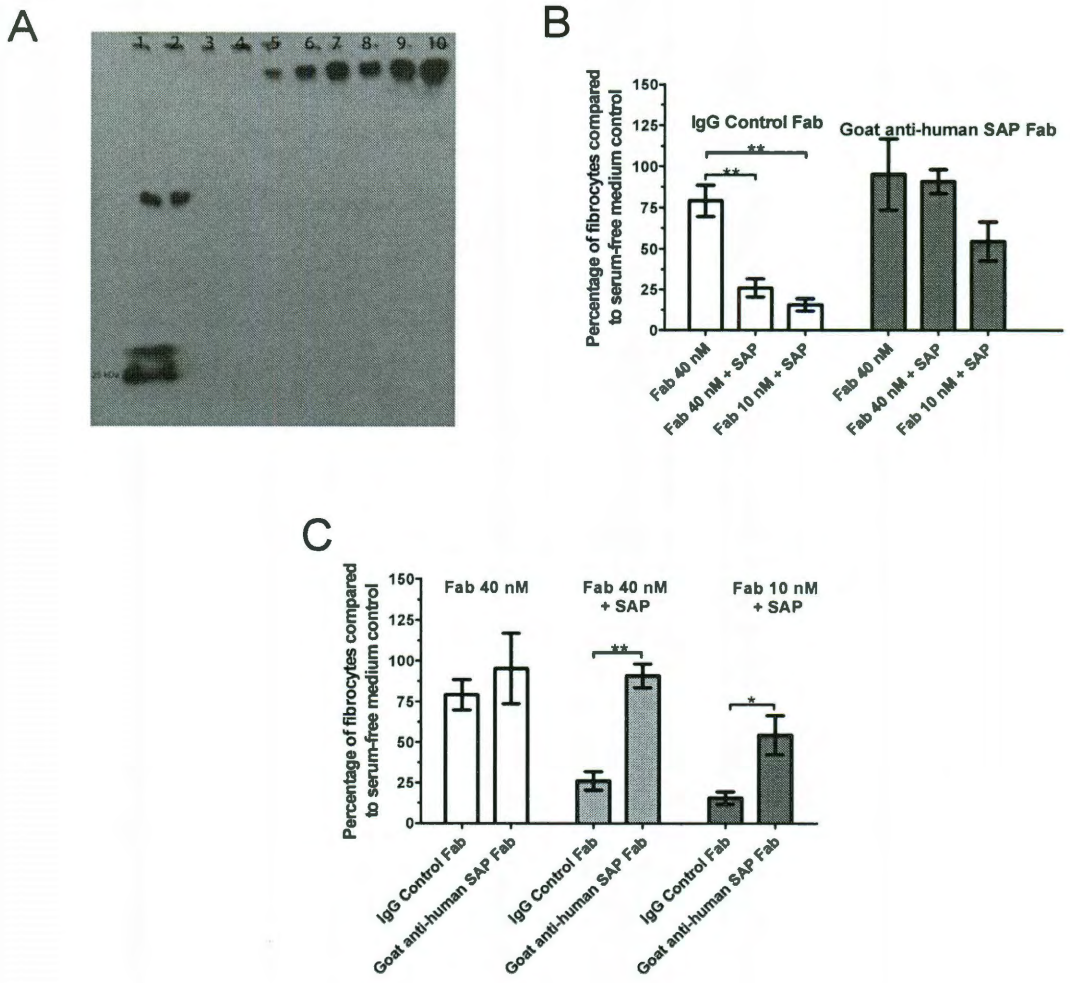

Figure 3.2: Goat anti-SAP Fab blocks SAP bioactivity. SAP antibody was made by Bethyl in a goat against the human SAP peptide[165]PPENILSAYQGT[176]. To assay the blocking activity of the antibody, we removed the nonspecific Fc portion of the antibody via papain digestion.

(A) Papain digestion of goat anti-SAP antibody gives rise to Fab fragments, as 25-26 kDa dimers. Fab fragments and full-length antibodies were detected using a biotinylated donkey anti-goat $F(ab')_2$ (Jackson ImmunoResearch), along with Extravidin-HRP (Sigma). Lane 1 – Goat anti-SAP Fab 1:50 dilution, lane 2- goat Fab control 1:100 dilution, lane 3- goat anti-SAP Fab 1:200, lane 4 – goat Fab control 1:500, lanes 5-7 – full length goat anti-SAP antibody, lanes 8-10 – full length goat IgG.

(B and C) SAP inhibits fibrocyte differentiation in the presence of nonspecific goat IgG Fab, but SAP's bioactivity is significantly reduced in the presence of goat anti-SAP Fab. PBMCs at $2x10^5$ cells/ml were cultured for 5 days in the presence of 5.5 nM SAP and/or Fab, or an equal volume of buffer in serum-free medium (SFM). Results are normalized to the number of fibrocytes per 2.5×10^5 cells/ml in SFM only wells, and the results are expressed as the mean percentage ± SEM (n=3). SAP significantly reduced the fibrocyte level in IgG Fab treated wells, but not in wells treated with goat anti-SAP (1-way ANOVA, Dunnett's test). *, $p < 0.05$; **, $p < 0.01$; ***. SAP's bioactivity was significantly decreased in wells treated with goat anti-SAP compared to wells treated with nonspecific IgG Fab (1-way ANOVA, Dunnett's test).

Table 3.1: SAP peptides tested for bioactivity.

Biomer Technology Peptides:	
Peptide	**Location**
Biotin-^{171}SAYQGTPLPANILDWQ^{186}	centered around ^{327}ALPAPI^{333} IgG-like domain
Biotin-^{178}LPANILDWQALNYEIRGY^{195}	Shifted towards c-terminus
Biotin-^{163}VLPPENILSAYQGTPLPA^{179}	Shifted towards n-terminus, contains residues critical in SAP-FcγRIIa crystal structure
Biotin-^{61}LLVYKERVGEYSLYIGRHK^{79}	Opposite side of protein, LPS/agarose binding domain
Bethyl peptide:	
^{165}PPENILSAYQGT^{176}	Contains residues critical in SAP-FcγRIIa crystal structure

The first three peptides were selected to cover the entire region around the ^{327}ALPAPI^{333} IgG-like domain (see Table 1, Figure 3). The fourth peptide was selected as a negative control since the sequence lies on the opposite side of the SAP planar disc (Figure 1.1), where SAP can opsonize bacteria and still bind to Fcγ receptors. The Bethyl peptide was available since our lab had an antibody synthesized, and the sequence contains residues critical in the SAP- FcγRIIa crystal structure (Figure 2.1).

as they failed to inhibit fibrocyte differentiation beyond buffer controls (Figure 3.3). Because SAP is pentameric in its native state and activates receptors via crosslinking, I also cross-linked the biotinylated peptides with a streptavidin-derivative (neutravidin) and tested for bioactivity. Initially, too high of neutravidin concentration was used, which depleted the biotin from the medium and resulted in cell death. Using a significantly lower neutravidin concentration as well as treating all samples with 5x excess biotin, I was able to mostly eliminate this effect except at the highest concentrations. However, the limited amount of peptide prevented me from pursuing further with the neutravidin binding assays.

Our lab had an anti-SAP antibody synthesized, and the peptide utilized for this synthesis happened to be centered around the FcγRIIa-SAP crystal structure residues (Figure 3.1B, Table 3.1). Therefore, I tested this peptide for bioactivity as a monomer and cross-linked. To be able to crosslink the peptide, I first biotinylated the peptide and then purified it (Figure3.4A - C). The monomeric form of the peptide failed to inhibit fibrocyte differentiation, nor did it block SAP's bioactivity (Figure 3.4D). Upon crosslinking with neutravidin, the cross-linked peptide still failed to block SAP bioactivity (data not shown), but the cross-linked peptide did manage to significantly inhibit fibrocyte differentiation ($p < 0.5$; 1-way ANOVA, Dunnett's test) when at 500 x molar excess compared to the bioactivity of SAP. At such high concentrations, the use of this peptide would not be biologically relevant and would be of no use as a potential therapeutic. Therefore, I did not further pursue the peptide studies.

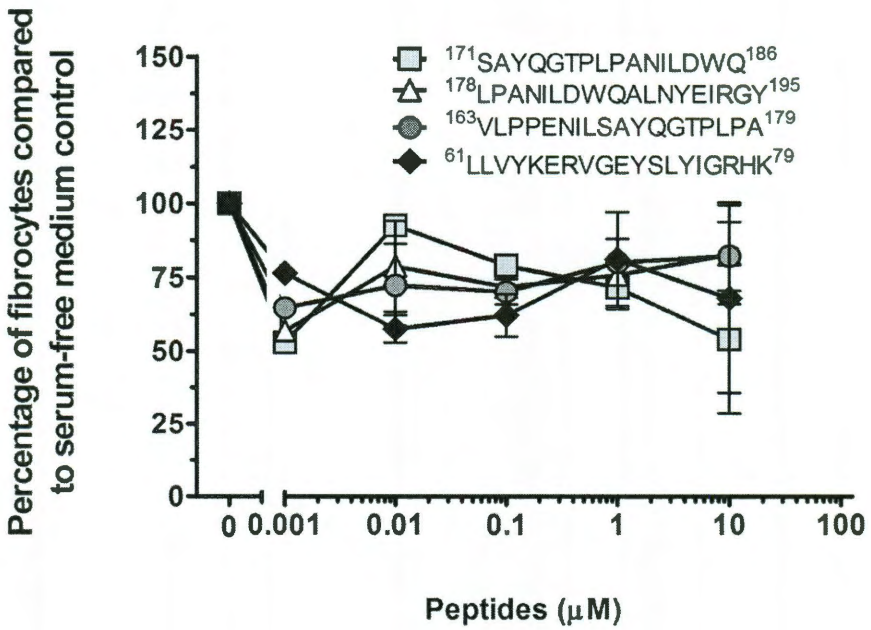

Figure 3.3: SAP peptides did not significantly alter fibrocyte differentiation. PBMCs at $2x10^5$ cells/ml were cultured for 5 days in the presence of the indicated peptide, neutravidin only, or a mixture of neutravidin and peptide. Results are normalized to the number of fibrocytes per 2.5 x 10^5 cells/ml in SFM only wells, and the results are expressed as the mean percentage ± SEM (n=3). All peptides, including the control ^{61}LLVYKERVGEYSLYIGRHK^{79}, reduced the number of fibrocytes across most concentrations without crosslinking. The presence of neutravidin crosslinker was initially found to be toxic to the cells. When added in 1/4th equimolar amounts compared to peptide, neutravidin only had a slight effect on the cells, and the cross-linked peptide-neutravidin complex did not appear to alter fibrocyte differentiation (n=1 only, ran low on peptide).

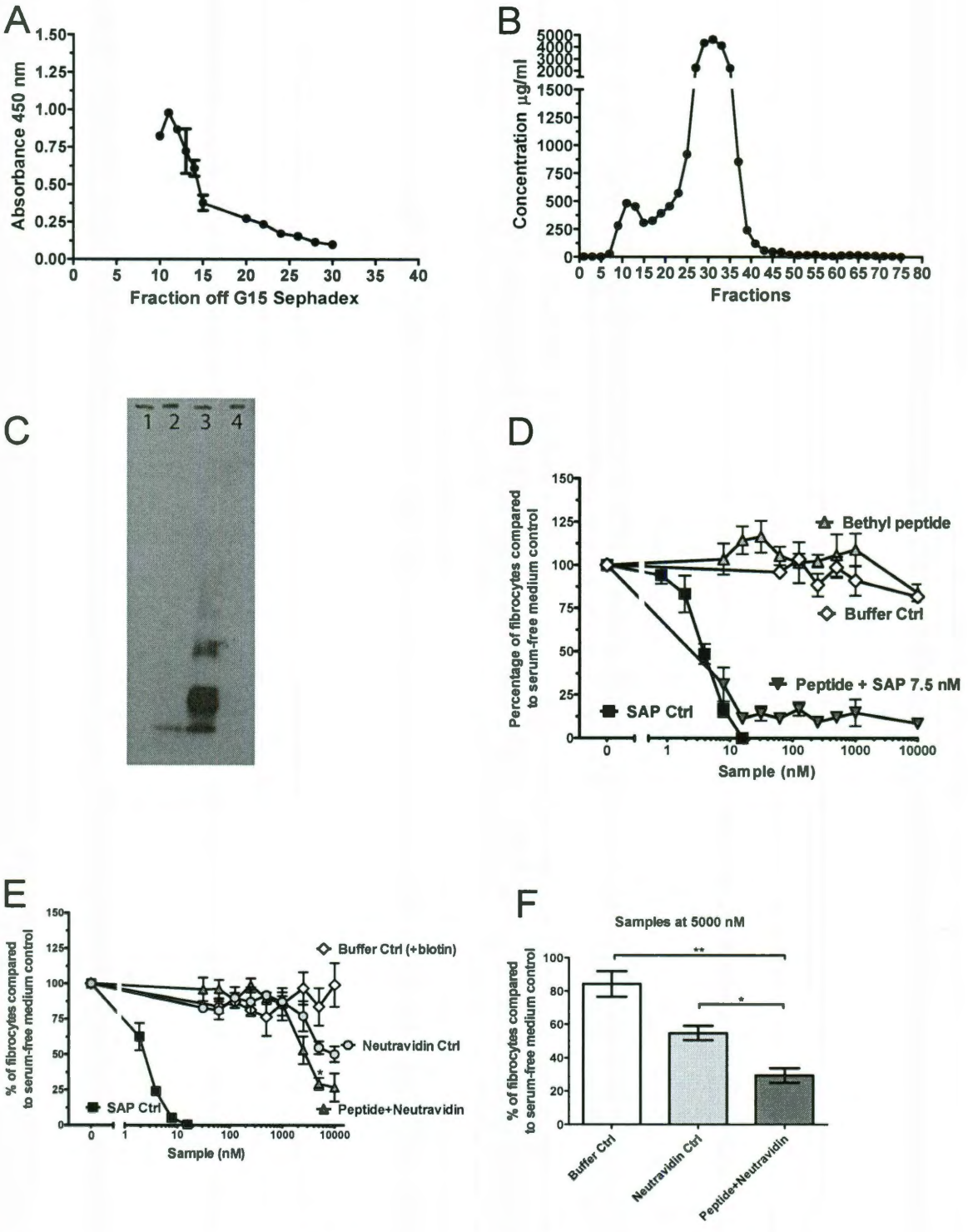

Figure 3.4: Biotinylation of ^{165}PPENILSAYQGT^{176} peptide and bioactivity. SAP peptide was biotinylated via available amine groups using NHS-PEG$_4$-Biotin (Thermo Scientific) and purified on a Sephadex G15 column (GE Healthcare).

(A) ELISA confirms biotinylation of the peptide with streptavidin-conjugated detection. Fractions off the Sephadex G15 column were tested on an ELISA plate for the ability of the newly attached biotin on the peptide to bind a streptavidin-conjugated peroxidase, which was then read at 450 nm on a plate reader.

(B) Biotinylation of the peptide results in two major peaks when collected off a Sephadex G15 column. Protein concentration was determined by Bradford. Fractions 10-15 composed the first, smaller peak, which was identified as biotinylated peptide through ELISA in (A).

(C) Biotinylated peptide binds neutravidin as seen by a shift in molecular weight. Neutravidin (Thermo Scientific) strongly binds up to 4 biotins and was mixed with biotinylated-peptide for 1 hour. The results were visualized on a Western blot using the goat anti-SAP antibody (Bethyl), with the neutravidin-bound biotinylated peptide shifted up from biotinylated-peptide only. Lane 1 – peptide, lane 2 – biotinylated peptide, lane 3 – biotinylated peptide bound to neutravidin, lane 4 – neutravidin.

(D) SAP peptide does not inhibit fibrocyte differentiation and does not compete with SAP bioactivity. PBMCs at $2x10^5$ cells/ml were cultured for 5 days in the presence of peptide and/or 7.5 nM SAP, or an equal volume of buffer in serum-free medium (SFM). Results are normalized to the number of fibrocytes per 2.5 x 10^5 cells/ml in SFM only wells, and the results are expressed as the mean percentage ± SEM (n=3).

(E &F) Neutravidin-conjugated SAP inhibits fibrocyte differentiation at 500x concentration compared to SAP. Neutravidin and PBS were premixed with biotin, biotinylated peptide was mixed initially with neutravidin and then with biotin. PBMCs at $2x10^5$ cells/ml were cultured for 5 days in the presence of neutravidin-bound biotinylated peptide, neutravidin-only, or an equal volume of buffer in serum-free medium (SFM). Results are normalized to the number of fibrocytes per 2.5 x 10^5 cells/ml in SFM only wells, and the results are expressed as the mean percentage ± SEM (n=4). Although neutravidin-only reduced the fibrocyte levels, the biotinylated peptide conjugated to neutravidin significantly reduced fibrocyte differentiation compared to buffer and neutravidin-only controls (1-way ANOVA, Dunnett's test). *, $p < 0.05$.

3.3.3 The binding of SAP to recombinant FcγRI can be detected via a direct ELISA.

We want to be able to test a variety of mutants for their ability to bind FcγRs. Therefore, I optimized a direct binding ELISA where the extracellular domain of the Fcγ receptor was bound to the plate, then mixed with SAP, and any bound SAP was visualized with anti-SAP antibodies and Extravidin-peroxidase. The recombinant FcγRs were bioactive, as they bound aggregated IgG, along with monomeric IgG for FcγRI (Figure 3.5A). I also determined that the rabbit anti-SAP polyclonal antibody (Calbiochem) and any antibody based on mouse IgG2 subtype like the SAP-5 monoclonal (Sigma-Aldrich) nonspecifically binds to FcγRI (Figure 3.5A & 3.5B). Therefore, one should avoid using any such antibodies for future assays. I also tested for SAP binding to the FcγRs using the SAP CBL304 mAb (Millipore). SAP was only detected binding to FcγRI, even though SAP has a higher affinity for FcγRIIa and III (Figure 3.5C; Castano *et al.*, 2009). I tried to improve upon SAP binding to the FcγRs by mimicking how SAP can opsonize apoptotic material, where SAP initially binds to a ligand like cellular debris on the "B" face of SAP and then binds to the FcγR with SAP's "A" face to elicit an immune response. (Figure 1.1A; Bharadwaj *et al.*, 2001; Mold *et al.*, 2002). To mimic this approach, I initially bound SAP to dextran in the presence of 2 mM $CaCl_2$, and then tried binding the complex to FcγRs. However, no difference in binding affinity was observed (Figure 3.5C). I also tried to fix any bound SAP to the receptor using 4% paraformaldehyde, but no improvement was observed (Figure 3.5C). For future ELISA experiments, I decided to use a PBS-1%BSA plus $CaCl_2$ binding buffer. The closely related pentraxin CRP requires Ca^{++} to bind to its receptor on a Biacore chip (Bodman-Smith *et al.*, 2002), and SAP requires Ca^{++} and

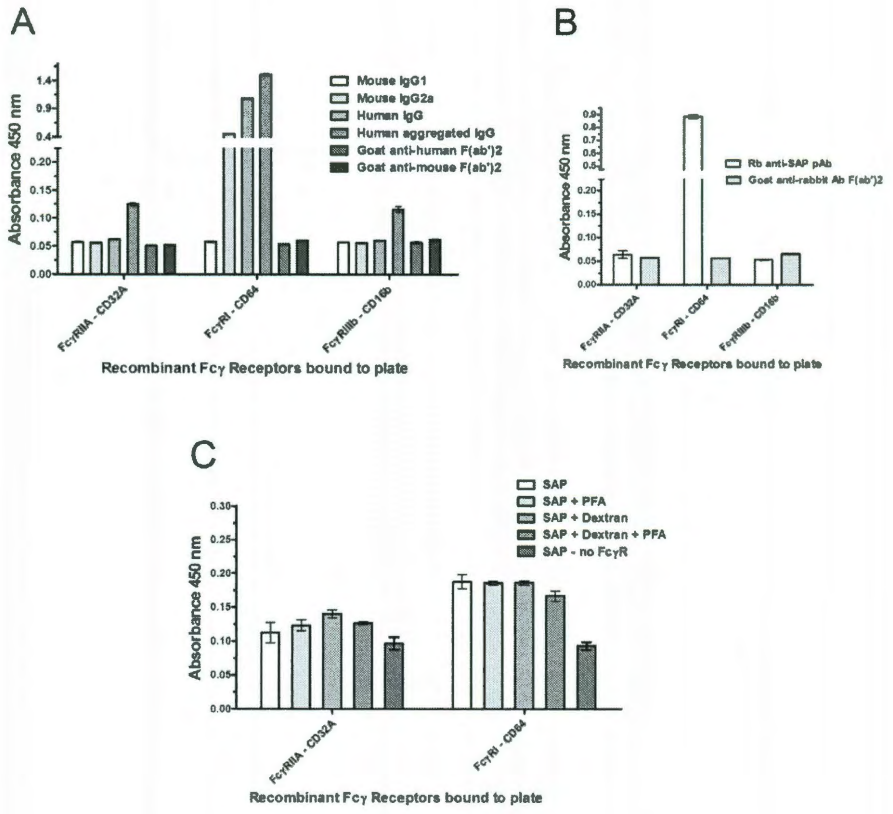

Figure 3.5: Receptor binding ELISA controls and SAP binding. Wells were coated with recombinant FcγR extracellular domains at 2 μg/ml. **(A & B)** Biotinylated human IgG was heated 45 minutes at 60 °C to heat aggregate. 30 μg/ml aggregated IgG and monomeric IgG were added to the wells as a positive control, along with the indicated negative control antibodies. The FcγRs all bind aggregated IgG as a functional control. The rabbit anti-SAP antibody and any mouse antibodies based on IgG2 subtype nonspecifically bind to FcγRI. Data are representative of 2 different experiments. **(C)** Native SAP was added to the wells at 30 μg/ml. SAP was preincubated with the dextran ligand when indicated. After binding SAP to the receptors on the plate, wells were washed, and when indicated fixed with 4% paraformaldehyde. Bound SAP was detected with the anti-SAP mAb CBL304 (Millipore), followed by Extravidin peroxidase (Sigma-Aldrich). SAP weakly bound FcγRI, while the remaining receptors showed no binding (IIb and III not shown). Fixing bound SAP to the receptor with 4% PFA, or pre-incubating SAP with a ligand such as dextran did not alter the ELISA read out. Data are representative of 3 different experiments.

dextran for receptor binding in surface plasmon resonance (Castano *et al.*, 2009). Although dextran did not improve the ELISA signal when assayed, BSA could potentially have made the dextran unnecessary since albumin is a weak ligand for SAP that can help stabilize the protein in the presence of Ca^{++} (Hutchinson *et al.*, 2000).

3.3.4 Biotinylated IgG binds to FcγRs and competes with "cold" IgG, while biotinylated SAP fails to do either.

In order to properly measure mutant SAP binding to the FcγRs, one should not use an anti-SAP antibody directly on the mutant. The reason is that a mutation could be in the same epitope that the antibody was raised against. Therefore, I performed an indirect competitive assay where I competed "hot" labeled protein with cold unlabeled protein such as the various SAP mutants. Aggregated biotinylated IgG was able to bind to the FcγRs (Figure 3.6A) as well as compete with cold IgG (Figure 3.6B). However, biotinylated SAP failed to do either when we were at least expecting to see the biotinylated SAP bind to FcγRI. The assay was repeated with 10 fold excess biotinylated SAP in case the biotinylation reduced SAP's ability to bind, but again no signal was observed (data not shown). Therefore, alternative competitors were assayed.

3.3.5 Aggregated IgG does not compete with SAP for receptor binding by ELISA.

As an alternative competition assay, SAP was tested for its ability to block aggregated IgG from binding to the FcγRs. After binding SAP and IgG to FcγRs, the

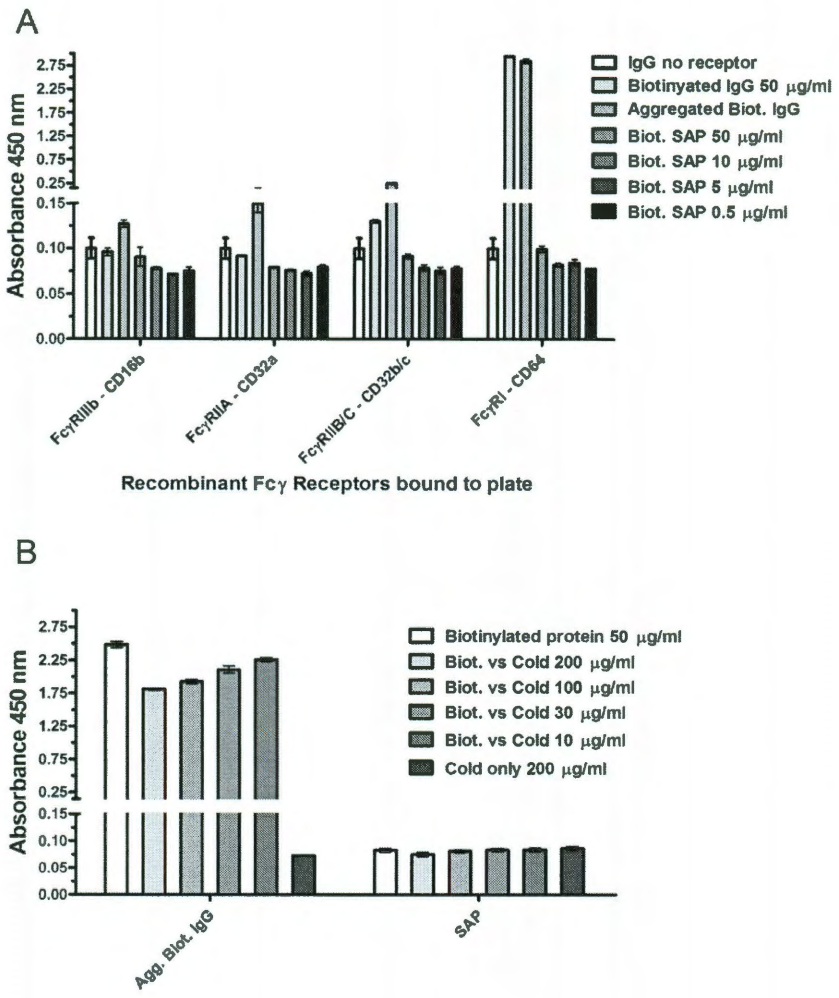

Figure 3.6: Biotinylated SAP is not detectable in receptor binding ELISA or competitive ELISA. Wells were coated with recombinant FcγR at 2 µg/ml. Biotinylated human IgG was heated 45 minutes at 60 °C to aggregate IgG. **(A)** Heat aggregated IgG was added to the wells at 50 µg/ml as a positive control. Biotinylated SAP was added to separate wells in concentration range of 0.5 – 50 µg/ml. Bound IgG or SAP was detected with streptavidin-conjugated peroxidase. **(B)** Biotinylated IgG or SAP were added to the wells at 50 µg/ml. Unlabeled "cold" IgG and SAP were added at the indicated concentrations to compete with biotinylated version of itself. The binding of biotinylated proteins was detected with Extravidin peroxidase (Sigma-Aldrich). Unlabeled aggregated IgG reduced the binding of aggregated biotinylated IgG, but no SAP binding was observed. Data are representative of 3 separate experiments.

amount of bound IgG was measured to determine if SAP lowered the degree of binding. SAP failed to compete against aggregated IgG in three out of four assays (Figure 3.7), and even in the 4th assay the competition was rather weak (data not shown). Therefore, a competitive assay between IgG and SAP is not a viable method to indirectly measure SAP's binding affinity. This also suggests that IgG and SAP may not bind to the same region on the FcγRs, as there was little to none competition between the two for the same receptor.

3.3.6 Improved ELISA signal when the FcγR extracellular domains are not bound to the plate.

To further optimize the ELISA assays, the orientation of the FcγRs was adjusted. The recombinant receptor's binding affinity could be altered when it randomly binds to an ELISA plate in an incorrect orientation. Therefore, the plates were coated with a rabbit anti-his capture antibody, and the his-tagged FcγR extracellular domains were then bound to the antibody. The signal was significantly improved and SAP binding to FcγRIIa was observed for the first time (Figure 3.8). However, the negative control wells had a high background signal that overshadowed the lowest concentrations of SAP. This method is the most promising but further optimizations would be needed for future measurements.

Alternatively, I tried a different coupling method for the receptor. Instead of binding the receptor to the plate, the receptor was cross-linked to tosylated Dyna beads through a free amine group. This method has the advantage of providing more surface

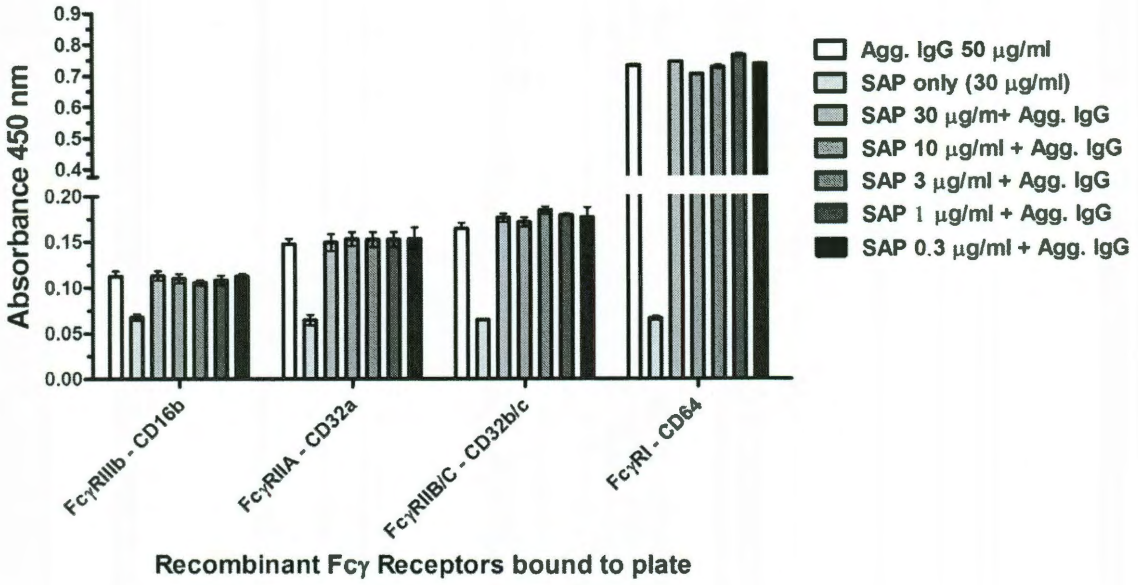

Figure 3.7: SAP does not compete with IgG binding to FcγRs. Human IgG was heated for 45 minutes at 60 °C to aggregate IgG. Wells were coated with recombinant FcγR at 2 µg/ml. SAP was added to each well in concentrations shown and was incubated for 15 minutes. Heat aggregated IgG at 50 µg/ml was added to the wells already containing SAP and then incubated for 45 minutes. The amount of human IgG bound to FcγR was detected with a biotinylated mouse anti-human IgG F(ab')2 and a streptavidin-conjugated peroxidase. Data are representative of 3 separate experiments.

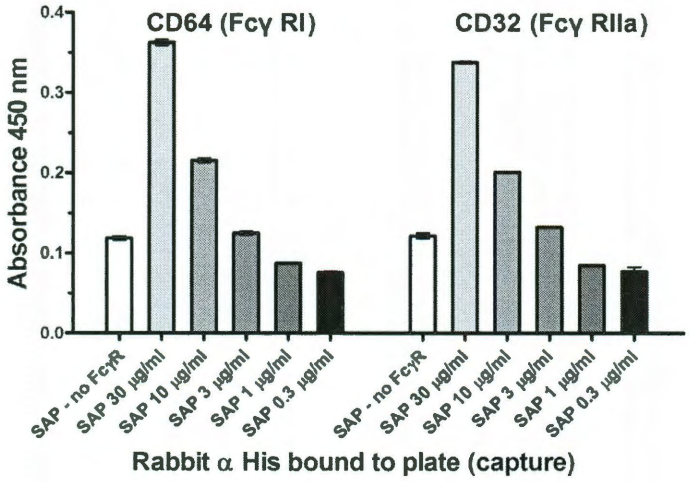

Figure 3.8: The receptor binding ELISA assay for SAP is improved when the receptor is not directly bound to the plate. Wells were coated with rabbit anti-his antibody. The his-tagged FcγRs were incubated the next day at 2 μg/ml for 1 hour, followed by SAP at the indicated concentrations in a PBS-1% BSA, 2 mM $CaCl_2$ buffer. Bound SAP was detected with a mouse monoclonal anti-SAP antibody (CBL304, Millipore), followed by Extravidin peroxidase (Sigma-Aldrich). Representative of n=2.

area for receptor binding, and the magnetic beads allowed for more efficient cleaning in reduced amounts. However, the blocking conditions had to be altered to reduce nonspecific SAP binding, by increasing the Tris and BSA concentrations. Promedior donated SAP conjugated with Alexa-594, which will allow for competitive binding assays. Therefore, we tested the binding of Alexa-594 SAP to FcγRI while competing with cold SAP and CRP. Cold SAP but not CRP was able to compete with the Alexa-SAP (Figure 3.9). This method will work for any future competitive binding assays, but the blocking step can be inconsistent, where one sometimes sees SAP binding in the absence of any bound receptor.

3.4 Discussion

To further elucidate the functional domain of SAP, peptides were tested that contained sequences from the two purported FcγR binding domains in Chapter 2. The peptides failed to block SAP activity and did not inhibit fibrocyte differentiation except in 500 fold molar excess. This negative result does not rule out these areas, but taken within the context of the mutagenesis study and the peptide analysis, we will need to look elsewhere for SAP's functional domain.

I was able to establish conditions that will allow us to measure the binding of mutant recombinant SAP to FcγRI and potentially FcγRIIa, although the system could use further refinement to reduce nonspecific binding. For the binding assay, coupling SAP with dextran was not necessary to obtain a signal, nor did it improve receptor binding. Previously, the coupling of SAP to dextran was necessary to measure receptor

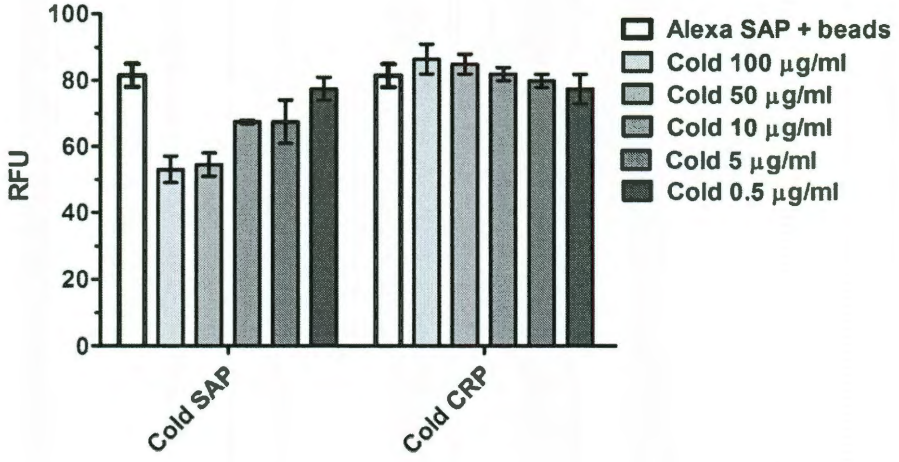

Figure 3.9: CRP does not compete with SAP binding to FcγRI when the receptor is bound to tosyl magnetic beads. 5 µg/ml of FcγRI extracellular domain was bound to tosylactivated M-280 dynabeads (Invitrogen) overnight at 37° C. The beads were blocked with sodium phosphate-3% BSA and 0.5 M Tris, pH 8.5 with 1% BSA. 50 µg/ml Alexa-594 conjugated SAP was mixed with cold SAP or CRP for 1 hour at 37° C at the indicated concentrations. After washes, beads were placed in a black 96 well plate (Nunc), and the fluorophore was excited at 594 nm and read at 620 nm using a Tecan plate reader (Durham, NC). Representative of 4 separate experiments. Negative controls were inconsistent across plates, where SAP was detected in the absence of FcγRI in 2 out of 4 experiments.

binding through surface plasmon resonance (Castano *et al.*, 2009). The binding of dextran would mimic how SAP can opsonize apoptotic material on one side of SAP's planar disc and then induce phagocytosis by binding to FcγRs on the opposite face (Bharadwaj *et al.*, 2002; Mold *et al.*, 2002). The prediction was that SAP could not efficiently bind to FcγRs unless SAP first bound a ligand in its Ca^{++}-dependent pattern recognition site. One possible explanation why pre-incubation with dextran did not improve receptor binding is that the assays were carried out in the presence of Ca^{++} and BSA, and BSA is a weak ligand for SAP that can help stabilize the protein (Hutchinson *et al.*, 2000).

In trying to develop a competition assay to indirectly measure SAP mutant binding, I found that SAP is not competitive with IgG or CRP for FcγRI binding. The lack of competition with IgG is consistent with the finding that monomeric IgG does not compete with SAP bioactivity *in vitro* and that there are distinct differences in the signaling cascade produced by SAP or IgG upon engagement to the receptor (Pilling *et al.*, 2006). However, Lu *et al.* (2008) found that SAP competes with IgG for binding to FcγRs through surface plasmon resonance (SPR). The contrasting results could be due to methodology or sensitivities in the assays, and Lu (2008) did not specifically look at FcγRI for SPR. Additionally, CRP likely did not compete because the FcγRI receptor is a lower affinity receptor for CRP, although a successful competition may be viable when using the high affinity receptor FcγRIIa (Bharadwaj *et al.*, 1999). For future competition assays, we can use fluorophore labeled SAP instead, either using the ELISA system with the rabbit anti-his capture antibody or the tosyl bead system.

Chapter 4: Improved serum-free culture conditions for spleen-derived murine fibrocytes

4.1 Introduction

Fibrocyte biology has been extensively studied in humans, but to delve further into how fibrocytes are involved in diseased states we need to find alternative cell sources from diverse genetic backgrounds. Thus, we can look to mouse disease model systems and murine genetic knock outs to see how fibrocyte differentiation is influenced. However, to do so efficiently, we need a quick, viable fibrocyte differentiation assay where we can eliminate outside influencing factors like the various components of serum.

In addition to human peripheral blood mononuclear cells (PBMCs), fibrocytes have also been cultured from murine PBMCs, although monocytes are only 1-4% of murine peripheral blood PBMCs compared to 10% for humans (Abe *et al.*, 2001; Kile *et al.*, 2003). However, a large reservoir of monocytes has recently been found in the subcapsular red pulp of the spleen, and these can be mobilized for wound repair (Swirski *et al.*, 2009). Niedermeier *et al.* (2009) recently used this splenic reservoir to show that fibrocytes differentiate from a subpopulation of CD11b+ CD115+ Gr1+ monocytes under the control of activated CD4+ T-cells. Their protocol involved culturing the cells in the presence of 10% FBS in RPMI for 14 days.

We previously found that culturing human and murine PBMC in serum-free medium results in fibrocytes appearing within 5 days (Pilling *et al.*, 2003, 2006, 2009a). In this chapter, I show that mouse spleen cells can differentiate into fibrocytes in serum

free conditions within 5 days. Conditions are determined where a large number of fibrocytes can be produced from a single mouse spleen, which will allow for future studies testing the effect of multiple factors on murine fibrocyte differentiation (Crawford *et al.*, 2010).

4.2 Methods

4.2.1 Isolation of murine SAP

Murine SAP was purified from murine serum (Gemini Bio-products, West Sacramento, CA) using calcium-dependent binding to phosphoethanolamine-conjugated agarose, as described previously (Haudek *et al.*, 2006; Pilling *et al.*, 2007), with the exception that Amicon Ultra-15 centrifugal filters (Millipore, Billerica, MA) were used for the 20 mM phosphate buffer exchange.

4.2.2 Cell fractionation

Human peripheral blood was collected into heparin vacutainer tubes (#367874; BD Bioscience, Franklin Lakes, NJ) with written consent from healthy adult volunteers and with specific approval of Rice University's Institutional Review Board. Peripheral blood mononuclear cells (PBMC) were isolated by Ficoll-Paque Plus (GE Healthcare Biosciences, Piscataway, NJ), as previously described (Pilling *et al.*, 2009a).

4-6 week male C57BL/6J mice (Jackson Laboratories, Bar Harbor, ME or Taconic, Hudson, NY) were used in this study. All work was done under Rice and Texas

A&M IACUC approved protocols. Murine peripheral blood was drawn by cardiac puncture using heparin-coated syringes, and mononuclear cells were purified by density centrifugation using Lympholyte-Mammal (Cedarlane, Burlington, NC), following the manufacturer's protocol. Spleens were harvested (~70-100 mg each) and cells were isolated by digesting in a cocktail of 450 U/ml collagenase I (EMD, San Diego, CA), 60 U/ml DNase I, and 60 U/ml hyaluronidase (Sigma-Aldrich, St. Louis, MO) in 1 ml RPMI (Sigma-Aldrich) for 30 minutes at 37°C. Alternatively, spleen cells were isolated by forcing diced spleen fragments through a 100 μm cell strainer (BD Biosciences, San Jose, CA) using the plunger of a 3 ml syringe (BD Medical, Franklin Lakes, NJ) and 5 ml of RPMI. Finally, some spleen cells were isolated with a combination of digest cocktail, followed by the use of a cell strainer. After digest or passage through a cell strainer, the cells were resuspended in 10 ml RPMI and collected by centrifugation at 300 x g for 10 minutes. Cells were further purified using ammonium chloride, potassium bicarbonate (ACK) lysis buffer (0.15 M NH_4Cl, 10 mM $KHCO_3$, 0.1 mM Na_2EDTA; Kruisbeek, 2000), or by density centrifugation using Lympholyte-Mammal or Ficoll-Paque Plus (GE Lifesciences, Piscataway, NJ). For ACK lysis, spleen cells were resuspended in 940 μl lysis buffer for 3 minutes at room temperature, and the reaction was stopped by the addition of 14 ml PBS. The cells were collected by centrifugation at 200 x g for 10 minutes, and the PBS wash step was repeated 3 additional times. A final wash was carried out by resuspending the cells in 1.5 ml Fibrolife basal media (Lifeline Cell Technology, Walkersville, MD) with the supplements listed below, and the cells were collected by centrifugation at 300 x g for 5 minutes at 4° C. For density centrifugation, spleen cells were resuspended in 10 ml RPMI and fractionated following the

manufacturer's protocol. The mononuclear fraction was then diluted to 14 ml with PBS and cells were collected by centrifugation at 300 x g for 10 minutes. The resuspension and centrifugation was repeated three times. The cells were resuspended in 1.5 ml Fibrolife basal media with supplements and collected by centrifugation at 300 x g for 5 minutes at 4° C.

4.2.3 Culture conditions and fibrocyte differentiation assay

PBMC and spleen cells were resuspended in 1 ml Fibrolife basal media (Lifeline Cell Technology), supplemented with 10 mM HEPES (Sigma-Aldrich), 2 x non-essential amino acids (Sigma-Aldrich), 2 mM sodium pyruvate (Sigma-Aldrich), 4 mM glutamine (Invitrogen, Carlsbad, CA), 100 U/ml penicillin, 100 g/ml streptomycin (Sigma-Aldrich), 2 x ITS-3 (Sigma-Aldrich), and 50 μm 2-mercaptoethanol (EMD). For some experiments, spleen cells were cultured in the presence or absence of 50 ng/ml murine IL-13 and 25 ng/ml murine M-CSF (Peprotech, Rocky Hill, NJ). Additionally, murine IL-4 (Peprotech), IL-13, and M-CSF were tested alone and in combination at the indicated concentrations. PBMC and spleen cells were cultured in flat-bottomed 96 well tissue culture plates (353072, BD Biosciences) at 200 μl per well at the indicated cell densities in a humidified incubator containing 5% CO_2 at 37° C. On day 3 of the incubation, wells with IL-13 and M-CSF were further supplemented with 5 μl of a cocktail containing 1 μg/ml IL-13 and 0.5 μg/ml M-CSF in Fibrolife SFM. After 5 days, plates were air dried, fixed with methanol, and stained with Hema 3 stain (Fisher Scientific, Hampton, NH). Fibrocytes were counted in five different 900 μm diameter fields of view for each well of a 96 well plate, using the following criteria: an adherent

cell with elongated spindle-shaped morphology and an oval nucleus (Pilling *et al.*, 2003, 2006, and 2009a; Shao *et al.*, 2008). The total number of fibrocytes per 10^5 input cells for each well was then calculated.

4.2.4 Immunohistochemistry

Mouse spleen cells, isolated by combination of digest cocktail, cell strainer, and ACK lysis, were cultured in 8 well glass slides (177402, Lab-tek, Nalge-Nunc, Naperville, IL) or 8 well CC2 glass slides (154941, Nalge-Nunc) at 4 x 10^6 cells/ml and 250 µl per well for 5 days in the presence or absence of IL-13 and M-CSF. Slides were air dried overnight, fixed in acetone, and stained as described previously (Pilling *et al.*, 2009a) with the following modifications. Slides were stained for CD34 (clone RAM34, rat IgG2a, eBioscience, San Diego, CA), CD11c (clone 223H7, rat IgG2a, MBL Int., Woburn, MA), CD11b (clone M1/70, rat IgG2b, BioLegend, San Diego, CA), CD45 (clone 30-F11, rat IgG2b, BD Biosciences), syk (sc-1077, rabbit polyclonal, Santa Cruz Biotech., Santa Cruz, CA), or collagen I (600-401-103-01, rabbit polyclonal, Rockland, Inc., Gilbertsville, PA). Negative controls were rat IgG2a and IgG2b (BioLegend) and rabbit IgG (Jackson Immunoresearch, West Grove, PA). Primary antibodies were incubated at 5 µg/ml in PBS/BSA for 1 hour, except anti-CD34 was incubated at 10 µg/ml. Slides were then washed in 5 changes of 50 ml PBS over 15 minutes and incubated for 30 minutes in PBS/BSA with 2.5 µg/ml biotinylated mouse $F(ab')_2$ anti-rat IgG (Jackson Immunoresearch) or 2.5 µg/ml biotinylated goat $F(ab')_2$ anti-rabbit IgG (Southern Biotech, Birmingham, AL). The slides were then washed and developed as previously described (Pilling *et al.*, 2009a).

4.2.5 Flow cytometry

For fibrocyte collagen analysis, spleen cells were cultured for 5 days in the presence of IL-13 and M-CSF. Adherent cells were dislodged with a 10 minute incubation in trypsin-EDTA (Sigma-Aldrich) at 37° C. Cells were washed with 14 ml PBS/10% mouse serum (Gemini) and collected by centrifugation at 300 x g for 10 minutes. The cells were resuspended in 100 µl ice-cold PBS containing 10% rat serum (Sigma-Aldrich), and incubated on ice for 15 minutes. Cells were collected by centrifugation at 300 x g for 5 minutes, and resuspended in 100 µl of PBS/4% BSA containing 2.5 µg/ml PE-conjugated anti-CD11b antibody (clone M1/70, rat IgG2b, eBioscience). After a 30 minute incubation on ice, the cells were washed twice with 1.4 ml ice-cold PBS and fixed with 100 µl of 4% paraformaldehyde in PBS for 15 minutes at room temperature. The cells were washed twice with 1.4 ml ice-cold PBS/4% BSA and permeabilized by resuspension in 100 µl PBS/4% BSA/0.1% saponin (Invitrogen). After a 15 minute incubation on ice, the cells were washed once with 1.4 ml ice-cold PBS/0.1% saponin, collected by centrifugation at 300 x g for 5 minutes, and then stained with antibodies against collagen type I (ab292-100, rabbit polyclonal, Abcam, Cambridge, MA), collagen type III (600-401-105-.1, rabbit polyclonal, Rockland), or syk (Santa Cruz) at 5 µg/ml in 100 µl PBS/4% BSA/0.1% saponin. After a 30 minute incubation on ice, cells were washed twice with 1.4 ml ice-cold PBS/0.1% saponin, and resuspend in 100 µl of PBS/4% BSA/0.1% saponin containing 2.5 µg/ml FITC-conjugated goat $F(ab')_2$ anti-rabbit IgG (Southern Biotech). After a 30 minute incubation on ice, cells were washed twice with 1.4 ml ice-cold PBS, resuspended in 100 µl PBS/BSA/saponin, and staining was analyzed using a C6 flow cytometer (Accuri, Ann Arbor, MI).

For monocyte analysis, mouse spleen cells were subjected to flow analysis as described previously (Pilling *et al.*, 2009a) with the following modifications. Cells were stained for Ly6G (clone 1A8, rat IgG2a, BioLegend). The secondary antibody was a FITC-conjugated mouse $F(ab')_2$ anti-rat IgG (Jackson Immunoresearch), used at 2.5 μg/ml. After incubating the cells with the secondary antibody and washing, the cells were resuspended in 100 μl ice-cold PBS containing 10% rat serum (Sigma-Aldrich), and incubated on ice for 30 minutes. Cells were collected by centrifugation at 300 x g for 5 minutes, and resuspended in 100 μl of PBS/4% BSA containing 2.5 μg/ml PE-conjugated anti-CD11b antibody (clone M1/70, rat IgG2b, eBioscience). After a 30 minute incubation on ice, cells were washed twice with 1.4 ml ice-cold PBS, resuspended in 100 μl ice-cold PBS/BSA, and then analyzed using a C6 flow cytometer (Accuri).

4.2.6 Monocyte enrichment and CD11b depletion of spleen cells

Mouse spleen cells were isolated by the combination of digest cocktail, cell strainer, and ACK lysis. Monocytes were enriched from spleen cells using an EasySep mouse monocyte negative selection kit (Stemcell Technologies, Vancouver, BC), following the manufacturer's protocol. Alternatively, CD11b+ cells were depleted from spleen cells using the EasySep Mouse CD11b positive selection kit (Stemcell Technologies), following the manufacturer's protocol. The CD11b-depleted cells were then subjected to ACK lysis. The purity of the cells was checked by morphology, with a monocyte defined as a large cell (10-15 μm) with a kidney-shaped nucleus. Cytospins were prepared by centrifugation at 400 rpm for 5 minutes in a Shandon Cytospin 2 (Thermo Scientific, Waltham, MA) and stained with a Hema 3 kit (Fisher). The purity

was also checked by staining for CD11b and Ly6G using flow cytometry, as described above. The cells were cultured for 5 days as described above, except the monocyte-enriched cells were plated at 5 x 10^5 cells/ml while the unfractionated spleen cells and CD11b-depleted cells were plated at 3 x 10^6 cells/ml.

4.2.7 Determining the effect of SAP and IgG on fibrocyte differentiation

Lympholyte-Mammal isolated murine PBMCs were cultured at 2.5 x 10^6 cells/ml. Spleen cells, isolated by the combination of digest cocktail, cell strainer, and ACK lysis, were cultured at 3.5 x 10^6 cells/ml. Murine and human SAP (EMD-Calbiochem) in 20 mM sodium phosphate buffer, pH 7.4, was added to the cells at the indicated concentrations. The cells were then cultured for 5 days, and fibrocytes were counted as described above.

Spleen cells were also tested for sensitivity to IgG. Chromopure murine IgG (Jackson Immunoresearch) was clarified by centrifugation at 14,000 x g for 15 minutes at 4° C to remove aggregates. Mouse spleen cells at 5 x 10^6 cells/ml in 500 µl were incubated with 100, 10, 1, or 0 µg/ml IgG for 30 minutes at 4° C. Cells were washed with 1.4 ml ice-cold Fibrolife medium and collected by centrifugation at 300 x g for 5 minutes at 4° C. Cells were resuspended in 500 µl Fibrolife medium and incubated with 500 ng/ml goat $F(ab')_2$ anti-mouse IgG (Southern Biotech) for 30 minutes at 4° C.

Cells were washed with 1.4 ml Fibrolife, collected by centrifugation at 300 x g for 5 minutes, and resuspended to 500 µl. Cells were counted and diluted to 3.5 x 10^6 cells/ml. The cells were then cultured for 5 days, and fibrocytes were counted.

4.3 Results

To study factors that regulate the differentiation of monocytes to fibrocytes, peripheral blood mononuclear cells can be isolated from blood and cultured *in vitro*. When murine PBMCs are utilized, the cells must be cultured at higher densities due to the low percentage of monocytes found in mouse blood (Wirth *et al.*, 1982; Kile *et al.*, 2003); therefore, the blood from multiple mice must be pooled together to obtain enough cells for a single experiment (Pilling *et al*, 2009a). Murine spleens have recently been shown to contain a monocyte population that can be mobilized for wound repair (Swirski *et al.*, 2009), and spleen cells have been shown to differentiate into fibrocytes, although this process requires serum and an incubation period of 14 days (Niedermeier *et al.*, 2009). Therefore, I tested if cultured mouse spleen cells can differentiate into fibrocytes in serum free conditions.

4.3.1 Spindle-shaped cells that appear in cultures of spleen cells express fibrocyte markers

We previously observed the appearance of spindle-shaped cells in 5 day serum-free cultures of human and murine PBMCs (Pilling *et al.*, 2003, 2006, 2009a; Shao *et al.*, 2008). These cells showed positive staining for markers that have been used to classify cells as fibrocytes, including the general leukocyte marker CD45, the stem cell marker CD34, the monocyte marker CD11b, and the matrix biosynthesis marker collagen I

(Bucala *et al.*, 1994; Abe *et al.*, 2001, Pilling *et al.*, 2003). To assess the viability of culturing mouse spleen cells to study fibrocyte differentiation, I first confirmed the presence of fibrocytes in mouse spleen cell cultures. Mouse spleen cells were initially isolated by passage through a cell strainer and further purified by density centrifugation. After a 5 day incubation in serum-free media, we observed spindle-shaped cells in the culture. To confirm the identity of the spindle-shaped cells, I stained the cells for a variety of markers. The spindle-shaped cells were positive for well-known markers of fibrocytes, including CD11b (Figure 4.1D), CD45 (Figure 4.1E), and weakly positive for collagen I (Figure 4.1H). The cells also stained positive for CD34 (Figure 4.1A) with variable expression levels, similar to the variability found in human fibrocytes (Pilling *et al.*, 2003 and 2009b; Phillips *et al.*, 2004). Fibrocytes are known to produce low levels of collagen (Wang *et al.*, 2007; Pilling *et al.*, 2009b), but to further confirm the presence of collagen, we measured the intracellular levels of collagen on 5 day cultured spleen cells by flow cytometry. The overall cell population (Figure 4.2A) showed little to no staining for collagen (Figure 4.2C), but CD11b+ cells (Figure 4.2B) stained positive for both collagen I and III (Figures 4.2D and 4.2E). Similar to the immunohistochemistry results, the CD11b+ cells only stained weakly positive for collagen I with a median fluorescent intensity of $3.4 \times 10^3 \pm 0.1 \times 10^3$ compared to $5.8 \times 10^4 \pm 0.6 \times 10^4$ for the positive control Syk (Figure 4.2D). To confirm that the spindle-shaped cells were not dendritic cells, I stained by immunohistochemistry for CD11c, a marker for dendritic cells (Shortman *et al.,* 2002). The cells in culture with a dendritic shape stained strongly for CD11c, while the spindle-shaped cells were either negative or very weakly positive (Figure 4.1B). This suggests that the spindle-shaped cells are fibrocytes rather than

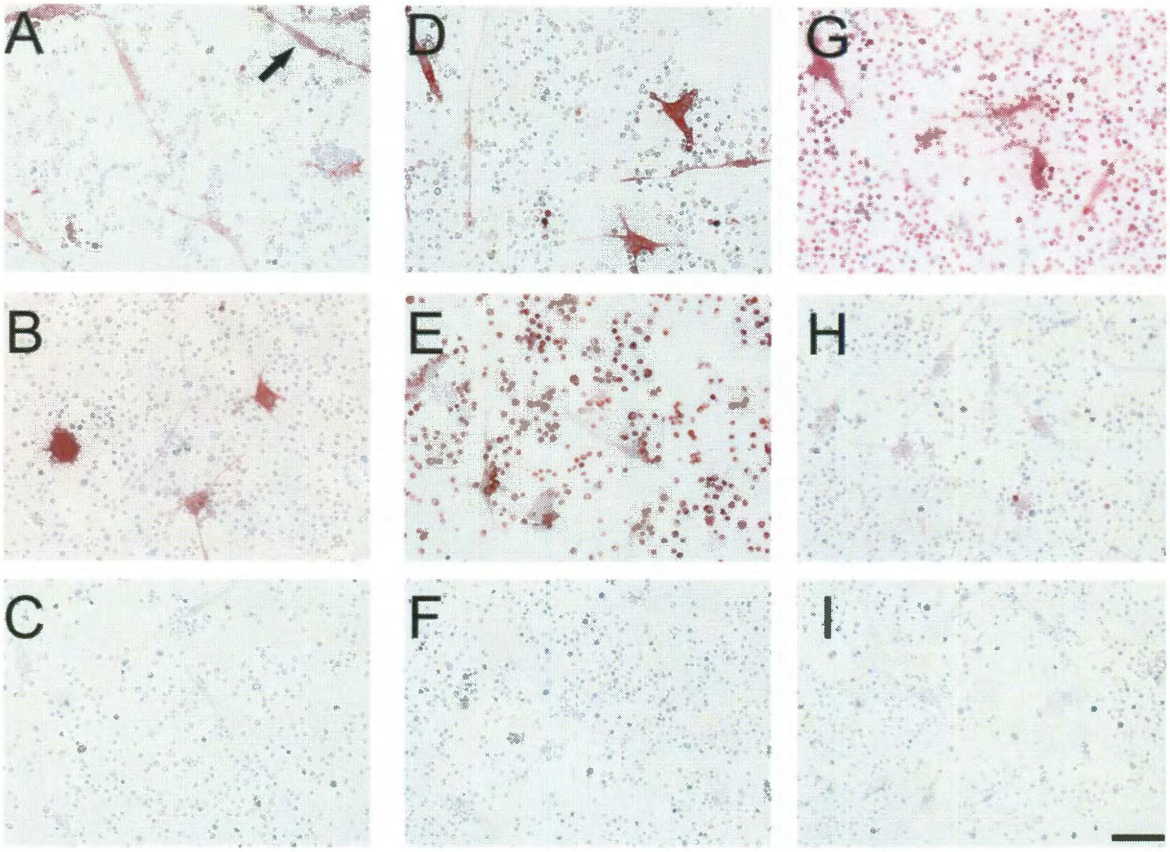

Figure 4.1: Cultured mouse spleen cells express markers of fibrocytes. Isolated spleen cells were cultured for 5 days at 4 x 10^6 cells/ml on 8 well CC2 slides, then air dried, fixed, and stained with antibodies against **(A)** CD34, **(B)** CD11c, **(C)** rat IgG 2a control for A and B, **(D)** CD11b, **(E)** CD45, **(F)** rat IgG 2b control for D and E, **(G)** syk, **(H)** collagen I, and **(I)** rabbit IgG control for G and H. Cells were counterstained with hematoxylin to identify nuclei. Bar is 50 μm, and arrow in A indicates a fibrocyte. Images are representative of four independent experiments.

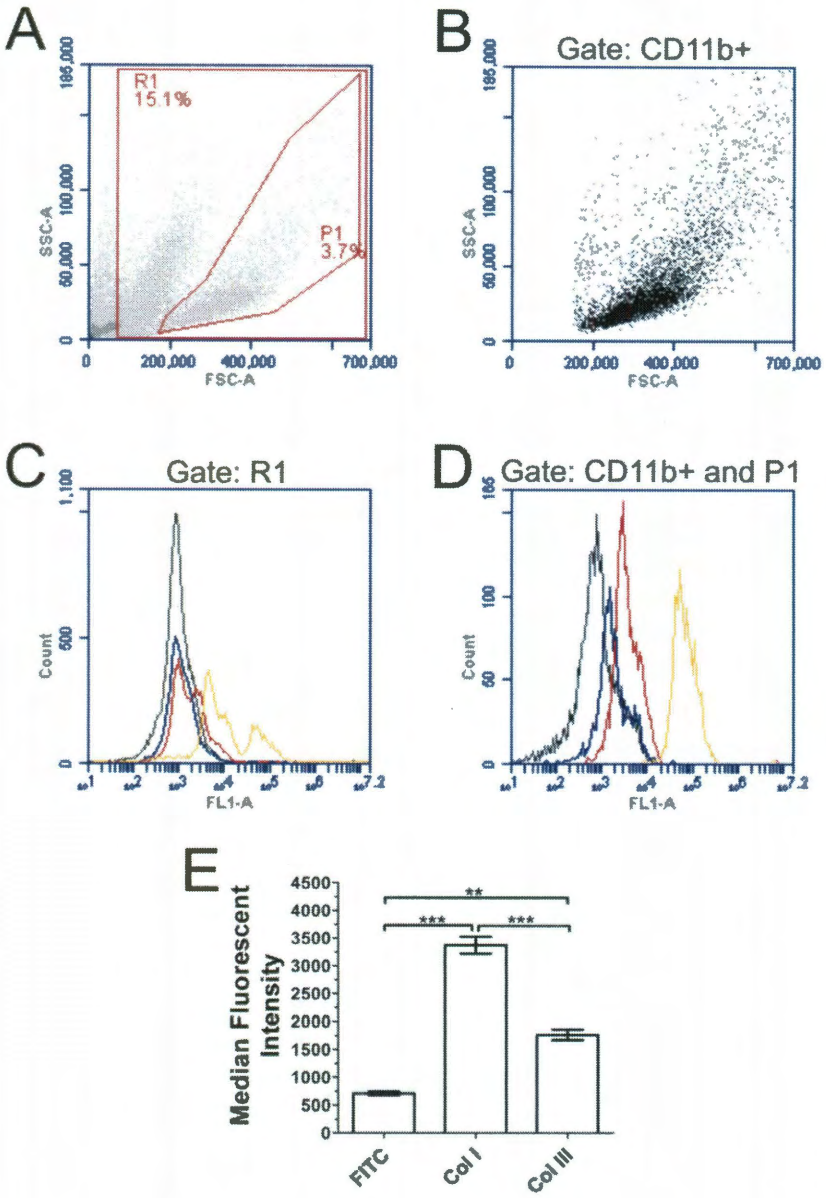

Figure 4.2: Expression of collagen by 5 day cultured spleen cells. ACK-treated spleen cells were cultured for 5 days at 3.5 x 10^5 cells per well in the presence of IL-13 and M-CSF. Adherent cells were removed by trypsin-EDTA treatment and stained for the presence of CD11b. The cells were then fixed, permeabilized, stained with rabbit polyclonal antibodies, and analyzed by flow cytometry. **A)** Forward and side scatter characteristics of 5 day cultured spleen cells. **(B)** Forward and side scatter analysis of CD11b+ cells. **C and D)** Histograms show fluorescence intensity of FITC-conjugated goat $F(ab')_2$ anti-rabbit 2° (black line) compared to collagen I (red line), collagen III (blue

line), and as a positive control syk (yellow line). Flow cytometry plots are representative of 3 independent experiments. **C)** When gating the entire live cell population R1 (from A), collagen was nearly undetectable, but when gating **(D)** for CD11b+ cells and region P1 (from A and B) there was an increase in the levels of both collagen I and III. **E)** Compared to FITC control, CD11b+ cells had a significant increase in median fluorescent intensity for collagen I and III staining (1-way ANOVA, Dunnett's test). **, $p < 0.01$; ***, $p < 0.001$.

dendritic cells. Together, these observations suggest that murine spleen cells cultured for 5 days in serum-free media can differentiate into fibrocytes. We can therefore use murine spleen cells to further study conditions that affect differentiation.

4.3.2 Effect of purification method on fibrocyte differentiation.

Murine splenocytes are typically isolated either by passage through a cell strainer or by digestion with enzymes (Swirski *et al.*, 2009). Mononuclear cells are typically further purified by density centrifugation, and leukocytes are purified by lysis of red blood cells (Kruisbeek *et al.*, 2000). I tested a variety of cell purification methods to optimize spleen cell recovery and fibrocyte differentiation. After removal of the spleen, cells were isolated by passage through a cell strainer, digestion with collagenase and DNase, or a combination of the two. The isolated spleen cells were further purified by density centrifugation with Lympholyte-Mammal or Ficoll, or by ACK lysis to remove red blood cells. For the initial isolation, the digest cocktail or the combination of cell strainer and digest resulted in the highest recovery of spleen cells (Figures 4.3A, 4.3C, and 4.3E). For the additional purification step, ACK lysis resulted in a significantly higher recovery of spleen cells compared to density centrifugation by Lympholyte-Mammal or Ficoll (Figures 4.3A, 4.3C, and 4.3E). For fibrocyte yield, there was no significant difference between the initial isolation techniques (Figures 4.3B, 4.3D, and 4.3F). However, for the additional purification step, ACK lysis showed a trend of increased fibrocyte differentiation compared to density centrifugation (Figures 4.3B, 4.3D, and 4.3F). Additionally, the cultures prepared by ACK lysis and density centrifugation were checked for the presence of any contaminating fibroblasts by

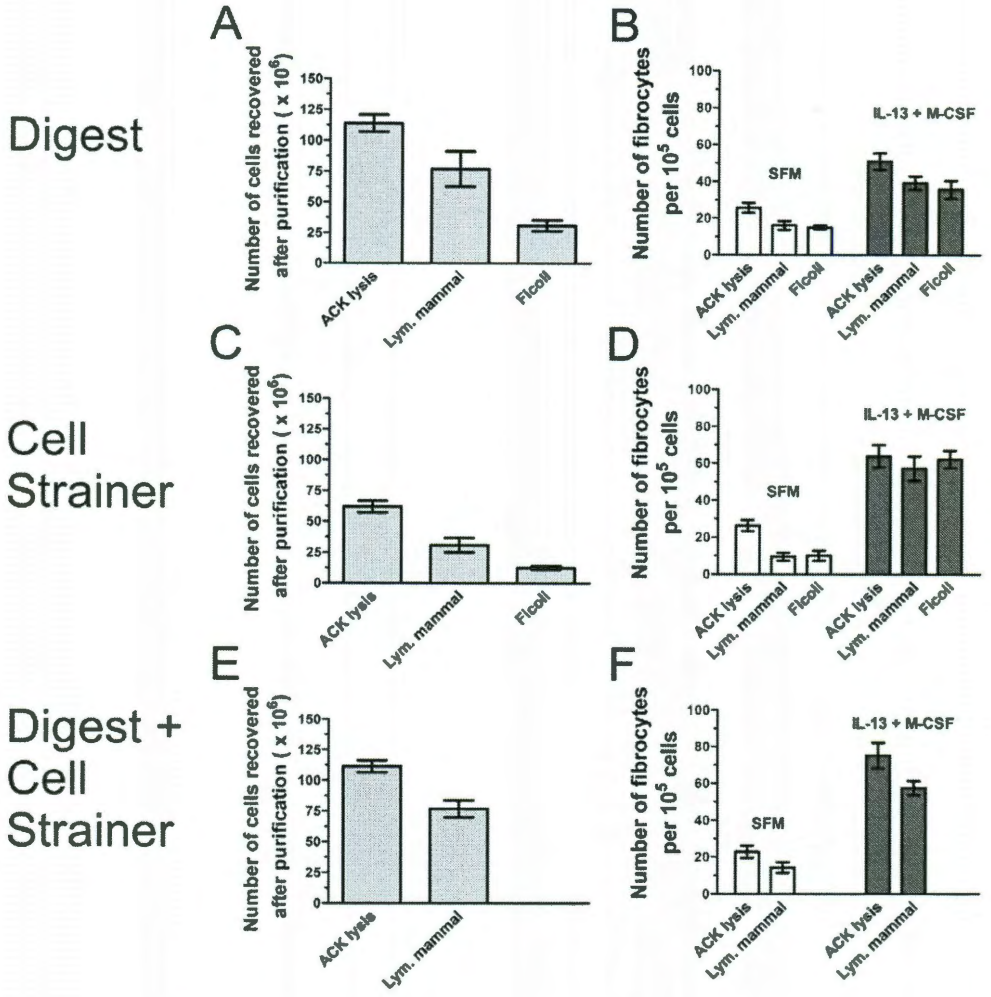

Figure 4.3: Effect of spleen cell isolation and purification techniques on fibrocyte differentiation. **A and B)** After removal, the spleen was treated with collagenase /DNase, and the cells were further purified through ACK lysis or density centrifugation. **C and D)** After removal, the spleen was passed through a 100 μm cell strainer, and the cells were further purified by ACK lysis or density centrifugation. **E and F)** After removal, the spleen was treated with collagenase/DNase and then passed through a 100 μm cell strainer. The cells were further purified by ACK lysis or Lympholyte-Mammal density centrifugation. For A, C, and E, the total number of cells recovered by the indicated purification technique was measured. For B, D, and F, the purified spleen cells were cultured in SFM in the presence or absence of IL-13 and M-CSF for 5 days. Cells were air dried, fixed, stained, and the number of fibrocytes was counted. Results are mean ± SEM (n=3).

morphology on day 1 and day 5 of the culture. The characteristic morphology of fibroblasts was never observed in the cultures, nor was there strong collagen staining of any cell in the culture, which would be indicative of a fibroblast. Finally, the influence of ACK lysis buffer on fibrocyte differentiation was examined to ensure that the higher fibrocyte yield compared to density centrifugation was not due to a biological effect by the ACK lysis buffer on the cells. Incubating Lympholyte-mammal (density centrifugation) purified cells with ACK lysis buffer did not significantly increase fibrocyte differentiation compared to density centrifugation alone (Figure 4.4), suggesting that the increased fibrocyte yield for ACK lysis is not due to the ACK lysis buffer directly promoting fibrocyte differentiation. Due to high spleen cell recovery and yielding the highest number of fibrocytes, the remaining experiments were performed using the digest cocktail plus cell strainer technique, followed by ACK lysis.

4.3.3 Effect of culture conditions on fibrocyte differentiation.

We previously found that human fibrocyte differentiation was increased when PBMC were cultured with the pro-fibrotic cytokines IL-4 and IL-13 (Shao *et al.*, 2008). Spleen monocytes have also been successfully cultured in the presence of GM-CSF and M-CSF (Swirski *et al.*, 2009), and fibrocyte differentiation from murine spleen cells was markedly enhanced using conditioned media from CD4+ T cells (Niedermeier *et al.*, 2009). Therefore, I tested the effect of cytokines on spleen cell differentiation in our serum-free medium culture conditions. ACK-treated spleen cells were cultured in the presence of murine M-CSF to promote monocyte survival, along with IL-4 and IL-13 as pro-fibrotic cytokines, both individually and in combination. Both M-CSF alone and the

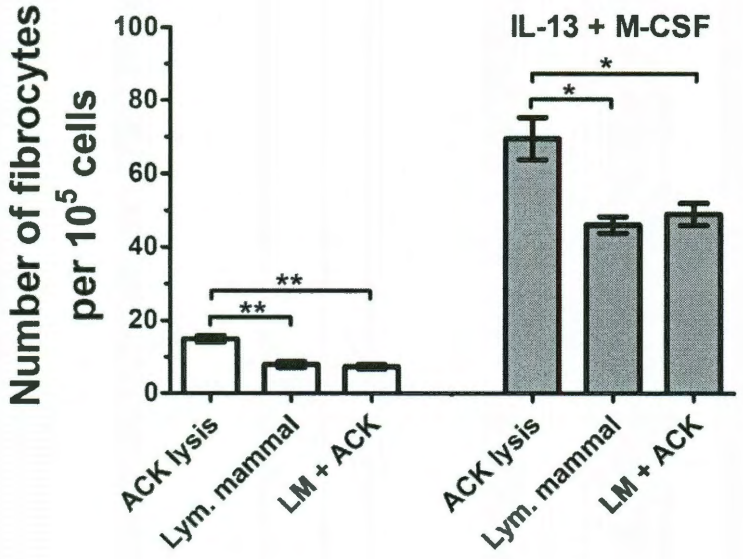

Figure 4.4: Treatment of spleen cells purified by density centrifugation with ACK lysis buffer does not enhance fibrocyte differentiation. After removal, the spleen was treated with collagenase/DNase and then passed through a 100 μm cell strainer. The cells were further purified through ACK lysis, density centrifugation using Lympholyte-Mammal (LM), or LM density centrifugation followed by a 3 minute incubation in ACK lysis buffer. Spleen cells were cultured in SFM in the presence or absence of IL-13 and M-CSF for 5 days at 3.5 x 10^5 cells per well. Cells were air dried, fixed, stained, and fibrocytes were counted. Cells purified by ACK lysis had increased fibrocyte differentiation compared to cells purified by density centrifugation (1-way ANOVA, Tukey's test). *, $p < 0.05$; **, $p < 0.01$. Treatment of spleen cells that have already been purified by density centrifugation with ACK lysis buffer did not significantly alter fibrocyte differentiation compared to cells only isolated with density centrifugation. Results are mean ± SEM (n=3).

combination of IL-13 and M-CSF increased the number of fibrocytes in culture, but M-CSF alone tended to promote macrophage and dendritic-like cell differentiation as well as spindle-shaped, pseudo-fibrocyte cells that did not meet the criteria of a fibrocyte, i.e., an elongated spindle-shaped cell with an oval nucleus (Figure 4.5A). These pseudo-fibrocytes tended to have round nuclei, shorter processes with increased width, and were not counted as fibrocytes. The addition of IL-13 and M-CSF resulted in significantly more elongated spindle-shaped cells with oval nuclei (Figures 4.5B), which also express the same fibrocyte markers found in Figure 1 (data not shown). When added individually, IL-4, at concentrations above 12.5 ng/ml, significantly decreased the number of fibrocytes, IL-13 had no effect on fibrocyte differentiation, and 25 ng/ml M-CSF significantly increased the number of fibrocytes (Figure 4.5C). When used in combination, IL-13 and M-CSF showed a significant increase in fibrocyte number compared to M-CSF alone (Figure 4.5D) and compared to cells not treated with cytokines (Figures 4.3B, 4.3D, 4.3F; Figure 4.5D; Figure 4.6). When IL-4 was cultured with M-CSF or in combination with M-CSF and IL-13, the number of fibrocytes was reduced to control levels, suggesting that the inhibitory effect of IL-4 counteracts the potentiating effects of M-CSF and IL-13 on fibrocyte differentiation (Figure 4.5D). Together, these results suggest that IL-13 and M-CSF can be used to promote the differentiation of fibrocytes from ACK-treated spleen cells in serum-free culture.

In vitro, human fibrocyte differentiation is dependent on cell density (Pilling *et al.*, 2009a). Therefore, ACK-treated spleen cells were cultured at different cell densities to determine the optimal culture condition. The highest yield of fibrocytes was observed

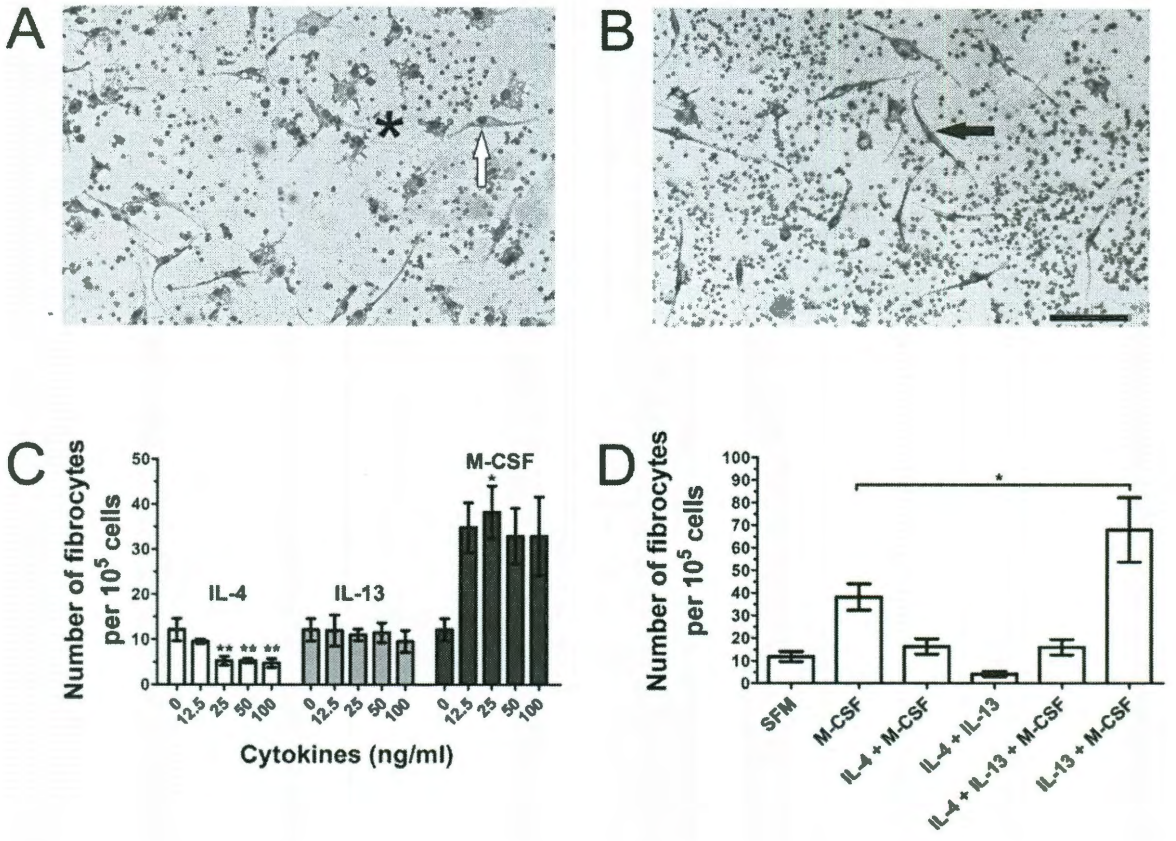

Figure 4.5: The effect of cytokines on spleen fibrocyte differentiation. ACK-treated spleen cells were cultured for 5 days at 3.5 x 10^5 cells per well in the presence of the indicated cytokines. Cells were air dried, fixed, stained, and the number of fibrocytes was counted. Wells treated with **(A)** M-CSF alone resulted in an increase of macrophage and dendritic-like cells (*) and pseudo-fibrocytes (white arrow), with round nuclei and shorter processes with increased width. Wells treated with **(B)** M-CSF and IL-13 in combination had more elongated, spindle-shaped cells with oval nuclei (black arrow). Bar is 100 μm, pictures are representative of 3 independent experiments. **(C)** IL-4, IL-13, and M-CSF were added to cultures individually to the indicated concentrations, or **(D)** in combination at 50 ng/ml for IL-4 and IL-13 and 25 ng/ml for M-CSF. Compared to SFM, ≥ 25 ng/ml IL-4 significantly reduced fibrocyte differentiation, while 25 ng/ml M-CSF significantly increased fibrocyte differentiation (1-way ANOVA, Dunnett's test). The combination of IL-13 and M-CSF significantly increased fibrocyte differentiation compared to M-CSF alone (1-way ANOVA, Dunnett's test). *, $p < 0.05$; **, $p < 0.01$. Results are mean ± SEM (n=3).

at $3.5x10^5$ cells per well (Figure 4.6). For the remaining assays, cells were cultured at 3.5 x 10^5 cells per well unless otherwise noted.

4.3.4 Monocyte origin of spleen-derived fibrocytes.

Fibrocyte precursors appear to differentiate from human CD14+ peripheral blood monocytes (Abe *et al.*, 2001 Yang *et al.*, 2002; Pilling *et al.*, 2003 & 2006). Niedermeier *et al.* (2009) found that murine fibrocytes derive from a GR-1+, Ly6G- monocyte subpopulation using splenocytes cultured for 14 days in serum. To confirm the origin of the fibrocytes in our serum-free 5 day culture system, I isolated monocytes from ACK-treated spleen cells. When the spleen cells were enriched for monocytes using an EasySep kit, the population of CD11b+, Ly6G- cells increased from less than 2.7% of total cells to more than 60% (Figures 4.7A, 4.7B, 4.7D, and 4.7E). Additionally, the monocyte-enriched population had an increase in the number of cells with kidney-shaped nuclei (Figures 4.7C and 4.7F) compared to spleen cell controls. The morphology of the cells along with the flow cytometry data suggests that the population was predominantly composed of monocytes. When cultured for 5 days, the monocyte-enriched population had a significant increase in fibrocyte differentiation (Figure 4.7G) compared to ACK-treated spleen cultures.

Niedermeier *et al.* (2009) found that the appearance of fibrocytes was dependent on CD11b+ monocytes. When monocytes and other CD11b+ cells were depleted from ACK-treated spleen cells using an EasySep CD11b kit, fibrocytes did not appear in our serum-free culture (data not shown). Together, the data suggest that the fibrocytes from

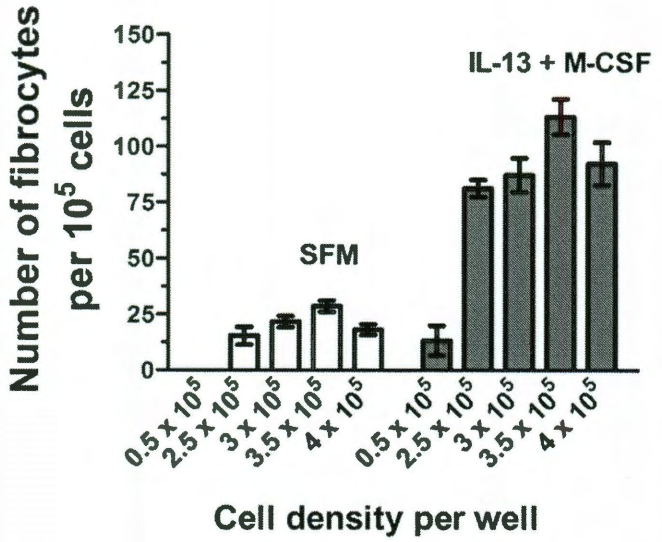

Figure 4.6: The effect of cell density on spleen fibrocyte differentiation. ACK-treated spleen cells were cultured in SFM in the presence or absence of IL-13 and M-CSF for 5 days at a range of cell densities. Cells were air dried, fixed, stained, and fibrocytes were counted. Results are mean ± SEM (n=3).

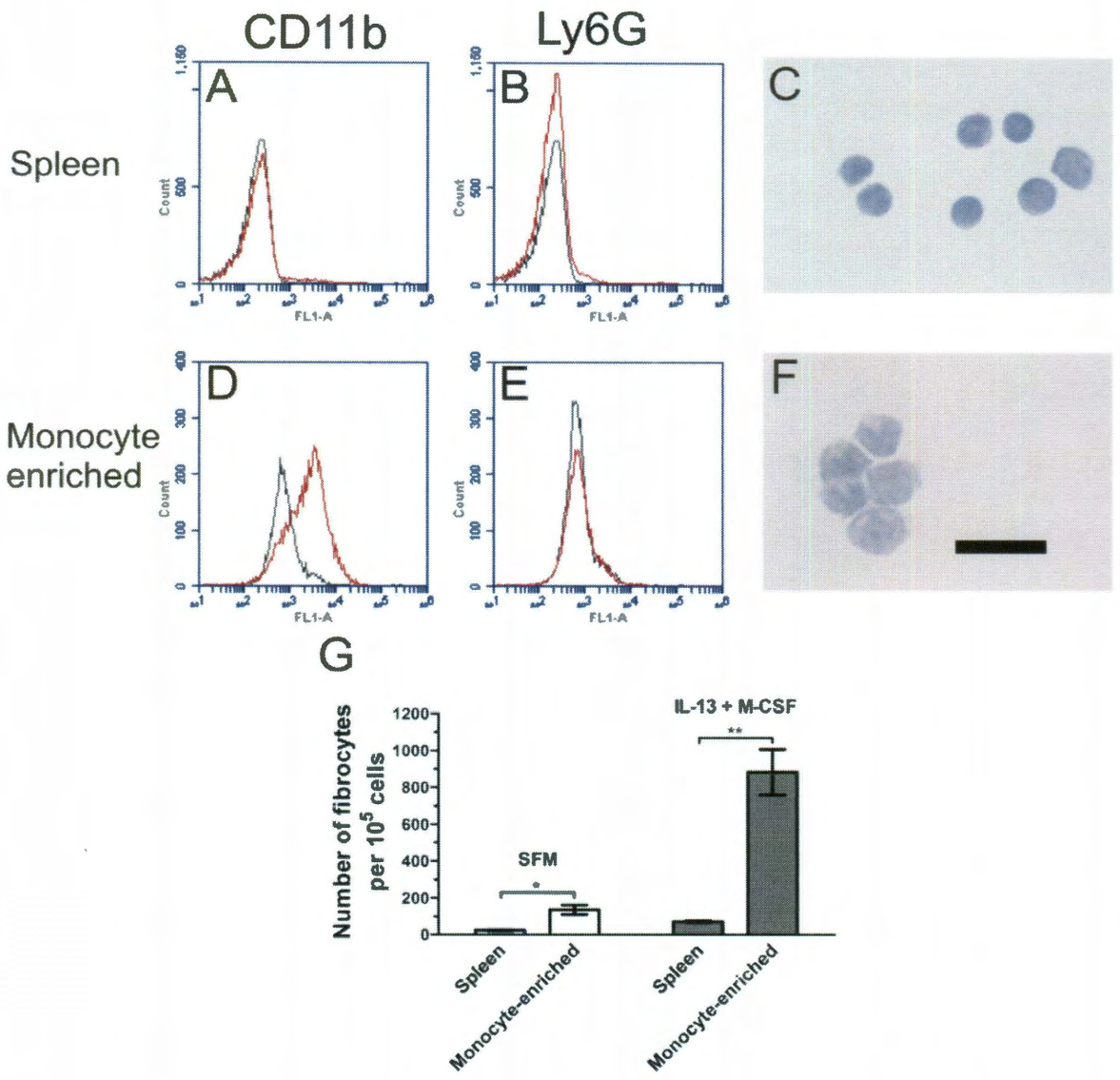

Figure 4.7: Enrichment of monocytes from spleen cells significantly enhances fibrocyte differentiation. Spleen cells were isolated through enzymatic digest, passed through a 100 μm cell strainer, and further purified by ACK lysis. The ACK-treated spleen cells were then enriched for monocytes through negative selection. ACK-treated spleen and monocyte-enriched cells were stained with rat monoclonal antibodies and analyzed by flow cytometry. Histograms show fluorescence intensity of isotype control antibody (black line) compared to the indicated antibody (red line). Compared to ACK-treated spleen cells **(A and B)**, monocyte-enriched cells **(D and E)** had an increased number of CD11b+, Ly6G- cells. Flow cytometry plots are representative of 3 independent experiments. ACK-treated spleen and monocyte-enriched cells were

analyzed for morphology. Monocyte-enriched cultures **(F)** showed an increased number of cells with kidney shaped nuclei (stained dark purple) compared to ACK-treated spleen cells **(C)**. Bar is 20 μm. Pictures are representative of 3 independent experiments. **G)** ACK-treated spleen and monocyte-enriched cells were cultured for 5 days at 3.5 x 10^5 cells per well and 0.5 x 10^5 cells per well, respectively, in the presence or absence of IL-13 and M-CSF. Cells were air dried, fixed, stained, and the number of fibrocytes was counted. Results are mean ± SEM (n=3). Monocyte-enrichment significantly increased the number of fibrocytes (t-test). *, $p < 0.05$; **, $p < 0.01$.

our serum free 5 day culture are of monocyte origin, comparable to what has been observed in other systems (Abe *et al.*, 2001; Pilling *et al.*, 2003; Niedermeier *et al.*, 2009).

4.3.5 SAP and cross-linked IgG inhibit the differentiation of spleen-derived fibrocytes.

We previously found that a number of factors can regulate the differentiation of human PBMCs into fibrocytes (Pilling *et al.*, 2003, 2006; Shao *et al.*, 2008). For instance, SAP and aggregated IgG inhibit fibrocyte differentiation (Pilling *et al.*, 2003, 2006). To determine if purified murine spleen cells can also be used to test the bioactivity of such factors, I cultured ACK-treated murine spleen cells with different concentrations of SAP. At concentrations above 80 nM, SAP significantly reduced the number of fibrocytes compared to serum-free medium and buffer controls (Figure 4.8). The IC50 values for SAP inhibition of murine spleen cells are comparable to those of murine PBMCs treated with SAP (Table 4.1). For both murine PBMCs and spleen cells, human SAP was significantly more effective at inhibiting fibrocyte differentiation than murine SAP. Together, these results suggest that cultured spleen cells can give similar biological responses as peripheral blood mononuclear cells. Interestingly, in the presence of IL-13 and M-CSF, the addition of 480 nM murine SAP did not fully inhibit fibrocyte differentiation (Figure 4.8B); however, the IC50 of murine SAP was not significantly altered (1-way ANOVA, Tukey's test, Table 4.1).

The differentiation of human PBMCs into fibrocytes is inhibited by cross-linked IgG (Pilling *et al.*, 2006). To determine if murine spleen cells have a similar biological

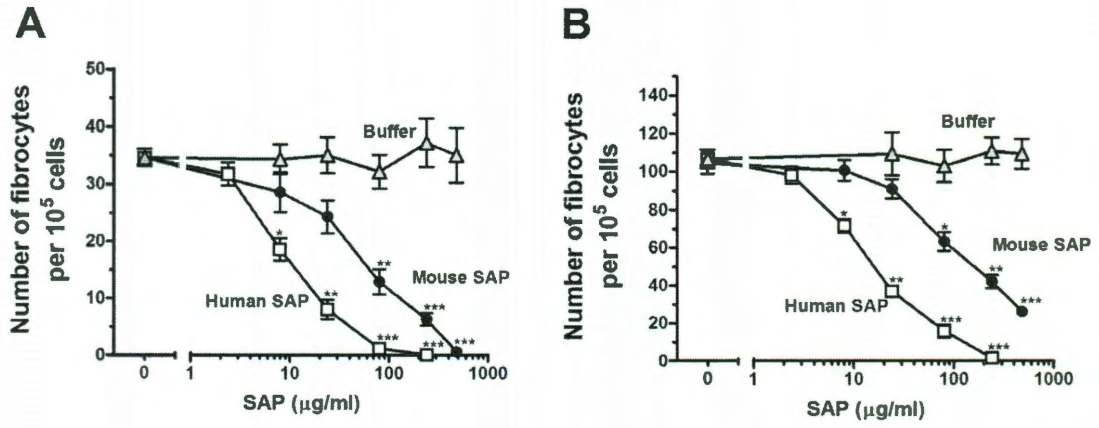

Figure 4.8: Murine and human SAP inhibit fibrocyte differentiation of cultured spleen cells. Murine, ACK-treated spleen cells were cultured for 5 days at 3.5 x 10^5 cells per well in the **(A)** absence or **(B)** presence of IL-13 and M-CSF, and the indicated mouse and human SAP concentrations. Cells were air dried, fixed, stained, and the number of fibrocytes was counted. Results are mean ± SEM (n=3). In the absence or presence of IL-13 and M-CSF, ≥ 10 μg/ml mouse SAP or ≥ 1 μg/ml human SAP significantly inhibited fibrocyte differentiation compared to buffer control (t-test). *, $p < 0.05$; **, $p < 0.01$; ***, $p < 0.001$.

Table 4.1: SAP IC50 values for the inhibition of fibrocyte differentiation in human and murine cell cultures.

Cells	Mouse SAP IC_{50} nM	Human SAP IC_{50} nM
Human PBMC	5.8 ± 1.1	3.0 ± 0.3 *
Murine PBMC	52.4 ± 7.4	11.8 ± 0.8 **
Murine Spleen	66.3 ± 15.7	9.6 ± 2.3 **
Murine Spleen + Cytokines	113.2 ± 27.7	14.2 ± 2.2 **

Human PBMCs, murine PBMCs, and murine spleen cells were cultured for 5 days at 5 x 10^4 cells per well, 2.5 x 10^5 cells per well, and 3.5 x 10^5 cells per well, respectively, in the presence of human and murine SAP. Murine spleen cells were also cultured in the presence or absence of the cytokines IL-13 and M-CSF. Cells were air dried, fixed, stained, and enumerated by morphology. Using fibrocyte counts normalized to SFM controls, IC_{50} levels were calculated by fitting SAP bioactivity to a sigmoidal dose response curve with variable slope. Results are expressed as mean ± SEM (n=5 for spleens, n=3 for mouse PBMCs, n=6 for human PBMCs). For the inhibition of fibrocyte differentiation by murine SAP, no significant difference was observed between the IC50 values for murine PBMCs and murine spleen cells (1-way ANOVA, Tukey's test). Human SAP was significantly more effective than murine SAP on both human cells ($p<0.05$) and mouse cells ($p<0.01$; t-test). *, $p < 0.05$; **, $p < 0.01$.

response, I cultured spleen cells in the presence or absence of monomeric and cross-linked IgG. Monomeric murine IgG at concentrations up to 100 μg/ml and goat-anti mouse IgG $F(ab')_2$ crosslinker alone had no effect on fibrocyte differentiation (Figure 4.9). The addition of goat $F(ab')_2$ anti-mouse IgG to monomeric IgG at concentrations as low as 10 μg/ml led to a significant reduction in fibrocyte differentiation (Figure 4.9). Similar to the ability of SAP and cross-linked IgG to inhibit the differentiation of human PBMCs into fibrocytes, the differentiation of mouse spleen cells into fibrocytes is inhibited by both SAP and cross-linked IgG. Since the biological response is consistent with those observed from human PBMC cultures, mouse spleen cultures appear to be a viable alternative to peripheral blood for studying factors that affect fibrocyte differentiation.

4.4 Discussion

We previously found that we could culture both human and murine PBMCs in serum-free culture for 5 days to obtain fibrocytes and use this system to test for factors that affect fibrocyte differentiation (Pilling *et al.*, 2003, 2006, 2009a; Shao *et al.*, 2008). However, to obtain enough mouse PBMCs, we had to pool blood from multiple mice. I therefore explored alternative sources for mononuclear cells, including the spleen. The spleen has been shown to contain monocytes that can participate in wound repair, and spleen cells have been shown to differentiate into fibrocytes in a 14 day serum culture

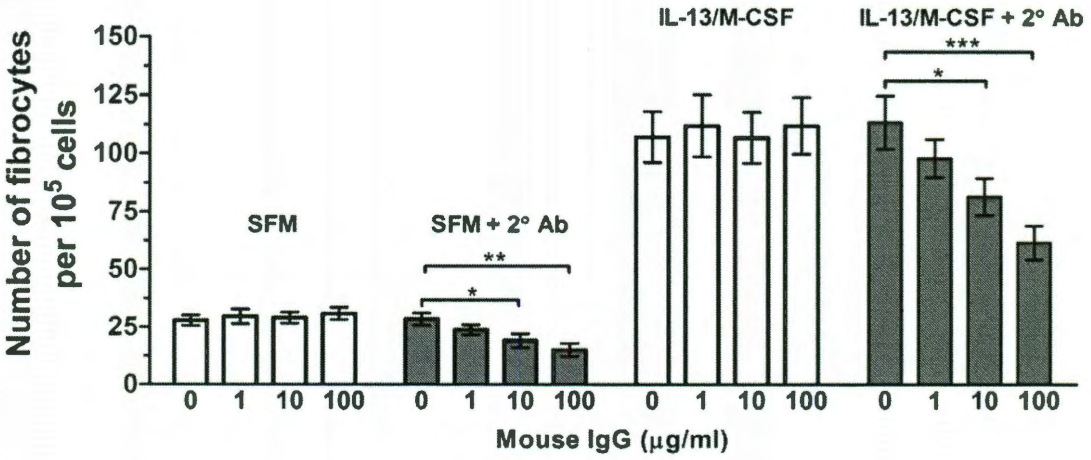

Figure 4.9: Cross-linked but not monomeric IgG inhibit fibrocyte differentiation of spleen cells. Murine, ACK-treated spleen cells were incubated with the indicated concentrations of murine IgG for 30 minutes, followed by incubation in the presence or absence of 500 ng/ml goat $F(ab')_2$ anti-mouse IgG cross-linker for 30 minutes. After washing the spleen cells, the cells were cultured for 5 days at 3.5 x 10^5 cells per well in the presence or absence of IL-13 and M-CSF. Cells were air dried, fixed, stained, and the number of fibrocytes was counted. Results are mean ± SEM (n=5). Compared to controls, cross-linked IgG at 10 and 100 µg/ml significantly reduced fibrocyte differentiation (1-way ANOVA, Dunnett's test). *, $p < 0.05$; **, $p < 0.01$; ***, $p < 0.001$.

(Swirski *et al.*, 2009; Niedermeier *et al.*, 2009). In this chapter, I found that murine spleen cells can also be cultured in our serum-free system to obtain fibrocytes and test for factors that can affect fibrocyte differentiation. My study focused on the common C57BL/6 strain. For other strains, the fibrocyte yield from spleen and blood cells, and response to cytokines, could be different, although results similar to C57BL/6 mice are expected.

I found that for optimal fibrocyte differentiation, leukocytes should be isolated from the spleen using a collagenase/DNase digest cocktail, followed by passage through a cell strainer and lysis of the red blood cells with ACK lysing buffer. The use of the digest cocktail led to an increase in the number of fibrocytes, which may be due to the release of monocytes attached to the matrix of the spleen. The number of non-red blood cells isolated from a spleen is ~ 40 times higher than the number of non-red blood cells isolated from approximately 1 ml of the peripheral blood of a mouse. However, the percentage of monocytes in the spleen cell preparation is 0.5% compared to 1-2% for the peripheral blood of C57BL/6 mice (Kile *et al.*, 2003; Swirski *et al.*, 2009). Thus, there are ~ 10 times more monocytes obtained from a spleen than peripheral blood. Approximately 6 % of the input monocytes from the spleen differentiated into fibrocytes, and this percentage increased 4-fold with the addition of IL-13 and M-CSF. For peripheral blood, ~ 8 % of the input monocytes differentiated into fibrocytes. These results are comparable to the differentiation in human PBMC, where ~ 5% of the input monocytes differentiate into fibrocytes, and this percentage is increased 4-fold with the addition of IL-13 (Pilling *et al.*, 2003 and 2009a; Shao *et al.*, 2008).

I further optimized fibrocyte differentiation by plating the cells at high cell density. The optimal cell density of 1.75 x 10^6 cells/ml is significantly higher than the optimal cell density of 2.5 x 10^5 cells/ml we observed for our serum free culture of human PBMCs (Pilling *et al.*, 2009a). One possible explanation for the higher optimal cell density for spleen cells is that the percentages of monocytes in murine blood and spleen are significantly lower than that of circulating monocytes in humans (Kile *et al.*, 2003; Swirski *et al.*, 2009; Robbins *et al.*, 2010). In addition, the promotion of fibrocyte differentiation by high cell density is may be due to both cell-to-cell contacts and soluble factors. In fact, T-cells have been shown to be required for the differentiation of spleen monocytes into fibrocytes (Niedermeier *et al.*, 2009), and Th2 cells can secrete pro-fibrotic cytokines such as IL-13, a factor known to enhance fibrocyte differentiation (Shao *et al*, 2008).

My final optimization was to repeat all assays in the presence of IL-13 and M-CSF. IL-13 was selected for its ability to enhance fibrocyte differentiation of human PBMCs (Shao *et al.* 2008) and M-CSF to promote monocyte survival (Becker *et al.*, 1987). Utilizing a combination of factors to promote leukocyte differentiation is a standard practice; for instance, GM-CSF and IL-4 are used to promote dendritic cells (Inaba *et al.*, 1992; Sallusto *et al.*, 1994), and M-CSF and serum are used to promote macrophages (Tushinski *et al.*, 1982). The use of IL-13 and M-CSF more than tripled the number of fibrocytes, while not significantly altering the biological response of the spleen cells to differing culture conditions and factors such as SAP and cross-linked IgG.

In contrast, IL-4 inhibited fibrocyte differentiation and negated the potentiating effects of IL-13 and M-CSF to control levels. We previously found that IL-4 promoted fibrocyte differentiation in human PBMCs (Shao *et al.*, 2008), but murine IL-4 has the opposite effect when incubated with murine spleen cells, which was also observed by Niedermeier *et al.* (2009). The ability of IL-4 to counteract IL-13 and M-CSF can partially be explained by the fact that mouse monocytes are significantly more sensitive to levels of IL-4 than IL-13 (Junttila *et al.*, 2008). Additionally, there is biological divergence between humans and mice for cytokine activity, such as the differential effects on B cells by IL-4 and IL-13 (Mestas *et al.*, 2004), but a possible divergence has not been fully explored for fibrocyte differentiation. It is known that IL-4 is non-essential in the bleomycin-induced model of murine lung fibrosis (Izbicki, *et al.,* 2002), while IL-13 deficient animals were protected from FITC-induced lung fibrosis (Kolodsick *et al.*, 2004). However, both cytokines and their receptors are induced in bleomycin-induced lung fibrosis (Jakubzick *et al.*, 2003)

I was able to culture over 3 x 10^4 fibrocytes from a single spleen, and this number increased to 1.1 x 10^5 fibrocytes in the presence of IL-13 and M-CSF. This is considerably higher than the 4 x 10^3 fibrocytes we could obtain from the peripheral blood of a single mouse (~ 1 ml). After 14 days in cultures containing serum, Abe *et al.* (2001) observed 8 – 40 x 10^3 fibrocytes from 1 ml of peripheral blood. The higher number of fibrocytes observed by Abe *et al.* (2001) could be due to the culturing of fibrocytes for 14 days in serum compared to our culturing of fibrocytes in serum-free medium for 5 days. Another possibility is that Abe *et al.* (2001) identified fibrocytes using flow cytometry

and staining for CD11b and collagen I, while I identified fibrocytes both morphologically and by marker expression.

The serum-free culture of mouse spleen cells resulted in the differentiation of fibrocytes over a short period of time compared to the typical 14 day period required in serum-based cultures. The delay in serum-based cultures is likely due to components in serum such as IgG and SAP that can inhibit fibrocyte differentiation. I was able to identify conditions to produce a high yield of fibrocytes from a single spleen, and the cells were sensitive to factors known to inhibit fibrocyte differentiation. This will allow for efficient testing of factors that can affect fibrocyte differentiation in multiple murine backgrounds.

Chapter 5: Determining which FcγR subtype regulates fibrocyte differentiation.

5.1 Introduction

An alternative means to determining how SAP functions is through the deletion or knockdown of SAP's only known receptor, FcγR. The current literature is unclear regarding how SAP interacts with FcγRs. One group found that human SAP (hSAP) has a lower affinity for binding to human FcγRs than IgG, and that hSAP has the highest affinity for FcγRI among the different receptor subtypes (Lu et al., 2008). Another group found that hSAP has a higher affinity for binding to human FcγRs than IgG, and that hSAP binds with highest affinity to FcγRIIa and III (Castano et al., 2009). A third group found that hSAP binds with highest affinity to FcγRI and FcγRIIa, and a lower affinity to FcγRIIIb (Bharadwaj et al., 2001).

Human SAP has previously been shown to bind to a 3T3 mouse fibroblast cell line expressing specific mouse FcγR subtypes with the relative rank order of FcγIV >Fcγ III ≥ FcγI > FcγIIb (Castano et al., 2009). Also, Castano *et al.* (2009) determined by surface plasmon resonance that human SAP binds with the following order of affinity: hFcγRIIA ~ hFcγRIII > hFcγRI >> hFcγRIIb. Again, there are differences in the biology between humans and mice, where human FcγRIIa and III have similar binding affinities, while mouse FcγRIV (the equivalent of human FcγRIIA) has significantly higher affinity than FcγIII. Therefore, when determining which receptor subtype is responsible for regulating fibrocyte differentiation, I will examine both human and mice cells.

Previously, we tested if SAP could act as a therapeutic in cardiac fibrosis-induced mice that lack the gamma chain required by all the activating FcγRs (Haudek et al., 2008). SAP was not able to reduce the level of fibrosis, suggesting that engagement of an activating FcγR (I, III, or IV) is necessary for SAP's function. However, this result does not reveal which specific receptor is necessary and does not give any information regarding the inhibitory receptor's (FcγRIIb) possible involvement in regulating fibrocyte differentiation.

We can use the *in vitro* fibrocyte differentiation assay from Chapter 4 to measure changes in SAP's bioactivity when incubated in mice spleen cells lacking the various FcγR subtypes. This will allow us to see more subtle shifts in SAP's bioactivity that might not be observable in a more complex biological system such as a fibrosis-induced mouse. SAP could act through multiple FcγRs and removing a single receptor subtype may not eliminate bioactivity, but would likely cause a noticeable shift in the bioactivity curve that could otherwise be missed *in vivo*. However, the differences in biology between human and mice FcγRs means that we should not rely solely on mouse knock outs for analysis. I will also be using siRNA against human FcγRs to study any changes in SAP bioactivity after knocking down various receptors singly and eventually in combination.

In this chapter, I will use a combination of FcγR KO and siRNA to determine which FcγRs are critical for SAP's ability to inhibit fibrocyte differentiation. We know that the γ chain (FcRγ) is necessary for SAP's bioactivity *in vivo*, so initially the FcRγ

KO mice and siRNA knockdown of FcRγ in human PBMCs can be tested as a positive control. Deletion of FcγRI and FcRγ in murine cells and reduction of FcγRI and FcRγ in human cells reduced sensitivity to SAP. Together, this suggests that SAP, at least in part, uses FcγRI and FcRγ to inhibit fibrocyte differentiation.

5.2 Methods

5.2.1 Cell fractionation of spleen cells

4-6 week male C57BL/6J mice (Jackson Laboratories, Bar Harbor, ME or Taconic, Hudson, NY), B6.129P2-*Fcgr3*$^{tm1Sjv/J}$ mice (Jackson Laboratories), B6.129S4-*Fcgr2b*^{tm1TtK} N12 mice (Taconic), B6.129P2-*Fcer1g*^{tm1Rav} N12 mice (Taconic) were used in this study. FcγRII/III/IV knock out mice in C57BL6/J background were kindly donated by Dr. Sjef Verbeek at Leiden University Medical Center. Spleen cells from FcγRI knockout mice (Ioan-Facsinay et al., 2002) were kindly donated by Dr. Bryce Binstadt at the University of Minnesota. All work was done under Rice and Texas A&M IACUC approved protocols. Spleens were harvested (~70-100 mg each) and cells were isolated by digesting in a cocktail of 450 U/ml collagenase I (EMD, San Diego, CA), 60 U/ml DNase I, and 60 U/ml hyaluronidase (Sigma-Aldrich, St. Louis, MO) in 1 ml RPMI (Sigma-Aldrich) for 30 minutes at 37°C. The digest was then forced through a 100 μm cell strainer (BD Biosciences, San Jose, CA) using the plunger of a 3 ml syringe (BD Medical, Franklin Lakes, NJ) and 5 ml of RPMI. The cells were resuspended in 10 ml RPMI and collected by centrifugation at 300 x g for 10 minutes. Cells were then resuspended in 940 μl ACK lysis buffer (0.15 M NH_4Cl, 10 mM $KHCO_3$, 0.1 mM Na_2EDTA; Kruisbeek, 2000) for 3 minutes at room temperature, and the reaction was stopped by the addition of 14 ml PBS. The cells were collected by centrifugation at 200

x g for 10 minutes, and the PBS wash step was repeated 3 additional times. A final wash was carried out by resuspending the cells in 1.5 ml Fibrolife basal media (Lifeline Cell Technology, Walkersville, MD) with supplements, and the cells were collected by centrifugation at 300 x g for 5 minutes at 4° C.

5.2.2 Fibrocyte differentiation assay for spleen cells

Fibrolife serum free media was prepared as discussed in section *4.2.3*, including the addition of 50 ng/ml murine IL-13 and 25 ng/ml murine M-CSF (Peprotech) for select wells. Spleen cells were cultured in flat-bottomed 96 well tissue culture plates (353072, BD Biosciences) at 3.5 x 10^5 cells per well in 200 µl in a humidified incubator containing 5% CO_2 at 37° C. Murine and human SAP (EMD-Calbiochem) in 20 mM sodium phosphate buffer, pH 7.4, were added to the cells at the indicated concentrations. On day 3 of the incubation, wells with IL-13 and M-CSF were further supplemented with 5 µl of a cocktail containing 1 µg/ml IL-13 and 0.5 µg/ml M-CSF in Fibrolife SFM. After 5 days, plates were air dried, fixed with methanol, and stained with Hema 3 stain (Fisher Scientific).

Flow cytometry

Mouse spleen cells were subjected to flow analysis as described previously (Crawford et al., 2010; Pilling et al., 2009) with the following modifications. Cells were stained using 5 µg/ml of antibodies against CD3 (clone 17A2, rat IgG2b, BD Biosciences), CD45R/B220 (clone RA3-6B2, rat IgG2a, BD Biosciences), CD11c (clone 223H7, rat IgG2a, MBL Int., Woburn, MA), CD16/32 (clone 2.4G2, rat IgG2b, BD

Biosciences), CD94 (clone HMa2, rat IgG2a, eBioscience, San Diego, CA), Ly6G (clone 1A8, rat IgG2a, BioLegend), GR-1 (clone RB6-8C5, rat IgG2b, BD Biosciences), F4/80 (clone BM8, rat IgG2a, Biolegend), and isotype-matched irrelevant rat monoclonal antibodies (Biolegend) as controls. The secondary antibody was a FITC-conjugated mouse $F(ab')_2$ anti-rat IgG (Jackson Immunoresearch, West Grove, PA), used at 2.5 μg/ml. After blocking with PBS/10% rat serum (Sigma-Aldrich) for 30 minutes at 4° C, cells were collected by centrifugation at 300 x g for 5 minutes, and resuspended in 100 μl of PBS/4% BSA containing 2.5 μg/ml PE-conjugated anti-CD11b antibody (clone M1/70, rat IgG2b, eBioscience) and 5 μg/ml biotinylated anti-CD45 antibody (clone 30-F11, rat IgG2b, BD Biosciences). After a 30 minute incubation on ice, cells were washed twice with 1.4 ml ice-cold PBS and resuspended in 100 μl ice-cold PBS/BSA containing 2 μg/ml streptavidin-APC (Biolegend). After a 30 minute incubation on ice, cells were washed twice, resuspended in 100 μl ice-cold PBS/BSA, and analyzed using a C6 flow cytometer (Accuri, Ann Arbor, MI).

5.2.3 SiRNA knockdown.

Silencer select siRNA's (Applied Biosystems/Ambion, Austin, TX) were reconstituted in H_2O to 50 μM. Human PBMCs were isolated and purified as described above. Transfection of human PBMCs was carried out with Lipofectamine 2000 (Invitrogen), following the manufacturer's protocol. 5.25 pmol siRNA was incubated in 25 μl Fibrolife basal media (Lifeline) + HEPES (Sigma-Aldrich) with 0.25 μl Lipofectamine 2000 for 20 minutes. The mixture was then diluted in 2.1 ml Fibrolife SFM lacking antibiotics to obtain a concentration of 2.5 nM siRNA. 200 μl siRNA was added to the top row of a 96

well plate, and 100 µl doubling dilutions were carried out using an equal volume of Fibrolife SFM lacking antibiotics to obtain 100 µl of the indicated concentrations of siRNA. 100 µl of PBMCs at $5x10^5$ cells/ml in SFM was added to each well, and the plate was incubated for 24 hours in a humidified incubator containing 5% CO_2 at 37° C. hSAP (EMD Calbiochem) was added at the indicated concentrations 24 hours later in 3 µl aliquots. The plate was returned to the incubator, and after 4 additional days the plates were air dried, fixed with methanol, and stained.

5.2.4 Determination of expressed protein levels of Fc gamma receptors after siRNA knockdown.

SiRNA plates were set up as described above except SAP was not added. After 2.5 days, the wells were washed with 100 µl PBS, fixed with 75 µl PBS/4% paraformaldehyde on ice for 15 minutes, washed twice for 5 minutes with 100 µl PBS, permeabilized with 75 µl PBS/0.1% Triton X-100 for 10 minutes at room temperature, and washed three times for 5 minutes with 100 µl PBS. The wells were blocked with 100 µl PBS/4% BSA at 4° C overnight. Cells were stained for one hour with primary antibody or IgG-matched controls (Biolegend and Epitomics) in 50 µl PBS/4% BSA using: 5 µg/ml rabbit anti-human FcεRI, γ subunit (06-727, Millipore), 5 µg/ml mouse anti-human CD64 (clone 10.1, mouse IgG1, BD Biosciences), 7.5 µg/ml goat anti-human CD32a (AF1875, R&D Systems), 1:100 rabbit anti-human CD32b (clone EP926Y, Epitomics), or 1:100 rabbit anti-human CD16a (clone EPR4333, Epitomics). The wells were washed four times for 5 minutes with 100 µl PBS. The primary antibodies were detected with biotinylated $F(ab')_2$ goat anti-rabbit IgG (Southern Biotech), biotinylated goat $F(ab')_2$

anti-mouse IgG (Southern Biotech), or biotinylated $F(ab')_2$ donkey anti-goat IgG (Jackson Immunoresearch). All secondary antibodies were incubated for 30 minutes at 2.5 μg/ml in 50 μl PBS/BSA, and the wells were then washed four times for 5 minutes with 100 μl PBS. After washing, the wells were incubated for 30 minutes with 2.5 μg/ml of streptavidin-conjugated Dylight-488 antibody (Thermo Scientific). The wells were washed four times for 5 minutes with PBS, and the wells were coated with 30 μl of Vectashield mounting media (Vector Labs, Burlingame, CA), containing 4',6-diamidino-2-phenylindole. Immunofluorescence images were captured using an Olympus FV1000 confocal microscope (Olympus, Center Valley, PA), and ImageJ (Rasband, WS, NIH, Bethesda, MD) was used for analysis. Mean fluorescent intensity was measured for each cell, excluding sizes smaller than 156 μm^2 to eliminate cell debris and lymphocytes.

5.3 Results

5.3.1 Murine FcRγ and FcγRI mediate sensitivity to SAP.

Because altering key residues of hSAP at the predicted FcγRIIa binding site (Lu et al., 2008) had only a modest effect on SAP bioactivity (Figure 2.13E), other FcγRs may bind SAP. The observation that FcRγ appears to be necessary for SAP to inhibit fibrosis *in vivo* (2 μg/g for lung or 20 μg/g for kidney) (Castano et al., 2009; Haudek et al., 2008), suggests that SAP might activate FcγRI or FcγRIII. To test this, I measured the inhibition of fibrocyte differentiation by SAP using cells from mice lacking specific FcγRs. I used the plentiful splenic reservoir of monocytes (Niedermeier et al., 2009; Swirski et al., 2009) to test for SAP bioactivity (Crawford et al., 2010), as outlined in Chapter 4.

With respect to fibrocyte differentiation, the bioactivity of murine and human SAP on FcRγ KO cells was significantly reduced compared to the bioactivity on wild-type cells (Figures 5.1A, 5.1B, and 5.2). These data suggest that fibrocyte differentiation is regulated by activating FcγRs and that the mouse spleen *in vitro* fibrocyte differentiation assay is a viable method for studying this effect in KO mice.

Compared to wild-type cells, FcγRI KO cells were significantly less sensitive to murine and human SAP (Figures 5.1C, 5.1D, and 5.2). The shift in bioactivity was obfuscated by an overall reduction in total fibrocyte number for the FcγRI KO cells compared to WT cells (Figures 5.1C and 5.1D). These data suggest that FcγRI mediates some of the effect of SAP on fibrocyte differentiation.

5.3.2 Murine FcγRIIb reduces sensitivity to SAP.

FcγRIIb KO and FcγRIII KO cells differentiated into an abnormally low number of fibrocytes (Figure 5.3A-D). FcγRIIb KO cells were more sensitive to murine SAP than wild-type cells, while FcγRIII KO cells showed a normal sensitivity (Fig. 5.2A). These data indicate that neither FcγRIIb nor FcγRIII are critical for the ability of SAP to inhibit fibrocyte differentiation.

5.3.3 Cells from FcγRIIb/III/IV KO mice have normal sensitivity to SAP.

As SAP inhibited fibrocyte differentiation from spleen cells of both FcγRIIb KO and FcγRIII KO mice, we determined if the deletion of multiple FcγRs affects the ability of SAP to inhibit fibrocyte differentiation. Spleen cells from FcγRIIb / FcγRIII / FcγRIV

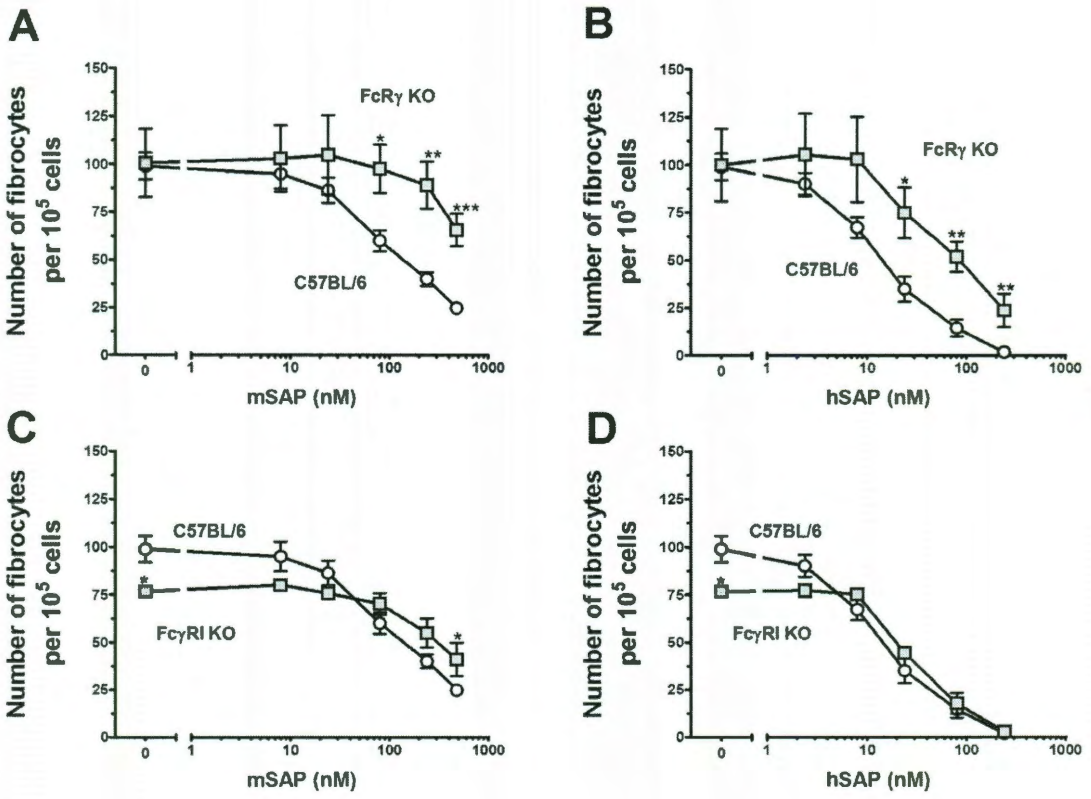

Figure 5.1: Murine FcRγ KO and FcγRI KO cells are less sensitive to SAP than wild-type C57BL/6 cells. Cells were cultured in the indicated concentrations of mSAP **(A and C)** or hSAP **(B and D)**. After a 5 day incubation, cells were air dried, fixed, stained, and the number of fibrocytes was counted. Results are mean ± SEM (n=5 for C57BL6, n=4 for FcRγ KO, n=3 for FcγRI). **(A and B)** At concentrations above 24 nM for mSAP and concentrations above 8 nM for hSAP, SAP bioactivity was significantly reduced for the FcRγ KO cells compared to wild-type cells, as determined by t test. *, $p < 0.05$; **, $p < 0.01$; ***, $p < 0.001$. **(C and D)** At 480 nM, mSAP bioactivity was significantly reduced for the FcγRI KO cells compared to WT spleen cells, as determined by t test. *, $p < 0.05$. FcγRI KO spleen cells had significantly fewer fibrocytes in the serum free control wells compared to WT spleens (t test, *, $p < 0.05$).

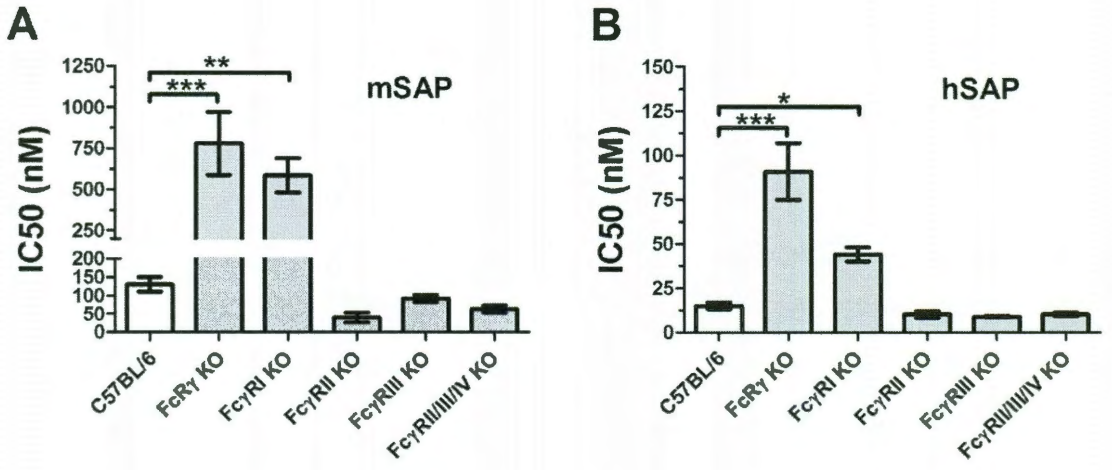

Figure 5.2: SAP IC50 values for the inhibition of fibrocyte differentiation in FcγR KO cell cultures. Spleen cells from the indicated strains of mice were cultured in the presence of **(A)** murine or **(B)** human SAP. Cells were air dried, fixed, stained, and enumerated by morphology. Using fibrocyte counts normalized to SFM controls, IC_{50} levels were calculated by fitting SAP bioactivity to a sigmoidal dose response curve with variable slope. Values are mean ± SEM (n=5 for C57BL/6, n=3 for FcγRIIb KO and FcγRIIIa KO, n=4 for FcRγ KO, FcγRI KO, and FcγRIIb/IIIa/IV KO). FcRγ KO and FcγRI KO spleen cells were significantly less responsive to SAP compared to the WT strain (1-way ANOVA, Dunnett's test) *, $p < 0.05$; **, $p < 0.01$, ***, $p < 0.001$. If the data is also examined by t-test, then FcγRIIb KO and FcγRIIb/IIIa/IV KO spleen cells were significantly more responsive to mouse SAP compared to WT cells ($p < 0.05$).

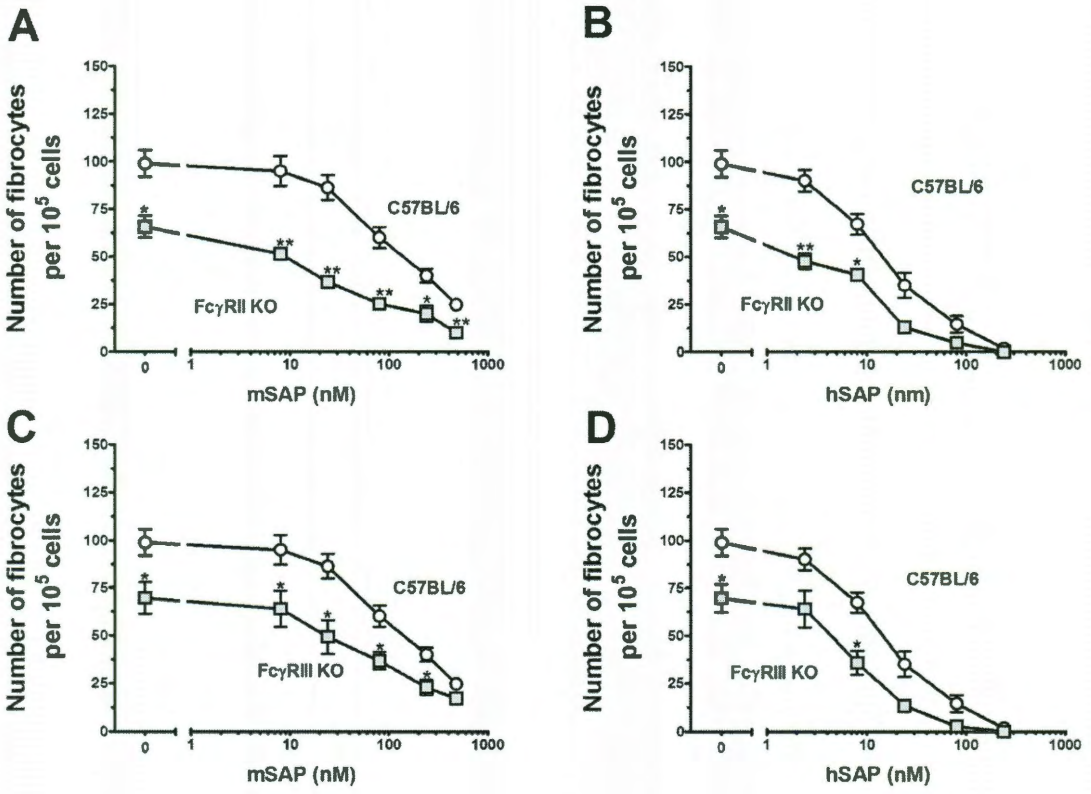

Figure 5.3: FcγRIIb KO cells have increased sensitivity to SAP, while FcγRIIIa KO cells have normal sensitivity. Cells from C57BL/6, FcγRIIb KO, and FcγRIIIa KO mice were cultured in the indicated concentrations of mSAP **(A and C)** or hSAP **(B and D)**. Values are mean ± SEM (n=3, except n=5 for C57BL/6). **(A and B)** FcγRIIb KO spleen cells had significantly fewer fibrocytes in the serum free controls compared to WT spleen cells, and had an increased sensitivity to **(A)** murine and **(B)** human SAP, as determined by t test. *, $p < 0.05$; **, $p < 0.01$. **(C and D)** FcγRIIIa KO spleen cells had significantly fewer fibrocytes in the serum free control wells compared to WT spleens (t test, *, $p < 0.05$).

triple KO mice also allowed us to examine if FcγRIV regulates fibrocyte differentiation, which we did not have access to as an individual knockout. The triple KO cells differentiated into an abnormally low number of fibrocytes (Figures 5.4A and 5.4B). However, the IC50 of hSAP in the triple KO spleen cells was comparable to that of WT mice (Figure 5.2B), although the triple KO spleen cells were about twice as sensitive to mSAP as wild-type cells (Figure 5.2A). The spleen cells from the triple KO mice responded to murine and human SAP to the same degree or with increased sensitivity compared to spleen cells from WT mice, suggesting that these receptors are not essential for SAP's ability to inhibit fibrocyte differentiation. To determine if the reduced fibrocyte number was due to a decrease in the number of monocytes in the spleen, we analyzed spleen cells for cell markers by flow cytometry. Spleens from the triple KO mice had normal numbers of total cells, monocytes (CD45+, CD11b+, GR1+ cells), and other leukocytes (Table 5.1). This suggests that the low fibrocyte yield was not due to a reduced number of monocytes in the spleen. These data indicate that SAP is still able to reduce fibrocyte differentiation in the absence of FcγRII, FcγRIII, and FcγRIV at least to the same degree as normal controls; however, the lack of these receptors does affect the development of fibrocytes in culture.

5.3.4 Reduction of FcRγ and FcγRI in human cells significantly reduces sensitivity to SAP.

Because of the differences in biology between mouse and human FcγRs, we also examined how reducing FcγR expression in human cells using siRNA (Table 5.2) affects the inhibition of fibrocyte differentiation by SAP. The siRNAs were transfected into

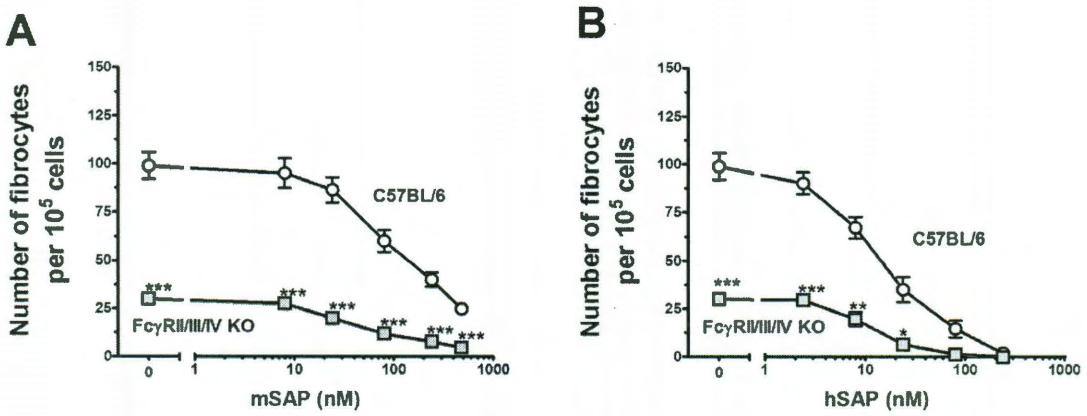

Figure 5.4: FcγRIIb/IIIa/IV KO spleen cells produce significantly fewer fibrocytes compared to WT C57BL/6 cells. Cells from WT C57BL/6 and FcγRIIb/IIIa/IV KO mice were cultured in the indicated concentrations of mSAP **(A)** or hSAP **(B)**. Values are mean ± SEM (n=4 for KO, n=5 for C57BL/6). **(A and B)** The FcγRIIb/IIIa/IV KO spleen cells had a significantly lower number of fibrocytes in the serum-free control wells compared to WT spleen cells, as determined by t test. *, $p < 0.05$; **, $p < 0.01$; ***, $p < 0.001$.

Table 5.1: Expression of surface markers on CD45+ spleen cells for wild-type and FcγRII/III/IV KO mice

Marker	C57BL/6 WT	FcγRII/III/IV KO
Rat IgG Control	0.7 ± 0.1	0.6 ± 0.1
CD3	37 ± 2	39 ± 2
B220	46 ± 1	49 ± 4
F4/80	1.6 ± 0.5	1.0 ± 0.3
CD11b	9.2 ± 0.3	8.0 ± 0.1
CD11c	2.9 ± 0.3	2.3 ± 0.3
Ly6G + CD11b	0.9 ± 0.1	1.0 ± 0.4
GR-1 + CD11b	2.1 ± 0.1	1.9 ± 0.3
CD94	1.6 ± 0.4	1.0 ± 0.5
CD16/32	62 ± 6	0.5 ± 0.1

Mouse spleen cells were stained with rat monoclonal antibodies and analyzed by flow cytometry. Average total cell number isolated from the spleens was 115 ± 6 x 10^6 for C57BL/6 and 110 ± 8 x 10^6 for the FcγRII/III/IV KO. All samples were gated for CD45+. Results are percent positive cells expressed as mean ± SEM (n = 3).

Table 5.2: Genes targeted for siRNA knockdown

Target gene	ID #	Sense 5′→3′	Successful reduction
FCER1G (FcRγ)	s5062	GCUCUGCUAUAUCCUGGAUtt	N
	s5064	CCAGCUAUGAGAAAUCAGatt	Y
FCGR1A (FcγRIa)	s5068	GAAAAAGUGGGAUUUAGAAtt	N
	s5070	GACUCUGGGUUAUACUGGUtt	Y
FCGR2A (FcγRIIa)	s5072	CUUCAACCAUUGACAGUUtt	Y
	s223524	AAACCAUCAUGCUGAGGUGtt	Y
FCGR2B (FcγRIIb)	s5073	CCUAUUCACUUCUCAUFCAtt	Y
FCGR3A(FcγRIIIa)	s5078	CAUUCGAAGCUCAACAAGAtt	Y
	s57396	CCUCCUGUCUAGUCGGUUUtt	Y
Scrambled	4390843		N/A

Succcessful reduction (Y) indicates a significant reduction in the protein levels of receptor after the addition of siRNA ($p < 0.05$; 1-way ANOVA, Dunnett's test). N – no reduction, N/A – not applicable.

human PBMCs using concentrations up to 1.25 nM, as concentrations above 1.25 nM (scrambled or specific siRNA) nonspecifically inhibited fibrocyte differentiation (data not shown). The addition of hSAP to the PBMCs was delayed 24 hours to give time for the siRNAs to act. Reduction of levels of FcRγ reduced sensitivity to hSAP (Figures 5.5A, 5.5N, and 5.6A). These effects were not observed with a scrambled siRNA control (Figures 5.5A and 5.6A). This suggests that hSAP acts through activating FcγRs in regulating human fibrocyte differentiation, which corresponds with the data from FcRγ KO mice (Figures 5.1A, 5.1B, and 5.2). Reducing the levels of FcγRI also significantly reduced sensitivity to hSAP (Figures 5.5A, 5.5C, and 5.6B). This suggests that hSAP acts at least in part through FcγRI to inhibit human fibrocyte differentiation.

5.3.5 Reduction of FcγRIIb in human cells increases sensitivity to SAP.

Reducing the levels of of FcγRIIa (Figure 5.7A) did not significantly affect sensitivity to hSAP (Figures 5.8A, 5.8C, and 5.8D). However, an increase in fibrocyte number was observed (Figure 5.8A), suggesting that this receptor could have a modest effect on fibrocyte differentiation. Reduction of FcγRIIb levels (Figure 5.7B) resulted in a significant decrease in the number of fibrocytes even in the absence of hSAP (Figure 5.8B), and an increase in sensitivity to hSAP (Figure 5.8E). This result is similar to the increased sensitivity observed in FcγRIIb knockout mice (Figures 5.2, 5.3A and 5.3B). Reduction of FcγRIIIa levels (Figure 5.7C) did not significantly alter sensitivity to hSAP (Figures 5.8B, 5.8F, and 5.8G). These data suggest that FcγRIIa and FcγRIIb may affect fibrocyte differentiation, and that FcγRIIb appears to counteract SAP's ability to inhibit fibrocyte differentiation.

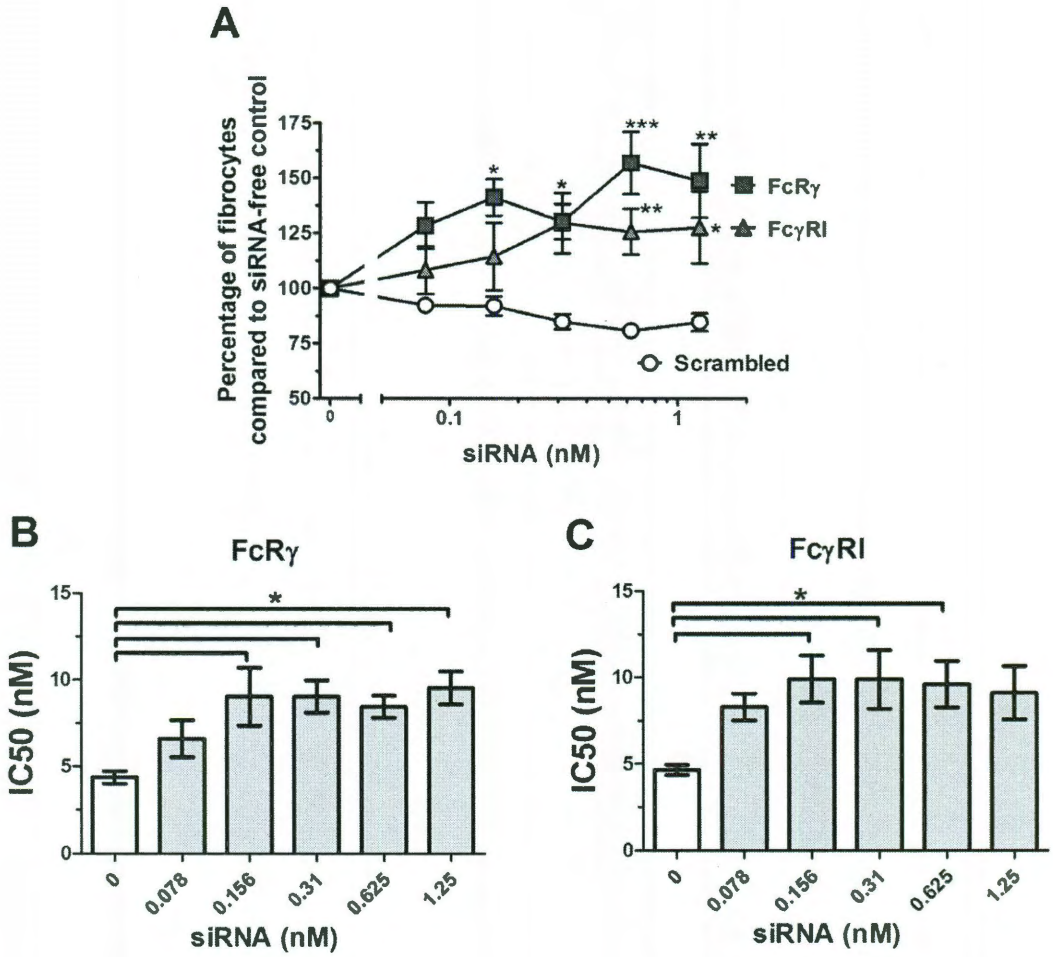

Figure 5.5: siRNA knockdown of FcRγ and FcγRI (CD64) in human PBMC significantly reduces hSAP bioactivity. Human PBMCs were cultured in the presence of siRNA or an equal volume of serum-free medium. After 24 hours, hSAP was added to the cultures at 2, 1, and 0.5 μg/ml. After 5 days, fibrocytes were counted. Results are normalized to the number of fibrocytes in the absence of siRNA. Values are mean percentage ± SEM (n=5 FcRγ, n=6 for FcγRI). **(A)** PBMCs were treated with 0.5 μg/ml hSAP, and the change in SAP bioactivity was measured through fibrocyte counts. siRNA knockdown of FcRγ and FcγRI significantly increased the number of fibrocytes compared to scrambled controls (t test). *, $p < 0.05$; ** $p < 0.01$. **(B and C)** IC50 levels were measured for hSAP's ability to inhibit fibrocyte differentiation. siRNA knockdown of FcRγ and FcγRI significantly increased the IC50 levels of hSAP compared to siRNA-free controls (1-way ANOVA, Dunnett's test). *, $p < 0.05$.

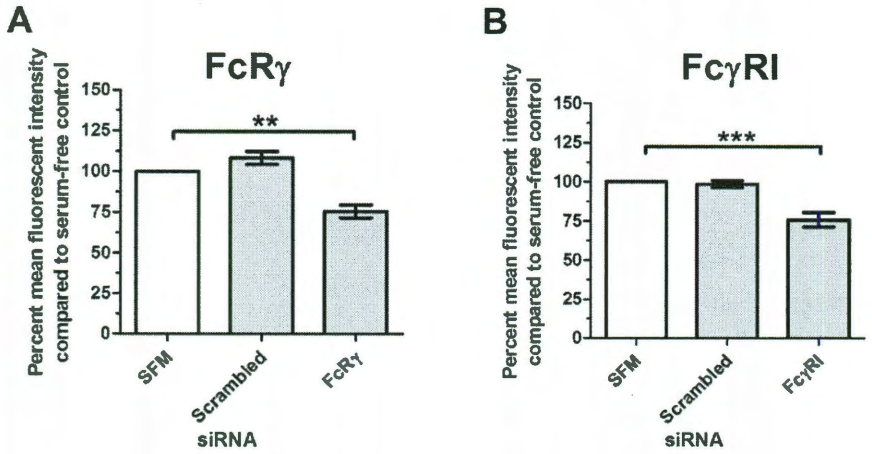

Figure 5.6: SiRNA knockdown of FcRγ and FcγRI (CD64) significantly reduces the corresponding protein levels. Cells were stained for FcRγ and CD64 and visualized with Dylight 488. Results are normalized to the mean fluorescent intensity of cells in the serum free control wells, and the results are expressed as the mean percentage ± SEM (n=3 for FcRγ, n=4 for FcγRI). A minimum of 100 cells was counted per condition. The levels of **(A)** FcRγ and **(B)** FcγRI were significantly reduced in cell cultures treated with siRNA (1-way ANOVA, Dunnett's test). **, $p < 0.01$; ***, $p < 0.001$.

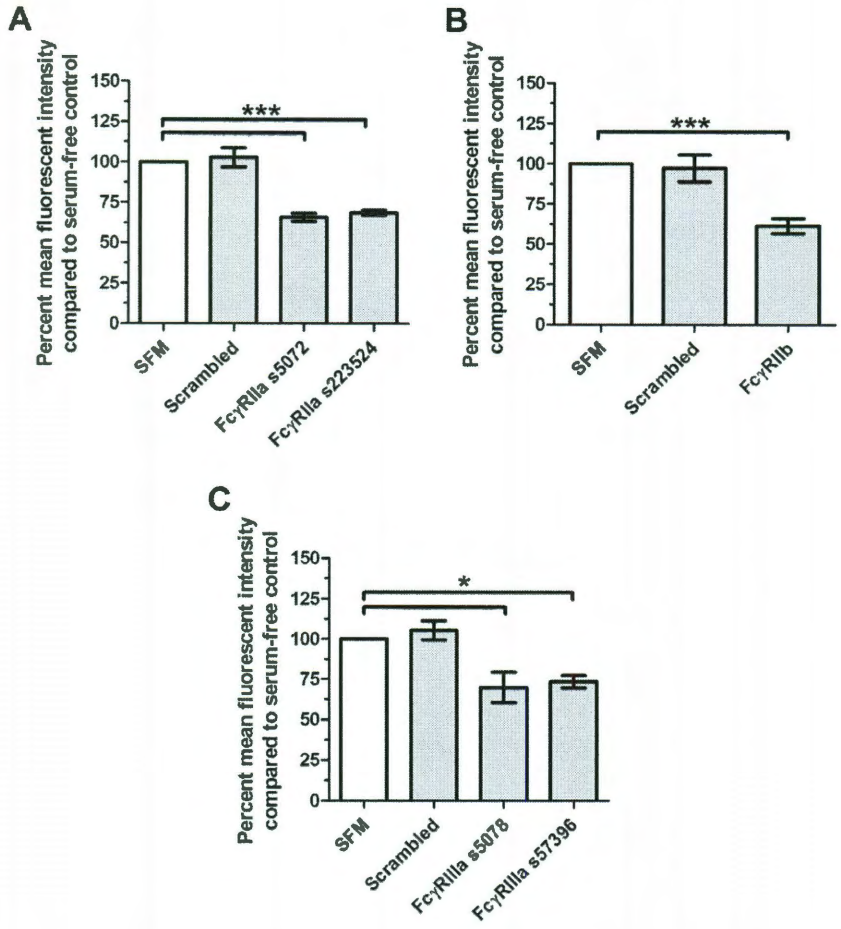

Figure 5.7: siRNA knockdown of FcγRIIa, -IIb, and -IIIa significantly reduces the corresponding protein levels. Human PBMCs were cultured for 3 days in the presence of siRNA or an equal volume of serum-free medium, and were then stained for the associated receptor. Results are normalized to the mean fluorescent intensity of cells in the serum free control wells, and the results are expressed as the mean percentage ± SEM (n=3). A minimum of 100 cells was counted per condition. The levels of **(A)** FcγRIIa, **(B)** FcγRIIb, and **(C)** FcγRIIIa were significantly reduced in cell cultures treated with siRNA (1-way ANOVA, Dunnett's test). *, $p < 0.05$; ***, $p < 0.001$.

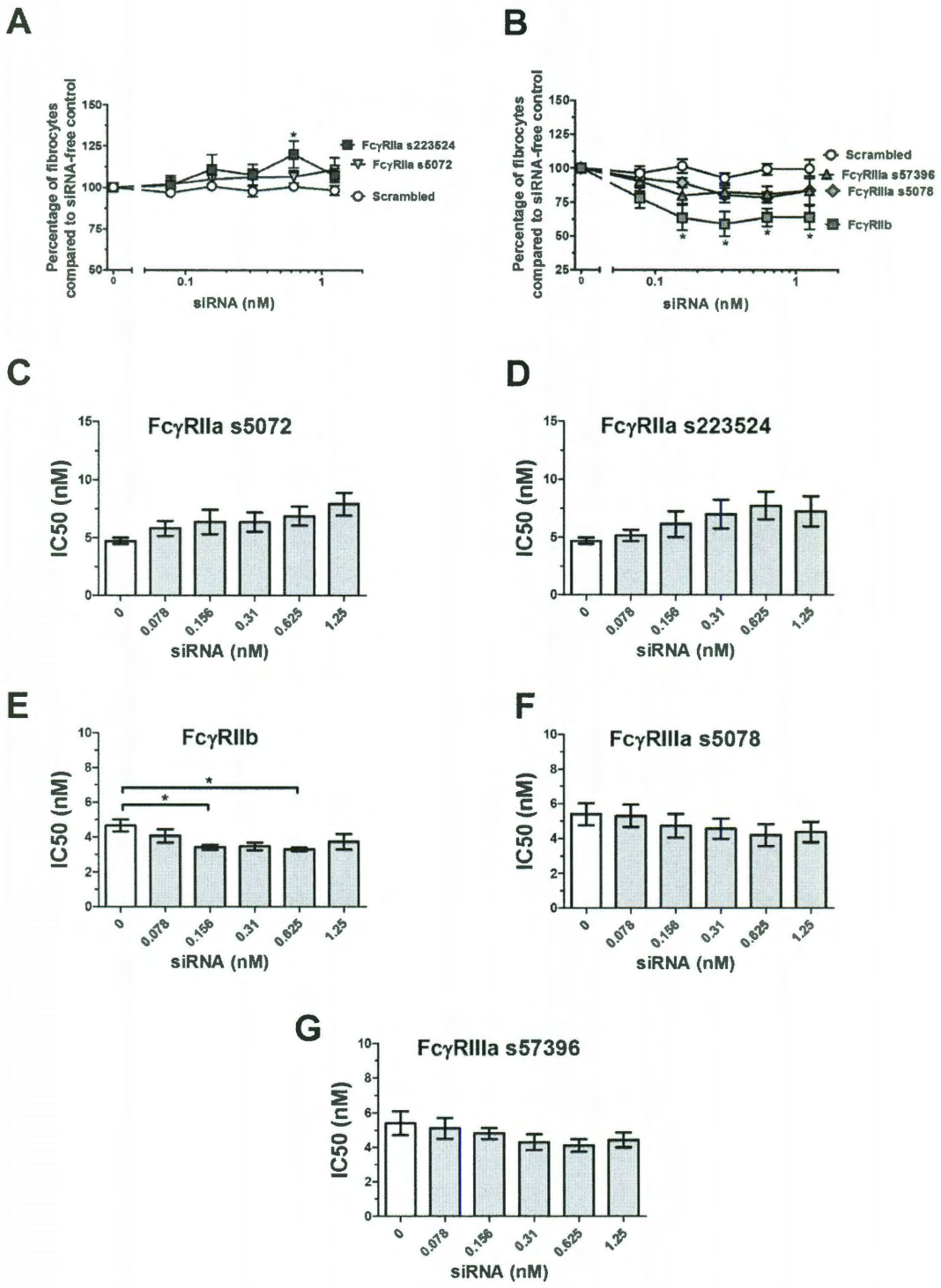

Figure 5.8: siRNA knockdown of FcγRIIa and FcγRIIIa does not significantly alter hSAP's bioactivity, while knockdown of FcγRIIb increases sensitivity to hSAP. Human PBMCs were cultured for 5 days in the presence of siRNA or an equal volume of

serum-free medium. At 24 hours, hSAP was added to the cultures at 2, 1, and 0.5 μg/ml. Results are normalized to the number of fibrocytes in siRNA-free wells, and the results are expressed as the mean percentage ± SEM (n=3, n=6 for FcγRIIa). **(A and B)** PBMCs were treated with 0.5 μg/ml hSAP, and the change in SAP bioactivity was measured through fibrocyte counts. siRNA knockdown of FcγRIIb significantly decreased the number of fibrocytes compared to scrambled controls (t test). *, $p < 0.05$. **(C – G)** IC50 levels were measured for hSAP's ability to inhibit fibrocyte differentiation. siRNA knockdown of FcγRIIb significantly decreased the IC50 levels of hSAP compared to siRNA-free controls (1-way ANOVA, Dunnett's test). *, $p < 0.05$.

5.4 Discussion

To elucidate key components of SAP bioactivity, I examined how the different Fcγ receptors affect the ability of SAP to inhibit fibrocyte differentiation. However, in the absence of added SAP, deletion of FcγRIIb in mice and reduction of FcγRIIb in human cells both decreased the number of fibrocytes observed in cultures. Deletion of other FcγRs in mice, or reduction of their levels in human cells, also affected fibrocyte numbers, but there was no correlation between the mouse and human data.

Deletion of FcγRI or the FcRγ chain in mice, and reduction of FcγRI or the FcRγ chain levels in human cells, significantly decreased but did not abolish the sensitivity of cells to SAP. This indicates that FcγRI and the FcRγ chain play a major role in the signal transduction pathway that SAP uses to inhibit fibrocyte differentiation. However, the ability of SAP to inhibit fibrocyte differentiation in cells lacking FcγRI or FcRγ suggests that SAP activates receptors in addition to FcγRI, and additionally activates a signaling pathway that does not require FcRγ.

In wild-type mice, SAP injections inhibit fibrosis, while in $FcR\gamma^{-/-}$ mice, injections of the same amounts of SAP do not inhibit fibrosis (Castano et al., 2009; Haudek et al., 2008). Based on my observation that in cultures of $FcR\gamma^{-/-}$ cells, only very high concentrations of SAP inhibit fibrocyte differentiation, we would predict that in $FcR\gamma^{-/-}$ mice, injections of high concentrations of SAP should inhibit fibrosis.

Deletion of FcγRIII in mice, and reduction of FcγRIIa or FcγRIIIa levels in human cells (mice do not have FcγRIIa) had no significant effect on the sensitivity of cells to SAP. This suggests that FcγRIIa and FcγRIIIa do not play a major role in the effect of SAP on fibrocyte differentiation. However, the mutagenesis data from Chapter 2 for the FcγRIIa-SAP interaction and the slightly increased fibrocyte numbers for the siRNA knockdown of FcγRIIa does mean that FcγRIIa could play a modest role.

Deletion of FcγRIIb in mice, and reduction of FcγRIIb levels in human cells, increased the sensitivity of cells to SAP. This suggests that FcγRIIb may activate a pathway that counteracts the ability of SAP to inhibit fibrocyte differentiation. An intriguing possibility is that signals that promote fibrocyte differentiation may be sensed by this receptor. The increased sensitivity to SAP could also be the result of FcγRIIb acting as a decoy receptor for SAP, although SAP does not have high binding affinity to FcγRIIb (Castano et al., 2009).

The FcγRIIb/IIIa/IV triple KO spleen cells retained full sensitivity to SAP. I did not have access to the single FcγRIV KO, but the SAP activity in the triple KO mice suggests that FcγRIV is not essential for SAP bioactivity. However, the triple KO cells differentiated into an abnormally low number of fibrocytes. This suggests that fibrocyte differentiation may be regulated by unknown factors that signal using one or more pathways that interact with pathways regulated by FcγRIIb/IIIa/IV. Combined with the observations that cytokines, angiotensin II, leukotrienes, TLR agonists, and hyaluronan fragments regulate fibrocyte differentiation (Haudek et al., 2010; Maharjan et al., 2010,

2011; Shao et al., 2008; Vannella et al., 2007), my results showing that SAP uses FcγRI as well as other unknown receptors, and FcRγ as well as other intracellular signaling components, indicates that a complex network regulates fibrocyte differentiation.

For future directions, we will be testing SAP bioactivity in a quadruple FcγR KO to determine if other receptors are involved in the regulation of fibrocyte differentiation, including other receptors that utilize FcRγ. The γ chain is known to associate with the FcεRI and dectin-2, mediators of the innate immune response involved in allergens and fungi, respectively (Sato *et al.*, 2006). Recently, SAP was also found to weakly bind to FcαRI with a K_d of 3.2 μM, while SAP binds to FcγRs with an affinity in the nM range (Castano *et al.,* 2009; Lu *et al.*, 2011). FcαRI activates through the common γ chain like FcγRs and similarly is expressed by monocytes, but FcαRI relies on engagement of IgA to elicit an immune response resulting in phagocytosis, antigen presentation, and the release of inflammatory cytokines (Herr *et al.*, 2003). However, neither heat aggregated IgA nor heat aggregated IgE were found to inhibit fibrocyte differentiation, suggesting that these receptors are not likely candidates (Pilling *et al.*, 2006). There remains some possibility, though, as SAP and IgG appear to inhibit fibrocyte differentiation through distinct but related pathways (Pilling *et al.*, 2006).

Chapter 6: Brain Serum amyloid P levels are reduced in individuals that lack dementia while having Alzheimer's disease neuropathology

6.1 Introduction

In addition to elucidating SAP's functional domain, we are also interested in the bioactivity of SAP in various disease states to further our understanding on how SAP functions *in vivo*. SAP was originally identified as a major component of amyloid deposits and is even co-localized with the amyloid plaques associated with Alzheimer's (Pepys *et al.*, 1982; Duong *et al.*, 1989). Two key neuropathological hallmarks of AD are amyloid plaques, formed by extracellular aggregates of beta amyloid (Aβ) peptide, and intracellular neurofibrillary tangles, composed of hyperphosphorylated tau protein. Mild cognitive impairment (MCI) is an intermediate state on the path to AD, where 10-15% progress to full stage Alzheimer's, and MCI individuals have a limited number of plaques and tangles (Guillozet et al., 2003). Interestingly, some people with high levels of beta amyloid plaques and neurofibrillary tangles, referred to as non-demented with AD neuropathology (NDAN), do not develop dementia (Aizenstein et al., 2008; Bennett et al., 2006; Reiman et al., 2009). Understanding the mechanism involved in such resistance would be important for the future development of novel, effective treatments for AD.

The exact cause and progression of AD is still poorly understood. The hallmark amyloid plaques and neurofibrillary tangles are found in the regions of the brain that deal with memory and higher cognitive function, such as the cortex, hippocampus, basal

forebrain, and amygdala (Mattson *et al.*, 2004). During the course of the disease, the patient experiences a loss of synapses, neuronal death, and neuroinflammation that is likely caused by soluble Aβ oligomers that eventually will form plaques, as well as disruption by the hyperphosphorylated tau proteins (Lee *et al.*, 2010). One risk factor for Alzheimer's is Apolipoprotein E (ApoE) which helps in the clearance of Aβ peptides by promoting proteolytic degradation (Jiang *et al.*, 2008). A specific allele of ApoE poses an increased risk for AD, APOE-ε4, while ε3 is neutral and ε2 is protective (Corder *et al.*, 1993).

SAP does not readily cross the blood brain barrier; however, neurons in the brain can produce SAP, and this production is upregulated in AD brains (Yasojima et al., 2000) although there is no difference in the cerebrospinal fluid (CSF) levels of SAP between AD patients and age-matched normal controls (Kimura et al., 1999; Mulder et al., 2002; Verwey et al., 2008). Among AD patients, one study using 70 patients found that higher CSF levels of SAP tended to correlate with less dementia (Kimura *et al.*, 1999), while a smaller study using 20 patients did not observe any trend (Mulder *er al.*, 2002). SAP potentially contributes to the pathogenesis of Alzheimer's disease through the binding of amyloid plaques and neurofibrillary tangles (NFTs) (Coria et al., 1988; Kalaria and Grahovac, 1990; McGeer et al., 2001). SAP has been found to enter neurons, and at elevated levels can induce apoptosis *in vitro* and *in vivo* (Urbanyi et al., 2003; Urbanyi et al., 2007). Additionally, SAP was described to stabilize amyloid plaques by preventing the proteolysis of Aβ fibrils (Tennent et al., 1995); however, other results suggest that addition of SAP actually inhibits initial fibril formation and dose-dependently increases

the solubility of Aβ peptide (Janciauskiene et al., 1995). SAP binds to fibrils in all types of amyloid deposits, but SAP is not essential for this deposition (Pepys, 2006). However, amyloid deposition throughout the body in reactive systemic amyloidosis is significantly delayed in SAP knockout mice, suggesting that SAP plays an important role in the pathogenesis of amyloid diseases (Botto et al., 1997; Togashi et al., 1997).

In this chapter, I show that SAP levels are reduced in the brains of NDAN individuals compared to the levels in the brains of AD patients. This reduction can be detected in both the hippocampus and frontal cortex. SAP staining is colocalized to the amyloid plaques and is reduced in NDAN hippocampal tissue compared to AD. This suggests that a reduced presence of SAP associated with senile plaques characterizes the amyloid deposits in the brain of individuals who do not develop dementia despite the presence of amyloid plaques and neurofibrillary tangles consistent with fully symptomatic AD.

6.2 Methods

6.2.1 Cases

Frozen brain tissue samples were obtained from the Oregon Brain Bank at Oregon Health and Science University (OHSU) in Portland, OR. Donor subjects were enrolled and clinically evaluated in studies at the NIH-sponsored Layton Aging and AD Center (ADC) at OHSU. Control subjects were participants in brain aging studies at the ADC. Subjects received annual neurological and neuropsychological evaluation, with CDR assigned by an experienced clinician. Autopsies were carried out post mortem from 2 to

24 hours, with most cases under 10 hours (Table 1). All cases (n=4) classified as Alzheimer's fulfilled the National Institute of Neurological and Communicative Disorders and Stroke and the Alzheimer's Disease and Related Disorders Association criteria for definitive Alzheimer's with histopathologic evidence of amyloid plaques and neurofibrillary tangles in the hippocampus and neo-cortex, as well as cognitive impairment with a mini-mental state exam (MMSE) score below 10. Control cases did not display cognitive impairment (MMSE of 28-30) and had either no or a very limited number of amyloid plaques and neurofibrillary tangles. Mild cognitive impairment cases had some cognitive impairment with MMSE scores in the mid 20s, and intermediate levels of amyloid plaques and neurofibrillary tangles. NDAN cases displayed little to no cognitive impairment (MMSE 26 to 30), while having extensive amyloid plaques and neurofibrillary tangles in the hippocampus and neo-cortex, comparable to full on-set Alzheimer's (Figure 1).

6.2.2 Western Blot

0.5 g of hippocampus or frontal cortex was homogenized in 1.5 ml of 0.32 M sucrose in 0.1 mM $CaCl_2$ with 1% protease inhibitor cocktail (Sigma Aldrich, St. Louis, MO) and 1x phosphatase inhibitor cocktail (Thermo, Waltham, MA). Samples were diluted 1:20 in PBS/0.2% SDS/Triton-X 100, and protein concentration was determined by Bradford (Sigma). Samples were normalized to 2 mg/ml in 50 µl SDS-PAGE sample buffer, run on 4-20% SDS-PAGE gels (Bio-Rad, Hercules, CA) and visualized by Coomassie stain to further confirm protein concentration. SAP concentration was determined by Western blotting as described previously (Pilling et al., 2003) with the

Table 6.1: Case studies

Diagnosis	Age	Sex	PMI	Braak Stage[a]	Plaque Score[a]	MMSE
Control[b]	82.7	M	14	1	4	N/A
Control[b]	83.1	M	2	1	1	N/A
Control[b]	77.4	F	12	0	4	N/A
Control	>89	F	18	0	4	28
Control	80	M	2	1	3	30
Control	28	F	15.5	0	4	N/A
Control	43	F	10	0	4	N/A
Control	51	M	9.5	0	4	N/A
Control	60	F	40.5	0	4	N/A
MCI[c]	>89	M	23	3	2	26
MCI[c]	89	F	20	3	2	22
MCI[c]	>89	F	12	3	2	27
MCI	>89	F	4	2	3	25
MCI	79	F	12	2	4	28
AD[b]	>89	M	3.25	6	1	2
AD[b]	61	M	4	6	1	2
AD[b]	79	N/A	6	6	1	N/A
AD	82	F	19	6	2	9
AD	60	N/A	4.5	6	2	N/A
AD	64	M	9.25	6	1	1
AD	62	F	6.5	6	2	7
AD	87	M	8.75	6	2	N/A
NDAN[b]	87.8	M	3	4	1	29
NDAN[b]	>89	F	4.5	6	1	27
NDAN[c]	87	F	2.5	2	3	29
NDAN	87.6	F	10.5	5	2	29
NDAN	89	F	2.5	5	2	27
NDAN	>89	F	18	6	4	30

Abbreviations are as follows: MCI - mild cognitive impairment, AD - Alzheimer's disease, NDAN, non-demented with Alzhiemer's disease neuropathology, M - male, F - female, PMI - postmortem interval in hours, MMSE - Mini-Mental State Examination, N/A - not available.

[a] Scoring based on Braak and Braak (Braak and Braak, 1991).

Tissue sample from hippocampus unless otherwise noted.
[b] Frontal cortex tissue only
[c] Hippocampus and frontal cortex tissue

	Ages	Sex	PMI	Braak	Plaque	MMSE
Control	28 - >89	4M/5F	13.7 ±3.8	1 ± 1	4 ± 1	29 ± 1
MCI	79 - >89	1M/4F	14.2 ±3.4	3 ± 1	3 ± 1	26 ± 1
AD	60 - 87	2M/2F	9.6 ±2.5	6 ± 0*	2 ± 1*	6 ± 2*
NDAN	87 - >89	1M/5M	6.8 ±2.6	5 ± 1*	2 ± 1*	29 ± 1

* denotes values significantly different than control values ($p < 0.05$; 1-way ANOVA, Dunnett's test)

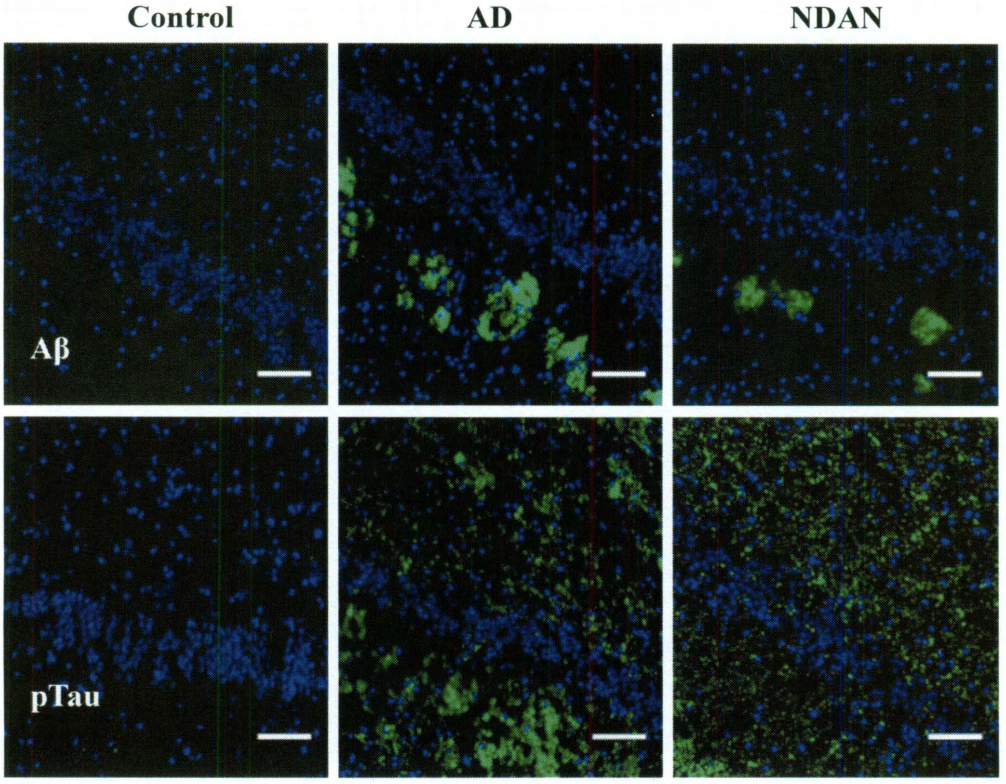

Figure 6.1: Pathological signatures of AD occur in cognitively intact individuals (NDAN). Reactivity for Aβ plaques (green, top row) and phosphorylated tau (green, bottom row) in the dentate gyrus of individuals classified as control (Braak 1, Plaque 3, MMSE 30), AD (Braak 6, Plaque 1, MMSE 2), or NDAN (Braak 6, Plaque 1, MMSE 27). DAPI mounting media was used to visualize nuclei (blue). Bar 100μm.

following modifications. Commercially available SAP (EMD Biosciences, Rockland, MA) was used as loading controls. SAP was detected using a rabbit anti-SAP antibody (Epitomics, Bulringame, CA) at a 1:10,000 dilution. Quantification of band intensity was performed via ImageJ (Rasband, WS, NIH, Bethesda, MD) and statistical analysis was done with GraphPad Prism (Graphpad Software, San Diego, CA).

6.2.3 Immunohistochemistry

Five mm sections of the mid hippocampus were brought out of storage at -80 °C and equilibrated to -20 °C before embedding in Tissue-Tek O.C.T. compound (Sakura Finetek USA, Torrance, CA). 10 μm sections were cut and affixed to Superfrost Plus slides (Thermo Fisher Scientific, Waltham, MA), for storage at -80°C. After briefly equilibrating to room temperature, sections were rinsed in 0.1 M PBS and then fixed in ice-cold 4% paraformaldehyde for 15 minutes. After two brief washes in 0.1 M PBS, the sections were blocked and permeabilized for 1 hour in 0.1 M PBS containing 10% goat serum, 0.03% Triton-X, and 0.1% phosphatase inhibitor (Thermo Fisher). Incubation with primary antibodies in 0.1 M PBS containing 10% serum and 0.1% phosphatase inhibitor was carried out overnight at room temperature. Antibodies used were 4G8 anti-beta amyloid (mouse, 1:800) and pTau (Ser202; mouse, 1:1000) from Pierce (Rockford, IL). Following two PBS washes, the slides were incubated for 1 hour with Alexa Fluor 488 and 594 secondaries (1:600; Invitrogen, Carlsbad, CA) in 0.1 M PBS containing 10% serum and 0.1% phosphatase inhibitor. Slides were again rinsed twice in PBS and once in distilled water before a 10 minute incubation with 0.3% Sudan Black B (EMD Chemicals, Gibbstown, NJ) in 70% ethanol to block lipofuscin autofluorescence (Romijn

et al., 1999). After two more rinses in distilled deionized water, Vectashield containing 4',6-diamidino-2-phenylindole (DAPI) was applied (Vector Laboratories, Burlingame, CA), and coverslips were mounted. Nail polish was applied to seal the edges.

For beta-amyloid and SAP staining, the same procedure was followed except that the sections were blocked and permeabilized for 1 hour in PBS/4% BSA/0.03% Triton X-100. Sections were incubated overnight at room temperature with 1:800 4G8 in PBS-4% BSA. The next day, the slides were briefly washed twice in PBS, and the sections were incubated with 1:500 rabbit anti-SAP antibody (Epitomics) for 1 hour at room temperature, along with negative control antibodies. After four 5-minute washes, the slides were incubated with donkey anti-mouse Dylight 488 and donkey anti-rabbit rhodamine red X (Jackson ImmunoResearch) in PBS-4% BSA for 30 minutes.

6.2.4 Image Analysis

Images were acquired using a confocal laser-scanning module (Bio-Rad Radiance 2000 with LaserSharp software; Hercules, CA) mounted on a Nikon E800 microscope with a 20x/0.75NA objective (Nikon USA; Melville, NY). Images were acquired with 488 nm and 568 nm excitation. Images for comparisons were acquired with constant settings for laser power, detector gain, amplification gain, and offset. For the beta-amyloid and SAP staining, DIC and fluorescence images were acquired using an Olympus FV1000 confocal microscope with a 20x/0.75NA objective and Micromanager software.

6.3 Results

6.3.1 SAP levels in the hippocampus and frontal cortex of NDAN individuals are significantly decreased compared to AD.

Previously, SAP levels were found to be elevated in Alzheimer's patients. (Yasojima *et al.*, 2000). We were therefore interested in looking at the level of SAP in NDAN patients who had the serious neurodegenerative hallmarks of AD but never had cognitive impairment. We also found that SAP levels were elevated in the hippocampus and frontal cortex of AD patients compared to controls with a four-fold increase to 110 ng of SAP/mg of protein in AD (Figure 6.2A, 6.2B). Our results differ from the 1 μg of SAP/mg protein previously reported, because we looked at total homogenate, while the SAP and total protein concentrations in supernatants after centrifugation of homogenates were previously reported (Yasojima et al., 2000). Interestingly, SAP levels were significantly elevated in both the hippocampus and frontal cortex for AD patients compared to NDAN samples, even though both sets of cases had comparable number of amyloid plaques and neurofibrillary tangles that SAP associates with (Figure 6.2A, 6.2B). In the NDAN samples, the level of SAP in the hippocampus and frontal cortex were comparable to the controls. Levels of SAP in MCI patients were intermediate in the hippocampus, while at normal levels in the frontal cortex, which is to be expected due to the significantly lower number of plaques and neurofibrillary tangles found in MCI compared to AD (Guillozet et al., 2003).

6.3.2 SAP staining is reduced at Aβ plaques for NDAN hippocampal sections compared to AD.

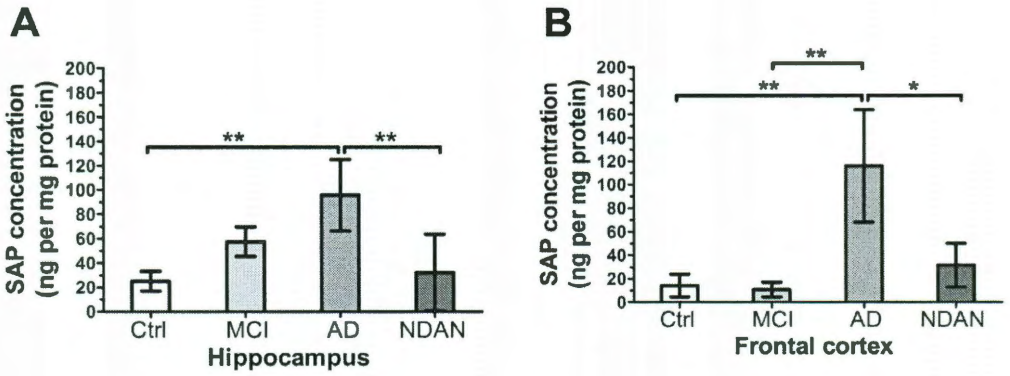

Figure 6.2: SAP levels in the hippocampus and frontal cortex of NDAN individuals are significantly decreased compared to Alzheimer's.

SAP levels in homogenized brain tissue were measured by Western blot and compared to normal brain controls. Statistical significance was determined by 1-way ANOVA, Tukey's test. *, $p < 0.05$; **, $p < 0.01$. Results are mean ± SEM (n=6 for control hippocampus, n=5 for MCI and AD hippocampus, n=4 for NDAN hippocampus; n=3 for frontal cortex).

SAP co-localizes with amyloid plaques in the brains of AD patients (Duong et al., 1989). On stained hippocampal tissue sections, no Aβ plaques or SAP staining was visible in the normal-age-matched controls (Figure 6.3). NDAN sections had numerous plaques with extremely light staining of SAP, also localized to the plaque (Figure 6.3). The number of plaques in AD patients was similar to NDAN, but AD tissue sections had relatively strong SAP staining co-localized to the plaques (Figure 6.3).

6.4 Discussion

SAP levels are elevated in the brains, but not the CSF, of patients with AD. These patients have cognitive impairment and a significant number of amyloid plaques and neurofibrillary tangles in the memory and cognitive function area of the brain (Lee et al., 2010; Yasojima et al., 2000). MCI patients only have slight cognitive impairment, fewer amyloid plaques, and significantly less neurofibrillary tangles (Guillozet et al., 2003). NDAN individuals have extensive amyloid plaques and neurofibrillary tangles like AD, while having little to no cognitive impairment (Aizenstein et al., 2008; Reiman et al., 2009). Here, I found that NDAN individuals have significantly lower levels of SAP compared to AD with levels approaching those of normal age matched controls. However, it is not possible at this point to mechanistically link the decreased levels of SAP to cognitive rescue.

SAP is expressed by neurons in the brain, and normal elderly will develop low levels of amyloid plaques and neurofibrillary tangles (Bouras et al., 1994; Yasojima et al., 2000). Therefore, at least low levels of SAP are expected to be, and were, found. The

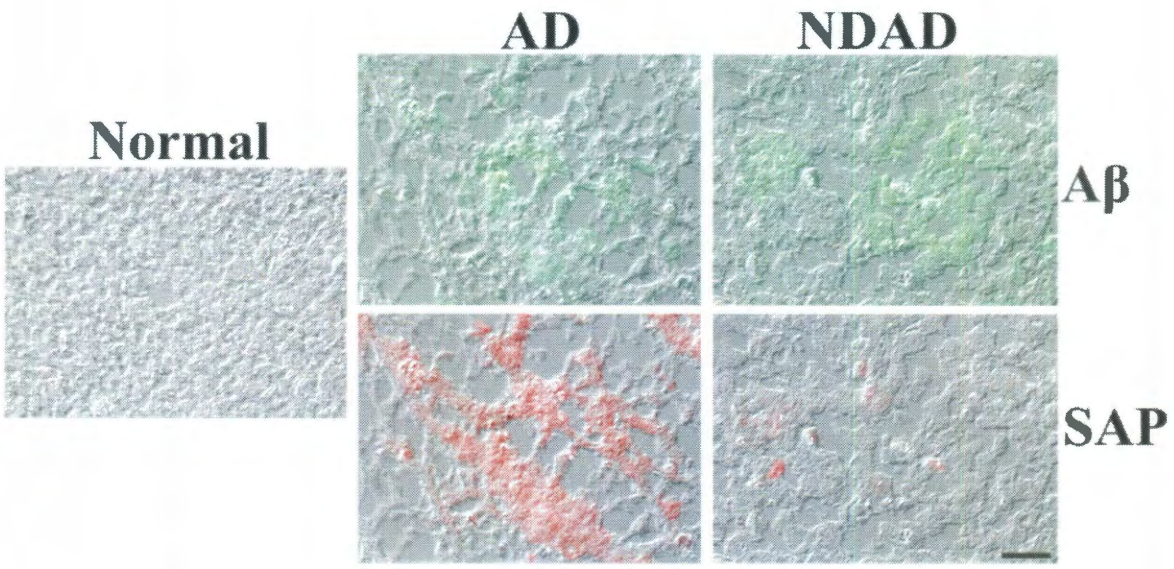

Figure 6.3: SAP staining is reduced at Aβ plaques for NDAN compared to Alzheimer's. Hippocampus sections were stained for Aβ (green) and SAP (red). Bar is 50 μm. Representative of n=3.

MCI samples showed intermediate levels (between AD and control) of SAP in the hippocampus, and in the frontal cortex the levels were indistinguishable from normal-age matched controls. This is also expected, since MCI individuals have significantly less infiltration of neurofibrillary tangles at that stage of the disease and possibly reduced plaque numbers. However, the low levels of SAP in NDAN individuals was not expected as high levels of plaques and tangles are located in both sections of the brains and SAP readily binds to both. This lack of SAP could therefore reflect biochemical changes leading to reduced SAP deposition. Further studies are needed to clarify the exact mechanisms involved.

The lack of dementia and low SAP levels in NDAN individuals could potentially be due to a reduced inflammatory response. Typically in Alzheimer's, the presence of amyloid plaques and neurofibrillaey tangless activate inflammatory cells, including the microglia and macrophages, resulting in the release of cytokines and other inflammatory agents (Lee et al., 2010). The microglia could upregulate SAP production, which can in turn bind more Aβ and result in additional plaques. For NDAN individuals, however, SAP could be acting predominantly in its role as an anti-inflammatory agent through opsonization and clearance of apoptotic neuronal cells, as well as downregulating the activation of infiltrating monocytes and macrophages with local IL-10 production (Castano et al., 2009). There would be a balance between SAP acting in a positive manner as an anti-inflammatory agent and SAP binding to amyloid plaques detrimentally as a pattern recognition protein. In the case of AD, the balance is shifted to SAP

predominantly binding to fibrils and plaques, while in NDAN individuals SAP is predominantly acting to reduce inflammation.

Additionally, there could be a connection between SAP levels and ApoE, a risk factor for AD (Jiang *et al.*, 2008). All NDAD patients in our study expressed the neutral APOE ε3 allele while the AD patients had a mixture of alleles (personal communication with Dr. G. Taglialatela, UTMB). However, SAP is involved in the stabilization of Aβ aggregates while ApoE promotes degradation of the soluble form (Tennet *et al.*, 1995; Jiang *et al.*, 2008). To explore any such connections, the study needs to be expanded to more cases.

The drug CPHPC cross-links SAP pentamers to increase the clearance of SAP from the body, resulting in decreased SAP levels in the serum and CSF of Alzheimer's patients (Kolstoe et al., 2009). An intriguing possibility is that CPHPC could be used to prevent the onset of dementia by removal of SAP from the brain. It remains to be seen how CPHPC will affect amyloid clearance in the long term, and if it will help restore cognitive function.

Concluding Remarks

As there is currently a large unmet medical need for treatments for fibrosing diseases, my work detailing how the potential therapeutic serum amyloid P regulates fibrocyte differentiation is of great interest. Fibrocytes have been implicated in two of the most prevalent and debilitating fibrosing diseases, cardiac and pulmonary fibrosis. We have previously shown that SAP can successfully treat both diseases in mice and rat model systems. Understanding specifically how SAP regulates fibrocytes could lead to improved or even new therapeutics.

Although I was not able to determine the specific functional domain of SAP in Chapter 2, the work is still of importance in developing an expression system for future mutagenesis experiments, and for eliminating two regions of SAP as the major functional domain. Expressing bioactive, native SAP was a long and arduous process that many commercial companies failed to do (personal correspondence with Promedior), and now we can use this method to evaluate new regions of SAP through mutagenesis. When the region of SAP was mutagenized that was similar to the IgG ^{327}ALPAPI^{333} binding region, there was no significant change in SAP's bioactivity, suggesting that SAP does not bind to the FcγR in the same manner as IgG. There was only a modest change in SAP bioactivity when residues were altered that were critical for SAP binding to FcγRIIa in a crystal structure. This result suggests that residues 173 and 174 may mediate some but not all of SAP bioactivity, and that the critical domain regulating fibrocyte differentiation lies elsewhere.

In Chapter 3, I developed an assay for measuring receptor binding for when we find a mutant that lacks bioactivity, and we want to see if the mutant still binds to the receptor. During the development of the assay, we expanded our knowledge of SAP biology. SAP has a pattern recognition site to bind apoptotic material or pathogens, and such binding does not appear necessary for efficient receptor binding to FcγR, although there is the possibility that BSA acts as a very weak ligand to SAP. Additionally, SAP does not compete with aggregated IgG for binding to FcγRs in our ELISA assay, suggesting that they bind to different locations on the receptor, which also agrees with our mutagenesis analysis for the IgG binding region.

In studying factors that regulate fibrocyte differentiation, we are very limited in genetic diversity and in studying diseased states if we only utilize human cells. Therefore, there was a specific need for a rapid assay to study such factors in mice, where one can knock out genes and/or induce a model diseased state. However, the amount of cells one gets from the blood of a single mouse is very limited. In Chapter 4, I solved this issue by developing a quick, efficient fibrocyte differentiation assay utilizing mouse spleen cells and pro-fibrotic cytokines. We are now able to test factors within a period of only 5 days in serum-free media to eliminate any non-specific serum effects. Additionally, we can get n=3 using 3 mice instead of the previous requirement of 9 or more, which is expensive when dealing with knock out mice.

Utilizing the assay from Chapter 4, I determined that FcγRI and the FcRγ chain play a major role in the signal transduction pathway that SAP uses to inhibit fibrocyte differentiation. However, the ability of SAP to inhibit fibrocyte differentiation in cells lacking FcγRI or FcRγ suggests that SAP activates receptors in addition to FcγRI, and additionally activates a signaling pathway that does not require FcRγ. Additionally, I found that FcγRII knock out spleen cells are even more sensitive to SAP, and a similar effect was observed in human cells when siRNA was used to knock down the level of the FcγRIIb. Using siRNA on the human FcγRs, I obtained results comparable to the mouse KOs, suggesting that a result in one system can potentially be extrapolated to the other. Overall, this finding of FcγRI as a major receptor in regulating fibrocyte differentiation is important since therapeutics could potentially be targeted to the specific SAP receptor, and knowledge of the specific receptor will help us investigate fibrocyte biology within fibrosing diseases.

Finally, I determined that SAP levels in NDAN individuals, that lack dementia, are significantly lower than Alzheimer's patients, when both have similar levels of amyloid plaques and neurofibrillary tangles. My findings are just a preliminary report, it is not possible at this time to mechanistically link decreased SAP levels to cognitive rescue. However, this finding could eventually be the basis for preventing disease progression in AD or used as a biomarker to determine if an individual will develop dementia.

References

Abe, R., Donnelly, S.C., Peng, T., Bucala, R., and Metz, C.N. (2001). Peripheral blood fibrocytes: differentiation pathway and migration to wound sites. J Immunol *166*, 7556-7562.

Aizenstein, H.J., Nebes, R.D., Saxton, J.A., Price, J.C., Mathis, C.A., Tsopelas, N.D., Ziolko, S.K., James, J.A., Snitz, B.E., Houck, P.R., *et al.* (2008). Frequent amyloid deposition without significant cognitive impairment among the elderly. Arch Neurol *65*, 1509-1517.

Aquilina, J.A., and Robinson, C.V. (2003). Investigating interactions of the pentraxins serum amyloid P component and C-reactive protein by mass spectrometry. Biochem J *375*, 323-328.

Becker, S., Warren, M.K., and Haskill, S. (1987). Colony-stimulating factor-induced monocyte survival and differentiation into macrophages in serum-free cultures. J Immunol *139*, 3703-3709.

Bennett, D.A., Schneider, J.A., Arvanitakis, Z., Kelly, J.F., Aggarwal, N.T., Shah, R.C., and Wilson, R.S. (2006). Neuropathology of older persons without cognitive impairment from two community-based studies. Neurology *66*, 1837-1844.

Bharadwaj, D., Stein, M.P., Volzer, M., Mold, C., and Du Clos, T.W. (1999). The major receptor for C-reactive protein on leukocytes is fcgamma receptor II. J Exp Med *190*, 585-590.

Bharadwaj, D., Mold, C., Markham, E., and Du Clos, T.W. (2001). Serum amyloid P component binds to Fc gamma receptors and opsonizes particles for phagocytosis. J Immunol *166*, 6735-6741.

Bodman-Smith, K.B., Melendez, A.J., Campbell, I., Harrison, P.T., Allen, J.M., and Raynes, J.G. (2002). C-reactive protein-mediated phagocytosis and phospholipase D signalling through the high-affinity receptor for immunoglobulin G (FcgammaRI). Immunology *107*, 252-260.

Botto, M., Hawkins, P.N., Bickerstaff, M.C., Herbert, J., Bygrave, A.E., McBride, A., Hutchinson, W.L., Tennent, G.A., Walport, M.J., and Pepys, M.B. (1997). Amyloid deposition is delayed in mice with targeted deletion of the serum amyloid P component gene. Nat Med *3*, 855-859.

Bouros, D., and Antoniou, K.M. (2005). Current and future therapeutic approaches in idiopathic pulmonary fibrosis. The European respiratory journal : J Eur Soc for Clin Resp Physiol *26*, 693-702.

Braak, H., and Braak, E. (1991). Neuropathological stageing of Alzheimer-related changes. Acta Neuropathol *82*, 239-259.

Bucala, R., Spiegel, L.A., Chesney, J., Hogan, M., and Cerami, A. (1994). Circulating fibrocytes define a new leukocyte subpopulation that mediates tissue repair. Mol Med *1*, 71-81.

Castano, A.P., Lin, S.L., Surowy, T., Nowlin, B.T., Turlapati, S.A., Patel, T., Singh, A., Li, S., Lupher, M.L., Jr., and Duffield, J.S. (2009). Serum amyloid P inhibits fibrosis through Fc gamma R-dependent monocyte-macrophage regulation in vivo. Science Transl Med *1*, 5ra13.

Chesney, J., Metz, C., Stavitsky, A.B., Bacher, M., and Bucala, R. (1998). Regulated production of type I collagen and inflammatory cytokines by peripheral blood fibrocytes. J Immunol *160*, 419-425.

Chi, M., Tridandapani, S., Zhong, W., Coggeshall, K.M., and Mortensen, R.F. (2002). C-reactive protein induces signaling through Fc gamma RIIa on HL-60 granulocytes. J Immunol *168*, 1413-1418.

Clark, R.A. (2001). Fibrin and wound healing. Ann NY Acad Sci *936*, 355-367.

Corder, E.H., Saunders, A.M., Strittmatter, W.J., Schmechel, D.E., Gaskell, P.C., Small, G.W., Roses, A.D., Haines, J.L., and Pericak-Vance, M.A. (1993). Gene dose of apolipoprotein E type 4 allele and the risk of Alzheimer's disease in late onset families. Science *261*, 921-923.

Coria, F., Castano, E., Prelli, F., Larrondo-Lillo, M., van Duinen, S., Shelanski, M.L., and Frangione, B. (1988). Isolation and characterization of amyloid P component from Alzheimer's disease and other types of cerebral amyloidosis. Lab Invest *58*, 454-458.

Cowper, S.E., and Bucala, R. (2003). Nephrogenic fibrosing dermopathy: suspect identified, motive unclear. Am J Dermatopathol *25*, 358.

Cowper, S.E., Kuo, P.H., and Bucala, R. (2007). Nephrogenic systemic fibrosis and gadolinium exposure: association and lessons for idiopathic fibrosing disorders. Arthritis Rheum *56*, 3173-3175.

Crawford, J.R., Pilling, D., and Gomer, R.H. (2010). Improved serum-free culture conditions for spleen-derived murine fibrocytes. J Immunol Methods *363*, 9-20.

Daeron, M. (1997). Structural bases of Fc gamma R functions. Int Rev Immunol *16*, 1-27.

DeLano, W.L. (2002). The PyMOL Molecular Graphics System. DeLano Scientific, San Carlos, CA, USA. http://www.pymol.org.

Dijstelbloem, H.M., van de Winkel, J.G., and Kallenberg, C.G. (2001). Inflammation in autoimmunity: receptors for IgG revisited. Trends in immunology *22*, 510-516.

Duong, T., Pommier, E.C., and Scheibel, A.B. (1989). Immunodetection of the amyloid P component in Alzheimer's disease. Acta Neuropathol *78*, 429-437.

Emsley, J., White, H.E., O'Hara, B.P., Oliva, G., Srinivasan, N., Tickle, I.J., Blundell, T.L., Pepys, M.B., and Wood, S.P. (1994). Structure of pentameric human serum amyloid P component. Nature *367*, 338-345.

Ebeling, W., Hennrich, N., Klockow, M., Metz, H., Orth, H.D., and Lang, H. (1974). Proteinase K from Tritirachium album Limber. Eur. J. Biochem. *47*, 91-7.

Ferreira, M.C., Tuma, P., Jr., Carvalho, V.F., and Kamamoto, F. (2006). Complex wounds. Clinics (Sao Paulo) *61*, 571-578.

Gomer, R.H., Pilling, D., Kauvar, L.M., Ellsworth, S., Ronkainen, S.D., Roife, D., and Davis, S.C. (2009). A serum amyloid P-binding hydrogel speeds healing of partial thickness wounds in pigs. Wound Repair Regen *17*, 397-404.

Gomperts, B.N., and Strieter, R.M. (2007). Fibrocytes in lung disease. J Leukoc Biol *82*, 449-456.

Grage-Griebenow, E., Flad, H.D., and Ernst, M. (2001). Heterogeneity of human peripheral blood monocyte subsets. J Leukoc Biol *69*, 11-20.

Guillozet, A.L., Weintraub, S., Mash, D.C., and Mesulam, M.M. (2003). Neurofibrillary tangles, amyloid, and memory in aging and mild cognitive impairment. Arch Neurol *60*, 729-736.

Hartlapp, I., Abe, R., Saeed, R.W., Peng, T., Voelter, W., Bucala, R., and Metz, C.N. (2001). Fibrocytes induce an angiogenic phenotype in cultured endothelial cells and promote angiogenesis in vivo. FASEB J *15*, 2215-2224.

Haslett, C. and Henson, P. (1988). Resolution of Inflammation. In *The Molecular and Cellular Biology of Wound Repair*. R. A. F. Clark and P. M. Henson, eds. Plenum Press, NY, 185-211.

Haudek, S.B., Xia, Y., Huebener, P., Lee, J.M., Carlson, S., Crawford, J.R., Pilling, D., Gomer, R.H., Trial, J., Frangogiannis, N.G., *et al.* (2006). Bone marrow-derived fibroblast precursors mediate ischemic cardiomyopathy in mice. Proc Natl Acad Sci USA *103*, 18284-18289.

Haudek, S.B., Trial, J., Xia, Y., Gupta, D., Pilling, D., and Entman, M.L. (2008). Fc receptor engagement mediates differentiation of cardiac fibroblast precursor cells. Proc Natl Acad Sci USA *105*, 10179-10184.

Herzog, E.L., and Bucala, R. (2010). Fibrocytes in health and disease. Exp Hematol *38*, 548-556.

Holm Nielsen, E., Nybo, M., Junker, K., Toftedal Hansen, P., Rasmussen, I.M., and Svehag, S.E. (2000). Localization of human serum amyloid P component and heparan sulfate proteoglycan in in vitro-formed Aβ fibrils. Scand J Immunol *52*, 110-112.

Hughes, A.L. (1996). Gene duplication and recombination in the evolution of mammalian Fc receptors. J Mol Evol *43*, 4-10.

Hulett, MD, and Hogarth PM. (1998). The second and third extracellular domais of FcγRI confer the unique high affinity binding to IgG2a. Mol. Immunol. 35: 989-996.

Hutchinson, W.L., Hohenester, E., and Pepys, M.B. (2000). Human serum amyloid P component is a single uncomplexed pentamer in whole serum. Mol Med *6*, 482-493.

Inaba, K., Steinman, R.M., Pack, M.W., Aya, H., Inaba, M., Sudo, T., Wolpe, S., and Schuler, G. (1992). Identification of proliferating dendritic cell precursors in mouse blood. J Exp Med *175*, 1157-1167.

Ioan-Facsinay, A., de Kimpe, S.J., Hellwig, S.M., van Lent, P.L., Hofhuis, F.M., van Ojik, H.H., Sedlik, C., da Silveira, S.A., Gerber, J., de Jong, Y.F., *et al.* (2002). FcgammaRI (CD64) contributes substantially to severity of arthritis, hypersensitivity responses, and protection from bacterial infection. Immunity *16*, 391-402.

Izbicki, G., and Breuer, R. (2003). IL-4 is not a key profibrotic cytokine in bleomycin-induced lung fibrosis model. J Immunol *171*, 2767-2768.

Jakubzick, C., Choi, E.S., Joshi, B.H., Keane, M.P., Kunkel, S.L., Puri, R.K., and Hogaboam, C.M. (2003). Therapeutic attenuation of pulmonary fibrosis via targeting of IL-4- and IL-13-responsive cells. J Immunol *171*, 2684-2693.

Janciauskiene, S., Garcia de Frutos, P., Carlemalm, E., Dahlback, B., and Eriksson, S. (1995). Inhibition of Alzheimer beta-peptide fibril formation by serum amyloid P component. J Biol Chem *270*, 26041-26044.

Jiang, Q., Lee, C.Y., Mandrekar, S., Wilkinson, B., Cramer, P., Zelcer, N., Mann, K., Lamb, B., Willson, T.M., Collins, J.L., *et al.* (2008). ApoE promotes the proteolytic degradation of Aβ. Neuron *58*, 681-693.

Junttila, I.S., Mizukami, K., Dickensheets, H., Meier-Schellersheim, M., Yamane, H., Donnelly, R.P., and Paul, W.E. (2008). Tuning sensitivity to IL-4 and IL-13: differential expression of IL-4Ralpha, IL-13Ralpha1, and gammac regulates relative cytokine sensitivity. J Exp Med *205*, 2595-2608.

Kalaria, R.N., and Grahovac, I. (1990). Serum amyloid P immunoreactivity in hippocampal tangles, plaques and vessels: implications for leakage across the blood-brain barrier in Alzheimer's disease. Brain Res *516*, 349-353.

Kile, B.T., Mason-Garrison, C.L., and Justice, M.J. (2003). Sex and strain-related differences in the peripheral blood cell values of inbred mouse strains. Mamm Genome *14*, 81-85.

Kimura, M., Asada, T., Uno, M., Machida, N., Kasuya, K., Taniguchi, Y., Fujita, T., Nishiyama, E., Iwamoto, N., and Arai, H. (1999). Assessment of cerebrospinal fluid levels of serum amyloid P component in patients with Alzheimer's disease. Neurosci Lett *273*, 137-139.

Kinoshita, C.M., Gewurz, A.T., Siegel, J.N., Ying, S.C., Hugli, T.E., Coe, J.E., Gupta, R.K., Huckman, R., and Gewurz, H. (1992). A protease-sensitive site in the proposed Ca(2+)-binding region of human serum amyloid P component and other pentraxins. Protein Sci *1*, 700-709.

Kisseleva, T., Uchinami, H., Feirt, N., Quintana-Bustamante, O., Segovia, J.C., Schwabe, R.F., and Brenner, D.A. (2006). Bone marrow-derived fibrocytes participate in pathogenesis of liver fibrosis. J Hepatol *45*, 429-438.

Kolodsick, J.E., Toews, G.B., Jakubzick, C., Hogaboam, C., Moore, T.A., McKenzie, A., Wilke, C.A., Chrisman, C.J., and Moore, B.B. (2004). Protection from fluorescein isothiocyanate-induced fibrosis in IL-13-deficient, but not IL-4-deficient, mice results from impaired collagen synthesis by fibroblasts. J Immunol *172*, 4068-4076.

Kolstoe, S.E., Ridha, B.H., Bellotti, V., Wang, N., Robinson, C.V., Crutch, S.J., Keir, G., Kukkastenvehmas, R., Gallimore, J.R., Hutchinson, W.L., *et al.* (2009). Molecular dissection of Alzheimer's disease neuropathology by depletion of serum amyloid P component. Proc Natl Acad Sci USA *106*, 7619-7623.

Kruisbeek, A.M. (2000). Isolation and fractionation of mononuclear cell populations. Curr. Protoc. Immunol. *39*:3.1.3-3.1.5.

Kumar, V., A. K. Abbas, and N. Fausto. (2005). Tissue Renewal and Repair: Regeneration, Healing, and Fibrosis. In Robbins and Cotran: Pathological Basis of Disease. V. Kumar,A. K. Abbas, and N. Fausto, eds. Elsevier Saunders, Philadelphia, pp. 87-118.

Lee, Y.J., Han, S.B., Nam, S.Y., Oh, K.W., and Hong, J.T. (2010). Inflammation and Alzheimer's disease. Arch Pharm Res *33*, 1539-1556.

Lu, J., Marnell, L.L., Marjon, K.D., Mold, C., Du Clos, T.W., and Sun, P.D. (2008). Structural recognition and functional activation of FcgammaR by innate pentraxins. Nature *456*, 989-992.

Lu, J., Marjon, K.D., Marnell, L.L., Wang, R., Mold, C., Du Clos, T.W., and Sun, P. (2011). Recognition and functional activation of the human IgA receptor (Fc{alpha}RI) by C-reactive protein. Proc Natl Acad Sci USA *108*, 4974-4979.

Lupher, M.L., Jr., and Gallatin, W.M. (2006). Regulation of fibrosis by the immune system. Adv Immunol *89*, 245-288.

Macdonald, S.L., and Kilpatrick, D.C. (2006). Human serum amyloid P component binds to peripheral blood monocytes. Scand J Immunol *64*, 48-52.

Maharjan, A.S., Pilling, D., and Gomer, R.H. (2010). Toll-like receptor 2 agonists inhibit human fibrocyte differentiation. Fibrogenesis Tissue Repair *3*, 23.

Maharjan, A.S., Pilling, D., and Gomer, R.H. (2011). High and Low Molecular Weight Hyaluronic Acid Differentially Regulate Human Fibrocyte Differentiation. PLoS One *6*, e26078.

Mattson, M.P. (2004). Pathways towards and away from Alzheimer's disease. Nature *430*, 631-639.

McGeer, E.G., Yasojima, K., Schwab, C., and McGeer, P.L. (2001). The pentraxins: possible role in Alzheimer's disease and other innate inflammatory diseases. Neurobiol Aging *22*, 843-848.

Mehrad, B., Burdick, M.D., Zisman, D.A., Keane, M.P., Belperio, J.A., and Strieter, R.M. (2007). Circulating peripheral blood fibrocytes in human fibrotic interstitial lung disease. Biochem Biophys Res Commun *353*, 104-108.

Mestas, J., and Hughes, C.C. (2004). Of mice and not men: differences between mouse and human immunology. J Immunol *172*, 2731-2738.

Mold, C., Gewurz, H., and Du Clos, T.W. (1999). Regulation of complement activation by C-reactive protein. Immunopharmacology *42*, 23-30.

Mold, C., Baca, R., and Du Clos, T.W. (2002). Serum amyloid P component and C-reactive protein opsonize apoptotic cells for phagocytosis through Fcgamma receptors. J AutoImmun *19*, 147-154.

Monteiro, R.C., and Van De Winkel, J.G. (2003). IgA Fc receptors. Annu Rev of Immunol *21*, 177-204.

Moreira, A.P., Cavassani, K.A., Hullinger, R., Rosada, R.S., Fong, D.J., Murray, L., Hesson, D.P., and Hogaboam, C.M. (2010). Serum amyloid P attenuates M2 macrophage activation and protects against fungal spore-induced allergic airway disease. J Allergy Clin Immun *126*, 712-721 e717.

Mori, L., Bellini, A., Stacey, M.A., Schmidt, M., and Mattoli, S. (2005). Fibrocytes contribute to the myofibroblast population in wounded skin and originate from the bone marrow. Exp Cell Res *304*, 81-90.

Mulder, C., Schoonenboom, S.N., Wahlund, L.O., Scheltens, P., van Kamp, G.J., Veerhuis, R., Hack, C.E., Blomberg, M., Schutgens, R.B., and Eikelenboom, P. (2002). CSF markers related to pathogenetic mechanisms in Alzheimer's disease. J Neural Transm *109*, 1491-1498.

Murray, L.A., Kramer, M.S., Hesson, D.P., Watkins, B.A., Fey, E.G., Argentieri, R.L., Shaheen, F., Knight, D.A., and Sonis, S.T. (2010). Serum amyloid P ameliorates radiation-induced oral mucositis and fibrosis. Fibrogenesis & Tissue Repair *3*, 11.

Naik-Mathuria, B., Pilling, D., Crawford, J.R., Gay, A.N., Smith, C.W., Gomer, R.H., and Olutoye, O.O. (2008). Serum amyloid P inhibits dermal wound healing. Wound Repair Regen *16*, 266-273.

Niedermeier, M., Reich, B., Rodriguez Gomez, M., Denzel, A., Schmidbauer, K., Gobel, N., Talke, Y., Schweda, F., and Mack, M. (2009). CD4+ T cells control the differentiation of Gr1+ monocytes into fibrocytes. Proc Natl Acad Sci USA *106*, 17892-17897.

Nimmerjahn, F., and Ravetch, J. (2005). Divergent immunoglobulin g subclass activity through selective Fc receptor binding. Science *310*, 1510-1512.

Nimmerjahn, F., and Ravetch, J.V. (2008). Fcgamma receptors as regulators of immune responses. Nat Rev Immunol *8*, 34-47.

Nimmerjahn, F., Lux, A., Albert, H., Woigk, M., Lehmann, C., Dudziak, D., Smith, P., and Ravetch, J.V. (2010). FcgammaRIV deletion reveals its central role for IgG2a and IgG2b activity in vivo. Proc Natl Acad Sci USA *107*, 19396-19401.

Pepys, M.B., and Dash, A.C. (1977). Isolation of amyloid P component (protein AP) from normal serum as a calcium-dependent binding protein. Lancet *1*, 1029-1031.

Pepys, M.B., Dash, A.C., Markham, R.E., Thomas, H.C., Williams, B.D., and Petrie, A. (1978). Comparative clinical study of protein SAP (amyloid P component) and C-reactive protein in serum. Clin Exp Immunol *32*, 119-124.

Pepys, M.B., Baltz, M.L., de Beer, F.C., Dyck, R.F., Holford, S., Breathnach, S.M., Black, M.M., Tribe, C.R., Evans, D.J., and Feinstein, A. (1982). Biology of serum amyloid P component. Ann NY Acad Sci *389*, 286-298.

Pepys, M.B., and Baltz, M.L. (1983). Acute phase proteins with special reference to C-reactive protein and related proteins (pentaxins) and serum amyloid A protein. Adv Immunol *34*, 141-212.

Pepys, M., Booth, D., Hutchinson, W., Gallimore, J., Collins, P., and Hohenester, E. (1997). Amyloid P component: a critical review. Amyloid *4*: 274.

Perez, A., Rogers, R., and Dauber, J. (2003). The prognosis of idiopathic pulmonary fibrosis. Am. J. Respir. Cell. Mol. Biol. *29*(3 Suppl): S19-S26.

Phillips, R.J., Burdick, M.D., Hong, K., Lutz, M.A., Murray, L.A., Xue, Y.Y., Belperio, J.A., Keane, M.P., and Strieter, R.M. (2004). Circulating fibrocytes traffic to the lungs in response to CXCL12 and mediate fibrosis. J Clin Invest *114*, 438-446.

Pilling, D., Buckley, C.D., Salmon, M., and Gomer, R.H. (2003). Inhibition of fibrocyte differentiation by serum amyloid P. J Immunol *17*, 5537-5546.

Pilling, D., Tucker, N.M., and Gomer, R.H. (2006). Aggregated IgG inhibits the differentiation of human fibrocytes. J Leukoc Biol *79*, 1242-1251.

Pilling, D., Roife, D., Wang, M., Ronkainen, S.D., Crawford, J.R., Travis, E.L., and Gomer, R.H. (2007). Reduction of bleomycin-induced pulmonary fibrosis by serum amyloid P. J Immunol *179*, 4035-4044.

Pilling, D., Fan, T., Huang, D., Kaul, B., and Gomer, R.H. (2009a). Identification of markers that distinguish monocyte-derived fibrocytes from monocytes, macrophages, and fibroblasts. PLoS One *4*, e7475.

Pilling, D., Vakil, V., and Gomer, R.H. (2009b). Improved serum-free culture conditions for the differentiation of human and murine fibrocytes. J Immunol Methods *351*, 62-70.

Querfurth, H.W., and LaFerla, F.M. (2010). Alzheimer's disease. The New England journal of medicine *362*, 329-344.

Radaev, S., Motyka, S., Fridman, W.H., Sautes-Fridman, C., and Sun, P.D. (2001). The structure of a human type III Fcgamma receptor in complex with Fc. J Biol Chem *276*, 16469-16477.

Ravetch, J.V., and Kinet, J.P. (1991). Fc receptors. Annu Rev Immunol *9*, 457-492.

Ravetch, J.V., and Bolland, S. (2001). IgG Fc receptors. Annu Rev Immunol *19*, 275-290.

Ravetch, J.V. (2003) Fc Receptors. In Fundamental Immunology, W.E. Paul, ed. (Philadelphia: Lippincott-Raven), 685-700.

Reiman, E.M., Chen, K., Liu, X., Bandy, D., Yu, M., Lee, W., Ayutyanont, N., Keppler, J., Reeder, S.A., Langbaum, J.B., *et al.* (2009). Fibrillar amyloid-beta burden in cognitively normal people at 3 levels of genetic risk for Alzheimer's disease. Proceedings of the National Academy of Sciences of the United States of America *106*, 6820-6825.

Robbins, C.S., and Swirski, F.K. (2010). The multiple roles of monocyte subsets in steady state and inflammation. Cell Mol Life Sci *67*, 2685-2693.

Romijn, H.J., van Uum, J.F., Breedijk, I., Emmering, J., Radu, I., and Pool, C.W. (1999). Double immunolabeling of neuropeptides in the human hypothalamus as analyzed by confocal laser scanning fluorescence microscopy. J Histochem Cytochem FIELD Full Journal Title:The journal of histochemistry and cytochemistry : official journal of the Histochemistry Society *47*, 229-236.

Sakai, N., Furuichi, K., Shinozaki, Y., Yamauchi, H., Toyama, T., Kitajima, S., Okumura, T., Kokubo, S., Kobayashi, M., Takasawa, K., *et al.* (2010). Fibrocytes are involved in the pathogenesis of human chronic kidney disease. Hum pathol *41*, 672-678.

Sallusto, F., and Lanzavecchia, A. (1994). Efficient presentation of soluble antigen by cultured human dendritic cells is maintained by granulocyte/macrophage colony-stimulating factor plus interleukin 4 and downregulated by tumor necrosis factor alpha. J Exp Med *179*, 1109-1118.

Sato, K., Yang, X.L., Yudate, T., Chung, J.S., Wu, J., Luby-Phelps, K., Kimberly, R.P., Underhill, D., Cruz, P.D., Jr., and Ariizumi, K. (2006). Dectin-2 is a pattern recognition receptor for fungi that couples with the Fc receptor gamma chain to induce innate immune responses. J Biol Chem *281*, 38854-38866.

Schmidt, M., Sun, G., Stacey, M.A., Mori, L., and Mattoli, S. (2003). Identification of Circulating Fibrocytes as Precursors of Bronchial Myofibroblasts in Asthma. J Immunol *171*, 380-389.

Shao, D.D., Suresh, R., Vakil, V., Gomer, R.H., and Pilling, D. (2008). Pivotal Advance: Th-1 cytokines inhibit, and Th-2 cytokines promote fibrocyte differentiation. J Leukoc Biol *83*, 1323-1333.

Shortman, K., and Liu, Y.J. (2002). Mouse and human dendritic cell subtypes. Nat Rev Immunol *2*, 151-161.

Srinivasan, N., White, H.E., Emsley, J., Wood, S., Pepys, M., and Blundell, T. (1994). Comparative analyses of pentraxins: implications for protomer assembly and ligand binding. Structure. *2*, 1017-1027.

Swirski, F.K., Nahrendorf, M., Etzrodt, M., Wildgruber, M., Cortez-Retamozo, V., Panizzi, P., Figueiredo, J.L., Kohler, R.H., Chudnovskiy, A., Waterman, P., *et al.* (2009). Identification of splenic reservoir monocytes and their deployment to inflammatory sites. Science *325*, 612-616.

Tennent, G.A., Lovat, L.B., and Pepys, M.B. (1995). Serum amyloid P component prevents proteolysis of the amyloid fibrils of Alzheimer disease and systemic amyloidosis. Proc Natl Acad Sci USA *92*, 4299-4303.

Thompson, D., Pepys, M.B., Tickle, I., and Wood, S. (2002). The structures of crystalline complexes of human serum amyloid P component with its carbohydrate ligand, the cyclic pyruvate acetal of galactose. J Mol Biol *320*, 1081-1086.

Togashi, S., Lim, S.K., Kawano, H., Ito, S., Ishihara, T., Okada, Y., Nakano, S., Kinoshita, T., Horie, K., Episkopou, V., *et al.* (1997). Serum amyloid P component enhances induction of murine amyloidosis. Lab Invest *77*, 525-531.

Urbanyi, Z., Laszlo, L., Tomasi, T.B., Toth, E., Mekes, E., Sass, M., and Pazmany, T. (2003). Serum amyloid P component induces neuronal apoptosis and beta-amyloid immunoreactivity. Brain Res *988*, 69-77.

Urbanyi, Z., Sass, M., Laszy, J., Takacs, V., Gyertyan, I., and Pazmany, T. (2007). Serum amyloid P component induces TUNEL-positive nuclei in rat brain after intrahippocampal administration. Brain Res *1145*, 221-226.

Vannella, K.M., McMillan, T.R., Charbeneau, R.P., Wilke, C.A., Thomas, P.E., Toews, G.B., Peters-Golden, M., and Moore, B.B. (2007). Cysteinyl leukotrienes are autocrine and paracrine regulators of fibrocyte function. Journal of immunology *179*, 7883-7890.

Verwey, N.A., Schuitemaker, A., van der Flier, W.M., Mulder, S.D., Mulder, C., Hack, C.E., Scheltens, P., Blankenstein, M.A., and Veerhuis, R. (2008). Serum amyloid p component as a biomarker in mild cognitive impairment and Alzheimer's disease. Dement Geriatr Cogn Disord *26*, 522-527.

Wang, J.F., Jiao, H., Stewart, T.L., Shankowsky, H.A., Scott, P.G., and Tredget, E.E. (2007). Fibrocytes from burn patients regulate the activities of fibroblasts. Wound Repair Regen *15*, 113-121.

Wirth, J.J., Theisen, M.A., and Crowle, A.J. (1982). Culture conditions required for primary isolation and study of mouse blood monocytes. J Reticuloendothel Soc *31*, 325-337.

Yang, L., Scott, P.G., Giuffre, J., Shankowsky, H.A., Ghahary, A., and Tredget, E.E. (2002). Peripheral Blood Fibrocytes from Burn Patients: Identification and Quantification of Fibrocytes in Adherent Cells Cultured from Peripheral Blood Mononuclear Cells. Lab Invest *82*, 1183-1192.

Yang, L., Scott, P.G., Dodd, C., Medina, A., Jiao, H., Shankowsky, H.A., Ghahary, A., and Tredget, E.E. (2005). Identification of fibrocytes in postburn hypertrophic scar. Wound Repair Regen *13*, 398-404.

Yasojima, K., Schwab, C., McGeer, E.G., and McGeer, P.L. (2000). Human neurons generate C-reactive protein and amyloid P: upregulation in Alzheimer's disease. Brain Res *887*, 80-89.